The Network Structure of Money Multiplier*

Ye Li† Yi Li‡ Sergey Sarkisyan§ Huijun Sun¶

March 7, 2026

Abstract

The role of deposits in the payment system creates both a liquidity constraint and a liquidity recycling mechanism for the banking system. When financing illiquid loans with deposits, a bank must rely on its liquid assets to cover depositors' outgoing payments. Therefore, the "money multiplier"—the ratio of loans funded by deposits to liquid assets (i.e., the bank's liquidity transformation relative to its liquidity base)—cannot be over-stretched. However, depositors' incoming payments relax this liquidity constraint. We develop a structural model to estimate the overall impact of payments (money velocity) on money multiplier using confidential payment data from Fedwire. The network topology of interbank payment flows plays an important role and determines banks' systemic importance for the equilibrium outcome.

Keywords: Payment network, deposits, credit supply, money multiplier, money velocity

*We are grateful for helpful comments from Juliane Begenau, Tobias Berg, Patrick Bolton, Markus Brunnermeier, Fabio Castiglionesi, Áureo de Paula, Mark Egan, Co-Pierre Georg, Simon Gilchrist, Michael Gofman, Ben Golub, Florian Heider, Bernard Herskovic, Peter Hoffmann, Arvind Krishnamurthy, Ricardo Lagos, Martin Schneider, René Stulz, Avanidhar Subrahmanyam, Pierre-Olivier Weill, for discussion by Enghin Atalay, Ana Babus, Yasser Boualam, Martin Brown, Selman Erol, and Zhentong Lyu, and for conference/seminar participants at Advances in Macro-Finance at Carnegie Mellon (Tepper-LAEF), American Finance Association, Bank of Canada Conference on Networks in Modern Financial & Payments Systems, Barcelona School of Economics Summer Forum, Boston College, Boston Fed, CEPR ESSFM Gerzensee, CESifo Conference on Money Macro and International Finance, Chicago Fed, European Banking Center Network Conference, European Finance Association, ECB, Federal Reserve Board, Federal Reserve Conference on the Interconnectedness of Financial Systems, Financial Intermediation Research Society, Frankfurt School of Finance & Management, Hong Kong University, INSEAD, Imperial College London, Nanyang Technological University, National University of Singapore, NYU Econ/Stern (macro seminar), Pacific Northwest Finance Conference, Philadelphia Fed, Singapore Management University, Stanford GSB (finance seminar), Tilburg University, UCLA (finance seminar), U Minnesota Finance Junior Conference, UNC Finance Junior Conference, U Toronto Econ Junior Conference, University of Zurich, U Penn/Wharton (macro brownbag), and Wharton (finance/micro brownbag). The views are those of the authors and do not reflect those of the Federal Reserve Board or its staff. This paper was previously circulated under the title "Bank Credit and Money Creation on Payment Networks: A Structural Analysis of Externalities and Key Players".

†University of Washington. E-mail: liye@uw.edu

‡Board of Governors of the Federal Reserve System. E-mail: yi.li@frb.gov

§The Ohio State University. E-mail: sarkisyan.1@osu.edu

¶Columbia University. E-mail: hsun25@gsb.columbia.edu

1 Introduction

At the core of a financial system are credit and money creation by banks. When extending loans, a bank grants borrowers newly issued deposits, engaging in a debt swap: The bank acquires borrowers' debts (loans) and issues debts (deposits) that borrowers hold as money.[1] This process expands the supply of inside money—the means of payment created within the private sector.

It may appear that banks possess the ability to create money ex nihilo thanks to the special status of their liabilities (deposits) as means of payment adopted by the rest of the economy. However, akin to other firms, banks' capacity to issue liabilities cannot be infinite in equilibrium as pointed out by Tobin (1963). What limits credit and money creation by banks? The answer also resides in the special status of deposits as money that circulates among depositors.

When the loan borrower turns the newly issued deposits into purchasing power, the bank faces three scenarios. First, the borrower withdraws cash, causing the bank to lose reserves. Second and more often, the borrower electronically pays depositors at other banks. The bank loses reserves and deposits to the recipients' banks. Lastly, should the recipients also be depositors at the lending bank, the bank simply alters the deposit ownership. In this scenario, the bank still faces liquidity loss if these recipients (the new depositors) pay others, triggering the first or second scenario.

Therefore, there is a liquidity constraint on credit and money creation: The ratio of loans funded by deposit issuance to the bank's liquid assets—the money multiplier—cannot be overstretched. Our notion of money multiplier differs from the traditional deposits-to-reserves ratio. What matters is not only the total amount of deposits issued by a bank but also the liquidity property of assets funded by deposits. Issuing deposits to acquire liquid assets is not liquidity transformation and therefore is not subject to the liquidity constraint, because payment outflows can be covered by selling the newly acquired liquid assets. In contrast, issuing deposits to fund loans requires the bank to have other (liquid) assets that buffer payment outflows because the loans are illiquid.

The money multiplier in equilibrium depends crucially on the liquidity churn among banks. In the second scenario of interbank payment, the payment sender's bank loses reserves while the recipient's bank gains reserves and sees its liquidity constraint relaxed. In response, it may decide to fund new loans by issuing deposits. Some of these deposits are then used in payment, sent to

[1] Money creation through bank lending was a popular theme in the classic literature (e.g., Wicksell, 1907; Schumpeter, 1954; Gurley and Shaw, 1960; Tobin, 1963). A growing literature revisits it (e.g., Gersbach, 1998; Cavalcanti and Wallace, 1999; Kiyotaki and Moore, 2002; Kahn and Roberds, 2007; Gu et al., 2013; Brunnermeier and Sannikov, 2016; Piazzesi and Schneider, 2016; Donaldson et al., 2018; Parlour et al., 2020; Bianchi and Bigio, 2022).

other banks alongside with reserves. This process results in a ripple effect of liquidity percolation. Such liquidity churn is large in magnitude: the average weekly volume of depositors' interbank payments in Fedwire—the primary payment settlement system in the U.S.—exceeds GDP.

In summary, banks are concerned about liquidity loss when financing lending with deposits but liquidity inflows from other banks relax the liquidity constraint. The problem is that when banks make decisions, they do not internalize the liquidity spillover to other banks as a result of their depositors paying depositors at other banks. This liquidity spillover effect leads to strategic complementarity: a bank will extend more loans funded by deposits when it receives payment inflows that in turn result from the rest of the banking sector extending loans funded by deposits.

We develop a structural model that captures banks' lending decisions in the presence of payment-induced liquidity externalities. Built upon insights from recent studies on payment and banking (e.g., Piazzesi and Schneider, 2016; Donaldson et al., 2018; Parlour et al., 2020; Bianchi and Bigio, 2022), our paper takes a step forward by modeling the structure of payment flows and estimating the network externality. A bank's decision to fund loans with deposits depends on the net interest margin, its liquid assets, and, importantly, its position in the payment network that determines its liquidity risk and liquidity spillover to other banks. Liquidity transformation capacity of the banking sector depends on topology of the entire network. When estimating the model, we map out the network using data from Fedwire. We find that strategic complementarity from payment externality amplifies the volatility of bank credit supply. By analyzing network topology, we identify systemically important banks that drive aggregate fluctuation.

Our paper revisits several classic concepts in monetary economics. Bank lending and liquidity percolation via payment are known to be the key ingredients of money multiplier, but little has been done in the modern literature to formalize the mechanism. Rather than relying on a binding reserve requirement, our model of money multiplier emphasizes banks' liquidity constraint that emerges from depositors' random payment needs, liquidity transformation in banks' choice of financing loans with deposits (inside money creation), liquidity redistribution in the payment system, and strategic complementarity in banks' decision to create credit and money.

Money velocity is a core ingredient in the literature on money demand theories (e.g., Alvarez et al., 2009). We focus on inside money supply: a higher velocity means more payments and greater liquidity risk for banks but also recycles liquidity faster among banks, so our structural model quantifies the overall impact on the equilibrium money multiplier and banks' money creation (deposit issuance) through lending. Moreover, when liquidity churns faster, strategic complemen-

tarity strengthens, making the system more sensitive to shocks. Our paper differs from studies on payment and bank liquidity shocks (e.g., Bianchi and Bigio, 2022) in its network perspective on money velocity and results on banks that are systemically important for shock propagation.

Recent studies on monetary assets focus on quantities and prices (or "liquidity premium"). Along the tradition of liquidity preference (Keynes, 1936; Baumol, 1952; Tobin, 1956; Sidrauski, 1967), much progress has been made in reviving money demand functions (e.g., Alvarez and Lippi, 2009; Krishnamurthy and Vissing-Jørgensen, 2012; Lucas and Nicolini, 2015; Nagel, 2016). On the supply side, it has been shown that banks play an important role in supplying monetary assets, earning liquidity premium (e.g., Krishnamurthy and Vissing-Jørgensen, 2015; Brunnermeier and Sannikov, 2016; Drechsler et al., 2018; Begenau, 2020; Piazzesi et al., 2019). Our paper goes beyond quantities and prices. By analyzing the circulation of inside money (deposits) among depositors at different banks and the resultant network of interbank flows, our approach highlights the defining feature of monetary assets—means of payment.

After the global financial crisis, banks have held a large quantity of reserves. Many hold the belief that banks are satiated with liquidity. However, evidence shows that reserve shortage still happens (Correa et al., 2020; Copeland et al., 2021; d'Avernas and Vandeweyer, 2021; Acharya et al., 2022; Afonso et al., 2022; Yang, 2022; Lopez-Salido and Vissing-Jørgensen, 2023). Our findings further this line of research by showing how payment-induced redistribution of liquidity across banks affects the supply of bank credit by allowing liquidity to be recycled.

Next, we explain the model setup and summarize the main findings from our structural estimation. The model has N banks, each endowed with reserves. A bank chooses the amount of loans funded by deposits; afterwards, its depositors make payments, which result in a random fraction of deposits flowing to other banks, draining reserves. Deposit and loan rates are endogenous and depend on the amounts of loans and deposits. The bank incurs an increasing and convex (quadratic) cost of reserve loss. It is costly to lose liquid assets that serve as precautionary savings or be used for regulatory and other purposes. Moreover, it is costly to replenish liquidity through interbank borrowing or other sources of external funds.[2] The bank also receives reserve inflows as a result of the other banks financing loans with deposits and their depositors making payments.

Therefore, banks are interconnected through depositors' payments. Payment flows churns

[2]If interbank markets operate frictionlessly, a bank in surplus can lend to a bank in deficit, costlessly reversing payment shocks (Bhattacharya and Gale, 1987). Therefore, our work builds on the literature on interbank market frictions (e.g., Afonso and Lagos, 2015; Bigio and Sannikov, 2019). The freeze of interbank market can be interpreted as strong convexity in the cost of reserve loss.

liquidity among banks. Under the increasing marginal cost of reserve loss, such liquidity churn makes banks' decisions to fund loans with deposits strategic complements. When one bank extends loans funded by deposits, its depositors' payment to other banks' depositors brings reserves to other banks. With more reserves, the other banks' marginal cost of reserve loss declines, so they are more willing to fund new loans with deposits.

In our model, money velocity manifests itself in a random graph of interbank payment flows that are directed by depositors and out of banks' control. For a single bank, such payment risk is a form of funding instability risk and constrains the elasticity of its balance sheet.[3] Beyond liquidity risk, payment also generates liquidity externality. When one bank expands its balance sheet, financing lending with deposits, it does not internalize the liquidity spillover that benefits its neighboring banks and relaxes their liquidity constraint. In equilibrium, bank i's lending depends on bank j's lending through a network-effect parameter, ϕ_i and the ij-th element of a network adjacency matrix that incorporates the first and second moments of pairwise payment flows between banks. The distribution of parameter ϕ_i is a key object of interest in our estimation. The larger its value is, the stronger the strategic complementarity is in banks' decision to finance lending with deposits.

Our model is a quadratic network game (Galeotti et al., 2010; Jackson and Zenou, 2015), and its equilibrium conditions map to a spatial model (Lee et al., 2010; de Paula, 2017; Redding and Rossi-Hansberg, 2017), which is common in the social interaction literature (e.g., Glaeser and Scheinkman, 2000; Ballester et al., 2006; Graham, 2008; Calvó-Armengol et al., 2009; Bramoullé et al., 2009; Blume et al., 2015) and has been recently adopted in financial economics (Cohen-Cole et al., 2014, 2015; Ozdagli and Weber, 2017; Herskovic, 2018; Lu and Luo, 2019; Herskovic et al., 2020; Denbee et al., 2021; Jiang and Richmond, 2021; Eisfeldt et al., 2022, 2023). Our equilibrium structure embeds the vast information of Fedwire payment flows in a network adjacency matrix, which includes the first and second moments of bank-pair level flows, and relates this network to banks' choices of lending funded by issuing deposits.

The equilibrium has another attractive feature, a two-step structure: first, we solve a bank's network-independent level of lending—that is, the bank's optimal choice should it be isolated from other banks; second, the network amplification mechanism works as an operator (formed by ϕ_i and

[3]Payment risk is distinct from run risk (Li and Li, 2021): depositors move money out of a bank to make payments, not out of concerns over the bank's solvency. Payment risk matters in normal times and applies to all deposits including insured deposits. The empirical banking literature has largely focused on run risk (e.g., Gorton, 1988; Calomiris and Mason, 1997; Iyer and Puri, 2012; Martin et al., 2018; Brown et al., 2020; Artavanis et al., 2022).

the adjacency matrix) which we apply to network-independent lending to obtain the equilibrium level of bank lending funded by deposits.

When estimating the model, our focus is on characterizing the network operator. We treat banks' network-independent lending as random variables that encapsulate banks' available reserves, shocks, and potentially other characteristics, and directly estimate their distributional properties (means and variances).[4] This approach allows us to stay agnostic about the amount of available reserves, which is empirically challenging to define. A bank may sell other assets for reserves, so available reserves depend on other assets' secondary-market liquidity are. The bank may also rely on external financing. Finally, the bank may hold reserves for different purposes, which implies the available reserves for covering payment outflows can be smaller than its reserve holdings.

We use simulated ML to estimate the mean and the variance of ϕ_i. The estimate of the mean is large in magnitude, which implies that the strategic complementarity is strong and the interbank payment network works as a shock amplification mechanism. Consider a positive shock that triggers all banks to extend loans funded by deposits. The neighboring banks, connected through depositors' payment flows, respond by further expanding balance sheets and thereby trigger another round of shock propagation. The network amplifies shocks by 23.4%. Accounting for network increases the R^2 in the regressions of lending on liquidity and NIM variables.

To address the concerns related to omitted variables, we consider an alternative network where banks are connected by the distance between their headquarters. Such a network does not depend on payments and only reflects geographic proximity and shared clients. We find no evidence for a positive network multiplier in this case.

To demonstrate the importance of network topology, we compare the mean and volatility of aggregate credit supply in equilibrium with those solved under a hypothetical network where banks are equally connected (payment flows are evenly distributed among bank pairs). Both networks amplify shocks. While the uniform network generates a slightly higher expected lending supply, the two networks significantly differ in volatility—the volatility from the real network of Fedwire payment flows is 20% higher.

Following Diebold and Yılmaz (2014), we decompose the volatility of aggregate credit supply into individual banks' contributions and develop a metric of systemic risk.[5] A bank's contribu-

[4]The shock to each bank can be interpreted as anything that contributes to the randomness of network-independent lending, such as shocks to net interest margin, regulatory cost, available reserves, etc.

[5]Our payment-based systemic risk metric adds to the literature (e.g., Billio et al., 2012; Acharya et al., 2016; Adrian and Brunnermeier, 2016; Benoit et al., 2016; Bai et al., 2018; Duarte and Eisenbach, 2021; Greenwood et al., 2015).

tion depends on the network amplification operator, which summarizes the routes of shock propagation via the payment linkages, and the volatility of its network-independent level of lending. We find that less than 20% of banks contribute to more than 90% of credit-supply volatility. We also show that the shocks propagate from the tightly-connected banks to the banks in the periphery.

Finally, we quantify the network externalities. In contrast to the market equilibrium, the planner's choice of bank lending internalizes the interbank liquidity spillover from depositors' payments. Therefore, by comparing the market equilibrium against the planner's solution, we demonstrate the impact of payment network externalities on bank lending. The market equilibrium generates a higher lending volatility and lower expected lending volume. In addition, the market equilibrium features stronger bank-level heterogeneity in expected lending and volatility. Under relationship lending, some borrowers cannot easily switch banks. Inefficiency arises from bank-borrower mismatch. For example, a borrower who prefers stable credit may be matched with a bank whose lending is volatile. Banks' lending volatility and expected level both depend on their locations in the payment network. In our setting, the bank-borrower mismatch is essentially between the bank's lending opportunities (i.e., the matched borrowers) and the payment characteristic of its deposits.

2 Model

2.1 The setup

There are N banks and three dates, $t = 0$, 1, and 2. We set up the model by describing bank i's problem. Bank i, $i \in \{1, ..., N\}$, has reserves, m_i, contributed by its owners (i.e., the equity investors or shareholders). At $t = 0$, bank i chooses y_i, the amount of loans financed by deposits and earns a net interest margin

$$(R_i - r_i + \varepsilon_i)y_i, \tag{1}$$

where the loan rate, R_i, and deposit rate, r_i, can be bank i-specific, depending on the characteristics of bank i and its customers, and ε_i represents a shock to bank i's profits that is realized before $t = 0$.[6] After solving the equilibrium, we will show that how the shock enters can be flexible.

The goal of our analysis is two-fold. First, we characterize the link between liquidity base,

[6]The shock can be related to credit demand, which in turn depends on collateral value and profitability of borrowers' projects, or shocks on the credit-supply side, for example, bank i's regulatory cost of expanding balance sheet.

m_i, and the equilibrium level of liquidity transformation, y_i, i.e., loans funded by deposits. Our second goal is to examine how ε_i is propagated and amplified in the banking system when depositors' payment flows generate interconnectedness between banks.

We can allow R_i and r_i to be dependent on y_i, the amount of lending and deposit issuance, to capture the elasticity of loan demand and deposit demand and the bank's market power. Specifically, as in the classic Klein-Monti model, we define the demand for bank i's loans as

$$y(R_i) = a_{L,i} - 2b_{L,i}R_i, \tag{2}$$

where $b_{L,i} > 0$, and the demand for deposits at bank i as

$$y(r_i) = a_{D,i} + 2b_{D,i}r_i, \tag{3}$$

where $b_{D,i} > 0$. The bank maximizes profits, i.e., $[R(y_i) - r(y_i) + \varepsilon_i]y_i$, with the following optimality condition for the choice of y_i:

$$R_i - r_i = \frac{a_{L,i}}{2b_{L,i}} + \frac{a_{D,i}}{2b_{D,i}} + \varepsilon_i - \left(\frac{1}{b_{L,i}} + \frac{1}{b_{D,i}}\right) y_i = a_i - b_i y_i + \varepsilon_i \,. \tag{4}$$

At $t = 1$, depositors at different banks make payments to one another. Let g_{ij} denote the fraction of bank i's deposits paid to depositors at bank j ($j \neq i$) by bank i's depositors. We define

$$z_i \equiv \sum_{j \neq i} g_{ij} y_i, \tag{5}$$

the total reserve and deposit outflow from bank i to other banks. Payment flows are risky: g_{ij} is random with mean μ_{ij} and variance σ_{ij}^2, and g_{ij} is out of bank i's control as the bank cannot interfere with depositors' payment decisions. Bank i transfers reserves, z_i, to the payment recipients' banks and deducts the corresponding amount of deposits, shrinking balance sheet, while the recipients' banks receive reserves and credit the recipients' deposit accounts with deposits, expanding balance sheets. On the liability side of balance sheet, a random fraction $\sum_{j \neq i} g_{ij}$ of deposits mature at $t = 1$ while the rest mature at $t = 2$.[7] The loans on asset side are illiquid and held until $t = 2$. At $t = 1$, bank i relies on reserves, m_i, to cover liquidity outflow. Therefore, its ability to

[7] As in Bolton et al. (2020), deposits are essentially debts with random maturities.

finance lending with deposits and its choice of y_i at $t = 0$ depends on m_i. We broadly interpret m_i to include both reserves and other liquid assets that can be readily sold to cover payment outflows.

At $t = 1$, bank i experiences liquidity inflows that result from other banks' depositors making payments to bank i's depositors. From bank j, bank i receives payment inflows equal to $g_{ji}y_j$, where g_{ji} has mean μ_{ji} and variance σ^2_{ji}. The correlation between g_{ij} and g_{ji} is denoted by ρ_{ij}.[8]

Bank i's cost of covering payment outflow at $t = 1$ is specified as follows:

$$\tau_1 \left(z_i - \sum_{j \neq i} g_{ji} y_j - m_i \right) + \frac{\tau_2}{2} \left(z_i - \sum_{j \neq i} g_{ji} y_j - m_i \right)^2 + \frac{\kappa}{2} z_i^2 \,, \tag{6}$$

where $z_i - \sum_{j \neq i} g_{ji} y_j - m_i$ is the liquidity shortfall and $\tau_1 > 0$, $\tau_2 > 0$, and $\kappa > 0$. This quadratic form will lead to a set of linear equilibrium conditions that map to the well-known empirical framework of spatial models (Anselin, 1988; Lee et al., 2010; de Paula, 2017). This modeling approach follows the literature on social interaction (Glaeser and Scheinkman, 2000; Ballester et al., 2006; Graham, 2008; Calvó-Armengol et al., 2009; Bramoullé et al., 2009; Galeotti et al., 2010; Blume et al., 2015; Jackson and Zenou, 2015) and recent applications in financial economics (Cohen-Cole et al., 2014, 2015; Ozdagli and Weber, 2017; Herskovic, 2018; Lu and Luo, 2019; Herskovic et al., 2020; Denbee et al., 2021; Jiang and Richmond, 2021; Eisfeldt et al., 2022, 2023). We add $\frac{\kappa}{2} z_i^2$ because netting may not happen instantaneously, so gross outflow adds liquidity stress.[9] We only need to add a quadratic form of z_i because a linear coefficient of z_i will be absorbed by τ_1.

Our model is built upon the assumption that interbank market is imperfect. If banks that experience payment inflows lend to banks that experience outflows freely and at zero interest rate, banks are no longer concerned about the interbank payment flows, facing τ_1, τ_2, and κ all equal to zero in (6) and (8). To simplify the notations, we define the *net* payment outflow for bank i:

$$x_i = z_i - \sum_{j \neq i} g_{ji} y_j = \sum_{j \neq i} g_{ij} y_i - \sum_{j \neq i} g_{ji} y_j \,, \tag{7}$$

If $x_i - m_i > 0$, the first two terms in (6) captures an increasing and convex cost of interbank

[8] We would expect $\rho_{ij} < 0$ if economic activities are directional, involving mainly bank i's customers paying j's customers. The correlation ρ_{ij} can also be positive if bank i's customers' payments to j's customers stimulate economic activities between the two depositor clienteles and result in j's customers making payments to i's customers.

[9] A large literature studied the intraday payment stress (Poole, 1968; Afonso, Kovner, and Schoar, 2011; Ashcraft, McAndrews, and Skeie, 2011; Ihrig, 2019; Copeland, Duffie, and Yang, 2021; d'Avernas and Vandeweyer, 2021; Afonso, Duffie, Rigon, and Shin, 2022; Yang, 2022). Kahn and Roberds (2009) review the studies on payment system.

borrowing. The convexity, as microfounded in Bigio and Sannikov (2019) and Parlour, Rajan, and Walden (2020), reflects the impact of interbank market frictions (Afonso and Lagos, 2015).[10] When $x_i - m_i < 0$, this quadratic form presents an increasing and concave return on interbank lending, and the concavity is again due to the attribution from interbank market frictions.

Typically, a bank's daily payment outflow is below its total stock of liquid assets. Thus, it is important to clarify the empirical counterpart of m_i. In our model, m_i represents liquid assets that bank i allocates towards buffering payment outflows; in other words, the bank may hold liquidity beyond m_i, but only a part of it is for covering payment outflows, while the rest are held for other reasons, such as liquidity needs from non-payment activities and investment opportunities that rely on internal funds. Payment-induced liquidity shortfall can potentially be covered by repurposing liquidity from other uses, and the associated cost is also captured by the quadratic form (6).

Incorporating both the net interest margin given by (1) and the liquidity cost from depositors' payment activities given by (6), we have the net profits for bank i:

$$R_i y_i - r_i y_i + \varepsilon_i y_i - \tau_1 \left(z_i - \sum_{j \neq i} g_{ji} y_j - m_i \right) - \frac{\tau_2}{2} \left(z_i - \sum_{j \neq i} g_{ji} y_j - m_i \right)^2 - \frac{\kappa}{2} z_i^2. \quad (8)$$

The first two terms of payment liquidity cost capture an increasing and convex cost of y_i. Note that y_i enters the payment liquidity cost via z_i (see (5)). The liquidity buffer, m_i, reduces the marginal cost of increasing y_i, suggesting a link exists between liquid assets, m_i, and bank i's optimal level of liquidity transformation (lending funded by deposits), y_i. In other words, when choosing y_i, bank i essentially faces a liquidity constraint: m_i is needed to buffer payment outflows.

Strategic complementarity emerges: An increase in y_j reduces bank i's marginal cost of y_i. This is the key force that we aim to capture in through the model and to quantify through our structural estimation. Intuitively, when bank j expands balance sheet by extending loans funded by deposits, it generates liquidity spillover to bank i through its depositors' payments to bank i's depositors. Such liquidity spillover relaxes the liquidity constraint on bank i's choice of y_i. A previously studied channel that also appears in our model is related to endogenous rates (Drechsler et al. (2017, 2021)). If NIM becomes more sensitive to changes in lending flows, banks lose their deposit franchise value advantage. As a result, the strategic complementarity motive declines.

In sum, when extending loans funded by deposits, individual banks face potential liquidity

[10] Banks may also borrow from the central bank but face the stigma effect (Copeland, Duffie, and Yang, 2021).

loss due to depositors' payment outflows and have to rely on their liquid assets. However, when depositors at different banks transact with one another, one bank's payment outflow is another bank's inflow. Such liquidity churn within the system relaxes individual banks' liquidity constraint.

Such liquidity spillover effect is not internalized in individual banks' choice of y_i, and the strength of such externality depends on the network structure of payment flows. Moreover, the liquidity spillover induces strategic complementarity in banks' choice of y_i, which may amplify the response of the banking system to individual banks' shock to net interest margin, ε_i.

So far, we have focused on bank i's liquidity needs captured by the quadratic cost (6). Next, we consider depositors' liquidity needs. When depositors incur large expenses (z_i is large), they face difficulty in managing liquidity.[11] Bank i may generate profits from extending lines of credit:

$$\theta_1 \left(z_i - \sum_{j \neq i} g_{ji} y_j \right) + \frac{\theta_2}{2} \left(z_i - \sum_{j \neq i} g_{ji} y_j \right)^2 = \theta_1 x_i + \frac{\theta_2}{2} x_i^2 \,. \tag{9}$$

Appendix B lays out the microfoundation. The first term captures depositors' liquidity loss, with $\theta_1 > 0$. The second term capture the increasing marginal impact: as depositors lose more liquidity, they are willing to pay more for lines of credit, which implies $\theta_2 > 0$.[12] The deposit base, y_i, enters via z_i with the coefficient equal to the fraction of deposits spent (see the definition of z_i in (5)). The profits increase in y_i but the marginal profits decrease in y_j. When bank i's depositors receive payment inflow, $g_{ji} y_j$, from bank j's depositors, they have more liquidity and are less willing to pay for bank i's lines of credit. This generates strategic substitution in banks' choices of y_i and counteracts the force of strategic complementarity from the payment liquidity cost given by (6).

An alternative interpretation of (9) is regulatory cost (Baron, 2020). Deposit inflows force banks to raise leverage and tighten the regulatory constraint on leverage, for example, the supplementary leverage ratio (SLR) requirement. When the constraint binds, the bank may be forced to raise costly equity (Bolton et al., 2020). Deposit outflow, z_i, alleviates the regulatory pressure by deleveraging the bank. Under this interpretation, θ_1 is positive, but the sign of θ_2 is unclear so we allow both positive and negative. The goal of incorporating (9) is to acknowledge different forces that may counteract or compound the channel of bank liquidity management captured through (6).

[11] For example, firms invest in inventory to boost sales but may not get paid in time by their customers, thus overstretching the cash conversion cycle. Households may incur large expenses before their payday.

[12] The increasing marginal value of liquidity arises in both static settings (see Appendix B) and dynamic settings (Riddick and Whited, 2009; Bolton, Chen, and Wang, 2011; Décamps, Mariotti, Rochet, and Villeneuve, 2011).

It is assumed that the revenues and costs in (1), (6), and (9) are all time-zero values. At $t = 0$, bank i chooses y_i to maximize the following expected profits:

$$\max_{y_i} \mathbb{E}\left[(R_i - r_i + \varepsilon_i)y_i - \tau_1(x_i - m_i) - \frac{\tau_2}{2}(x_i - m_i)^2 - \frac{\kappa}{2}z_i^2 + \theta_1 x_i + \frac{\theta_2}{2}x_i^2\right].^{13} \tag{10}$$

Several observations are in order. The expectation is taken over the randomness in g_{ij}, not ε_i that is known at $t = 0$. The spread between the loan and deposit rates can depend on y_i as we show in (4). Endogenizing rates helps to capture the banks' deposit franchise value. The net interest margin may be viewed as already reflecting an exogenous risk adjustment and henc constitutes a risk-adjusted return for the bank. This is without loss of generality, as long as the systematic shocks to loan return, driven by macroeconomic factors, are orthogonal to the randomness in interbank payment flows. Finally, our focus is on banks' normal-time operations, not crises or runs. We assume that even when the realized payment flows cause the maximum loss (which is finite since g_{ij} is bounded in $[0, 1]$), the bank's profits remain positive. Thus, a bank is always solvent.

Our model differs from the classic banking model in Diamond and Dybvig (1983). In our model, one bank's loss of deposits and reserves is another bank's gain. We model payment between depositors at different banks and emphasize the interconnectedness from payment flow and its network structure; in contrast, Diamond and Dybvig (1983) model depositors' cash withdrawal that does not lead to bank interconnectedness. Moreover, Diamond and Dybvig (1983) analyze bank run, while in our model, liquidity risk is solely from the role of deposits as means of payment.

Discussion: Money creation, liquidity transformation, and other assets and liabilities. When extending loans, a bank acquires borrowers' debts (loans) and issues debts (deposits) that borrowers can use as money. This practice has been adopted throughout the history of banking.[14] After obtaining the loan, the borrower may hold the newly issued deposits in her account at the lending bank or transfer the newly issued deposits to a depositor at the same bank. In both cases, the lending bank does not lose deposits. If the borrower transfers deposits to her account at another bank or pays a depositor at another bank, the lending bank loses deposits and must transfer reserves to

[13] The following parameter restriction ensures concavity in y_i: $\tau_2 + \kappa > \theta_2$.

[14] There is a classic literature and a growing modern literature on this topic (e.g., Gurley and Shaw, 1960; Tobin, 1963; Gersbach, 1998; Cavalcanti and Wallace, 1999; Kiyotaki and Moore, 2000, 2002; Kahn and Roberds, 2007; Gu et al., 2013; McLeay et al., 2014; Hart and Zingales, 2014; Quadrini, 2017; Brunnermeier and Sannikov, 2016; Piazzesi and Schneider, 2016; Donaldson et al., 2018; Wang, 2019; Parlour et al., 2020; Bianchi and Bigio, 2022).

the bank that receives the deposits, shrinking its balance sheet on both the asset and liability sides.

Liquidity transformation takes place the moment a bank extends loans at $t = 0$ because the bank may lose deposits at $t = 1$ before loans mature at $t = 2$. The bank can adjust capital structure after payment shocks (i.e., after g_{ij} and g_{ji} are realized). For example, the bank rebuilds its holdings of liquid assets by raising funds from bond or equity investors. The associated financing costs are captured through the cost of liquidity loss (6). A bank's capacity to create money (issue deposits) through lending is constrained by the amount of liquid assets it has to cover the potential deposit outflow, as the new loans are illiquid. In contrast, issuing deposits to purchase liquid assets is not constrained, as those newly acquired assets can be readily sold to cover deposit outflows.

To sum up, we model bank loans funded by deposit issuance, y_i, in line with the practice in banking and characterize the link between m_i, the liquidity base, and y_i. We do not model banks acquiring liquid assets with deposits as it is not liquidity transformation and is not constrained by m_i. On the asset side of balance sheet, we focus on loans. On the liability side, we do not explicitly model other bonds or equity, but allow these instruments to be used as costly sources of liquidity.

2.2 Equilibrium

We solve bank i's optimal choice of y_i, given other banks' choices, y_j ($j \neq i$). To simplify the notations, we introduce the mean of gross payment outflows as a fraction of y_i:

$$\overline{\mu}_{-i} \equiv \mathbb{E}\left[\sum_{j\neq i} g_{ij}\right], \tag{11}$$

and the variance of gross payment outflows as a fraction of y_i:

$$\overline{\sigma}^2_{-i} = \mathrm{Var}\left(\sum_{j\neq i} g_{ij}\right). \tag{12}$$

We derive the following first-order condition for y_i:

$$\begin{aligned} R_i - r_i + \varepsilon_i - b_i y_i = {} & (\tau_1 - \theta_1)\overline{\mu}_{-i} + y_i(\kappa + \tau_2 - \theta_2)(\overline{\sigma}^2_{-i} + \overline{\mu}^2_{-i}) - \tau_2 \overline{\mu}_{-i} m_i \\ & - (\tau_2 - \theta_2)\sum_{j\neq i}(\overline{\mu}_{-i}\mu_{ji} + \rho_{ij}\sigma_{ij}\sigma_{ji})y_j \end{aligned} \tag{13}$$

The net interest margin is adjusted for the bank's loan and deposit market power via the term, $-b_i y_i$, and is equal to the marginal cost associated with depositors' payment activities. The first two terms on the right side depend on the first and second moments of payment outflows, and the third term reflects the fact that having more liquid assets, m_i, reduces the marginal cost of liquidity loss. In the last term, $\overline{\mu}_{-i}\mu_{ji}y_j$ shows that if bank i experiences more outflow ($\overline{\mu}_{-i}$), the inflow from bank j (μ_{ji}) becomes more valuable. We call this term *liquidity externality* following Parlour et al. (2020). The other component is the covariance between g_{ij} and g_{ji}, $\rho_{ij}\sigma_{ij}\sigma_{ji}$. This *hedging externality* represents a form of risk sharing on the network (Eisfeldt et al., 2022).[15] A negative correlation, $\rho_{ij} < 0$, dampens the peer effect, while a positive correlation amplifies it.

Rearranging the first-order condition (13), we solve the optimal y_i:

$$y_i^* = \phi_i \sum_{j \neq i} w_{ij} y_j^* + a_i, \tag{14}$$

where the network attenuation factor, ϕ_i, is given by

$$\phi_i = \frac{\tau_2 - \theta_2}{\kappa + \tau_2 - \theta_2 + \bar{b}_i}, \tag{15}$$

with $\bar{b}_i = b_i(\overline{\sigma}_{-i}^2 + \overline{\mu}_{-i}^2)^{-1}$, and the ij-th element of the network adjacency matrix, $\mathbf{W}$, is given by

$$w_{ij} = \frac{\overline{\mu}_{-i}\mu_{ji} + \rho_{ij}\sigma_{ij}\sigma_{ji}}{\overline{\sigma}_{-i}^2 + \overline{\mu}_{-i}^2}, \tag{16}$$

a_i is the optimal y_i without peer effect, i.e., the solution under $g_{ji} = 0$, $j \neq i$.

Note that in the case of a fixed R_i and r_i (i.e., in the absence of loan and deposit market power), the network attenuation factor is no longer bank-dependent:

$$\phi = \frac{\tau_2 - \theta_2}{\kappa + \tau_2 - \theta_2}. \tag{17}$$

Since $\bar{b}_i > 0$, ϕ_i is less than ϕ, which indicates that the peer effect tends to be weaker in the absence of banks' loan and deposit market power. This case of homogeneous ϕ turns out to be econometrically much more tractable. It can be estimated with the standard maximum likelihood estimation (MLE) approach and will serve as a baseline case for comparison with the model under

[15] In our derivation, g_{ij} is assumed to be uncorrelated with g_{ki} ($k \neq j$), consistent with our data.

heterogeneous ϕ_i that is estimated with simulated ML. When implementing the simulated ML, we consider ϕ_i as drawn from a Normal distribution and estimate the distribution's mean and variance. The estimated mean is close to the MLE estimate of the homogeneous ϕ.

The overall peer effect depends on $\phi_i w_{ij}$, the attenuation factor, ϕ_i, and the ij-th element of the adjacency matrix. If $\phi_i w_{ij} > 0$ (< 0), strategic complementarity (substitution) dominates. As will be shown later, in our sample, there are only 0.39% of non-zero w_{ij} that are negative. Therefore, whether the pair $\{i, j\}$ exhibits strategic complementarity or substitution depends on the sign of ϕ_i. As previously discussed, an increase in y_j has two opposing implications on bank i's choice of y_i. First, bank i receives liquidity inflows as its depositors receive payment from bank j's depositors; with a larger liquidity buffer, the marginal cost of liquidity loss declines, so bank i increases y_i. Second, the payment inflows to bank i's depositors also bring these depositors liquidity, so they rely less on bank i for liquidity provision (and thus there are fewer opportunities for bank i to profit from depositors' liquidity needs). Moreover, deposit inflow can push the bank against regulatory constraints on leverage. Therefore, when y_j increases, bank i can be less interested in raising deposits against loans. If $\tau_2 > \theta_2$ ($\phi_i > 0$), the first force dominates, and strategic complementarity emerges: y_i is increasing in y_j. The expected payment flow from j to i, μ_{ji}, is valuable especially when bank i's expected outflow, $\overline{\mu}_{-i}$, is large. If $\tau_2 < \theta_2$ ($\phi_i < 0$), the second force dominates, and strategic substitution emerges: Bank i is averse to payment inflows from j.

Proposition 1 *Suppose the network feedback is stable in the sense that*

$$\rho(\Phi \mathbf{W}) < 1, \tag{18}$$

where $\rho(\cdot)$ denotes the spectral radius and Φ is a diagonal matrix where the diagonal is populated with $\boldsymbol{\phi} = (\phi_1, \ldots, \phi_N)^\top$. Then there exists a unique interior Nash equilibrium outcome given by

$$y_i^* = \{\mathbf{M}(\Phi, \mathbf{W})\}_{i.} \mathbf{a}, \tag{19}$$

where $\mathbf{I}$ is the $N \times N$ identity matrix, $\{\}_{i.}$ returns the i-th row of its argument, and

$$\mathbf{M}(\Phi, \mathbf{W}) \equiv \sum_{k=0}^{\infty} (\Phi \mathbf{W})^k = \mathbf{I} + \Phi \mathbf{W} + (\Phi \mathbf{W})^2 + (\Phi \mathbf{W})^3 + \ ... = (\mathbf{I} - \Phi \mathbf{W})^{-1} \ . \tag{20}$$

The i-th element of the $N \times 1$ column vector $\mathbf{a}$, $\{\mathbf{a}\}_i = a_i$, records bank i's optimal choice of y_i

under $g_{ji} = 0$. a_i *satisfies* $\frac{da_i}{dm_i} > 0$, $\frac{d^2a_i}{dm_i d\bar{\mu}_{-i}} > 0$, $\frac{da_i}{d\tau_1} < 0$, $\frac{d^2a_i}{d\tau_1 d\bar{\mu}_{-i}} < 0$, $\frac{da_i}{d\bar{\sigma}^2_{-i}} < 0$, *and* $\frac{da_i}{d\varepsilon_i} > 0$.

Proposition 1 summarizes the equilibrium solution. In vector form, we can rewrite (19) as

$$\mathbf{y}^* = \mathbf{M}(\Phi, \mathbf{W})\,\mathbf{a} = (\mathbf{I} - \Phi\mathbf{W})^{-1}\,\mathbf{a}\,. \tag{21}$$

The stability condition $\rho(\Phi\mathbf{W}) < 1$ states that network externalities must be small enough to prevent feedback triggered by spillover effects from escalating without bounds.[16] Proposition 1 characterizes the link between m_i, the liquidity base, and y_i, the equilibrium level of liquidity transformation and shows how the shocks to individual banks, ε_i, are propagated in the system. Note that it is sufficient to prove that Proposition 1 holds under the homogeneous ϕ given by (17), since for any i, $\phi_i \leq \phi$ under $\bar{b}_i > 0$.[17] In the case of homogeneous ϕ, the stability condition would be $|\phi\lambda^{\max}(\mathbf{W})| < 1$ where the function $\lambda^{\max}(\cdot)$ returns the largest eigenvalue.

The equilibrium multiplier that links m_i to y_i has a two-step structure: First, the liquidity base, m_i, enters into a_i; then the network operator, $\mathbf{M}(\Phi, \mathbf{W})$, is applied to a_i, accounting for the interconnectedness between banks. The properties of a_i are intuitive. The liquidity base, m_i, contributes to "network-independent" lending financed by deposits, $\frac{da_i}{dm_i} > 0$, because it buffers bank i's liquidity loss from payment outflows. When bank i expects more payment outflows, having liquid assets becomes more important, $\frac{d^2a_i}{dm_i d\bar{\mu}_{-i}} > 0$. In bank i's liquidity cost given by (6), τ_1 represents a baseline cost of borrowing reserves, which has a negative impact on bank lending, $\frac{da_i}{d\tau_1} < 0$, in line with the evidence (Jiménez et al., 2012, 2014). When bank i expects more liquidity loss, the negative impact of τ_1 is amplified, $\frac{d^2a_i}{d\tau_1 d\bar{\mu}_{-i}} < 0$. Finally, when bank i faces more payment liquidity risk, a_i becomes smaller, $\frac{da_i}{d\bar{\sigma}^2_{-i}} < 0$, in line with the findings in Li and Li (2021).

Proposition 1 also shows that bank i's shock, ε_i, enters into the equilibrium in two steps. First, it affects a_i, i.e., $\frac{da_i}{d\varepsilon_i} > 0$, and then the network operator, $\mathbf{M}(\Phi, \mathbf{W})$, is applied to a_i, and the shock impact is transmitted to the other banks. In our model setup, ε_i hits bank i's net interest margin before bank i chooses y_i at $t = 0$. In fact, we can be very flexible about how the shock is specified. Any source of randomness in a_i will be propagated through the system via the network operator, $\mathbf{M}(\Phi, \mathbf{W})$. For example, we may assume that a shock to a_i originates from a shock to bank i's liquidity buffer, m_i, rather than its net interest margin. When mapping the model to data,

[16] The Neumann series in (20) converges under $\rho(\Phi\mathbf{W}) < 1$; see, e.g., standard results on matrix power series convergence. The equilibrium definition is akin to that of Calvó-Armengol, Patacchini, and Zenou (2009).

[17] This means that if banks' optimality conditions form a contraction mapping under the fixed R_i and r_i, they still form a contraction mapping with a unique fixed point (equilibrium) under endogenous (y_i-dependent) R_i and r_i.

we shall treat a_i as a random variable that has an expected level and a random component:

$$a_i = \bar{\alpha}_i + \nu_i, \tag{22}$$

where ν_i has a zero mean and variance δ_i^2. We estimate the mean and volatility of a_i directly (in full sample and rolling windows) without unpacking the structure of a_i. Doing so has several advantages. Beyond a flexible interpretation of ε_i, we can stay agnostic about the empirical counterpart of m_i, as m_i enters y_i only through a_i. It is challenging to specify m_i empirically, as it depends on bank i's reserves, holdings of liquidity securities, liquidity that can be obtained by selling or pledging other assets, and liquidity from external sources (e.g., central bank liquidity facilities). It is also unclear how banks allocate liquidity between covering payment outflows and other activities.

When estimating and quantifying the model, our focus is on the network operator $\mathbf{M}(\Phi, \mathbf{W})$, which jointly captures network topology and heterogeneous network exposure. Define $\bar{\boldsymbol{\alpha}} = [\bar{\alpha}_1, \ldots, \bar{\alpha}_N]^\top$ and $\boldsymbol{\nu} = [\nu_1, \ldots, \nu_N]^\top$. Using (21), the equilibrium outcome can be written as

$$\mathbf{y}^* = \underbrace{\mathbf{M}(\Phi, \mathbf{W})\, \bar{\boldsymbol{\alpha}}}_{\text{level propagation}} + \underbrace{\mathbf{M}(\Phi, \mathbf{W})\, \boldsymbol{\nu}}_{\text{risk propagation}}. \tag{23}$$

The matrix $\mathbf{M}(\Phi, \mathbf{W})$ has a natural economic interpretation as a generalized network multiplier. It aggregates all direct and indirect links among banks, allowing for heterogeneous attenuation across nodes. Specifically, the diagonal matrix $\Phi = \mathrm{diag}(\boldsymbol{\phi})$ governs how strongly each bank transmits shocks through the network. As in Katz (1953), longer paths are penalized geometrically, but in our setting the rate of decay depends on the originating bank. Formally, the Neumann expansion in (20) implies that the identity matrix captures each bank's direct exposure to its own shock, the term $\Phi\mathbf{W}$ captures all direct network spillovers, $(\Phi\mathbf{W})^2$ captures spillovers transmitted through paths of length two steps, and so on. The (i, j) element of $\mathbf{M}(\Phi, \mathbf{W})$,

$$m_{ij}(\Phi, \mathbf{W}) \equiv \sum_{k=0}^{\infty} \left\{ (\Phi\mathbf{W})^k \right\}_{ij},$$

aggregates paths of one, two, and any k steps from bank j to bank i.

Multiplying the rows (columns) of $\mathbf{M}(\Phi, \mathbf{W})$ by a conformable unit vector yields the generalized indegree (outdegree) Katz–Bonacich centrality measures. The indegree centrality measure summarizes how strongly a bank loads on shocks originating elsewhere in the network, while the

outdegree centrality measure captures how strongly shocks originating at a given bank propagate to others. Accordingly, the i-th row of $\mathbf{M}(\Phi, \mathbf{W})$ reflects how bank i is exposed to the network as a whole, whereas the i-th column captures how the network as a whole loads on bank i.

The matrix $\mathbf{M}(\Phi, \mathbf{W})$ alone is not sufficient to determine a bank's systemic importance. Regardless of the network topology or propagation mechanism, banks subject to larger idiosyncratic shocks (higher δ_i^2) exert a larger influence on other banks and on aggregate lending, $Y = \sum_i y_i$. Moreover, the network does not only propagate shocks but also amplifies the impact of the level component $\bar{\boldsymbol{\alpha}}$. In Section 3.5, we show how to combine the equilibrium structure with our parameter estimates to empirically identify systemically important banks.

2.3 The planner's solution

We benchmark the market equilibrium against the planner's solution. We consider a planner that equally weights the objective of each bank and chooses $\{y_i\}_{i=1}^N$,

$$\max_{\{y_i\}_{i=1}^N} \mathbb{E}\left[\sum_{i=1}^{N}(R_i - r_i + \varepsilon_i)y_i - \tau_1(x_i - m_i) - \frac{\tau_2}{2}(x_i - m_i)^2 - \frac{\kappa}{2}z_i^2 + \theta_1 x_i + \frac{\theta_2}{2}x_i^2\right]. \quad (24)$$

We do not aim for welfare implications as the planner's objective only incorporates banks' profits instead of the total welfare of banks, borrowers, and depositors. The focus is on characterizing network externalities that emerge from payment flows. In addition, for this benchmark, we consider fixed R_i and r_i (i.e., the case of homogeneous ϕ under $b_i = 0$), which do not depend on y_i and thus does not reflect banks' loan and deposit market power, so that when the planner solves y_i, the only inefficiency she corrects is the liquidity externality induced by interbank payment flows.

The planner's first order condition for bank i's lending amount, y_i, yields:

$$\begin{aligned} R_i - r_i + \varepsilon_i =& y_i\left(\kappa + \tau_2 - \theta_2\right)\left(\overline{\sigma}_{-i}^2 + \overline{\mu}_{-i}^2\right) - \tau_2\overline{\mu}_{-i}m_i - \left(\tau_2 - \theta_2\right)\sum_{j\neq i}\left(\overline{\mu}_{-i}\mu_{ji} + \rho_{ij}\sigma_{ij}\sigma_{ji}\right)y_j \\ &+ y_i(\tau_2 - \theta_2)\overline{\sigma}_{-i}^2 - (\tau_2 - \theta_2)\sum_{j\neq i}(\overline{\mu}_{-j}\mu_{ij} + \rho_{ij}\sigma_{ij}\sigma_{ji})y_j \\ &+ (\tau_2 - \theta_2)\sum_{j\neq i}\left(\sum_{k\neq j}\mu_{kj}y_k\right)\mu_{ij} - \sum_{j\neq i}\tau_2 m_j\mu_{ij} \end{aligned} \quad (25)$$

The planner's marginal cost of bank i's lending is on the right side of (25). Its first three terms also

appear on the right side of first-order condition (13) in the market equilibrium, but the rest differ and reflect the planner internalizing spillover effects. First, bank i's costs or benefits associated with the expected outflow, $(\tau_1 - \theta_1)\overline{\mu}_{-i}$ in (13), disappear because, from the planner's perspective, bank i's expected outflow is the other banks' expected inflow and thus i's losses are offset by j's gains. Second, the new term, $y_i(\tau_2 - \theta_2)\overline{\sigma}^2_{-i}$, reflects the fact that when bank i lends more, it adds payment-flow risk not only to itself (via the first term on the right side of (25)) but also to its neighboring banks. Third, the fifth term, $-(\tau_2 - \theta_2)\sum_{j\neq i}(\overline{\mu}_{-j}\mu_{ij} + \rho_{ij}\sigma_{ij}\sigma_{ji})y_j$, captures the liquidity externality and hedging externality of bank i's lending on bank j ($j \neq i$). In particular, the liquidity externality of bank i's marginal lending (through the marginal outflow, μ_{ij}) has a stronger impact on bank j when j expected a large outflow $\overline{\mu}_{-j}$. The sixth term, $(\tau_2 - \theta_2)\sum_{j\neq i}(\sum_{k\neq j}\mu_{kj}y_k)\mu_{ij}$, shows that if bank j already receives inflows due to bank k's lending ($k \neq j$), the marginal impact of liquidity from bank i (i.e., μ_{ij}) is smaller. Finally, the last term shows that if bank j already has large reserve holdings, the marginal impact of liquidity from bank i is smaller.

Rearranging the planner's first-order condition (25), we solve the optimal y_i:

$$y_i = \widetilde{\phi}_i \sum_{j\neq i} \widetilde{w}_{ij} y_j - \widetilde{\phi}_i \sum_{j\neq i} \mu_{ij} \left(\sum_{k\neq j} \mu_{kj} y_k \right) + \widetilde{a}_i \tag{26}$$

where the network attenuation factor for bank i, $\widetilde{\phi}_i$, is given by,

$$\widetilde{\phi}_i = \frac{(\tau_2 - \theta_2)(\overline{\sigma}^2_{-i} + \overline{\mu}^2_{-i})}{(\kappa + \tau_2 - \theta_2)(\overline{\sigma}^2_{-i} + \overline{\mu}^2_{-i}) + (\tau_2 - \theta_2)\overline{\sigma}^2_{-i} + b_i} = \left(\frac{1}{\phi_i} + \frac{\overline{\sigma}^2_{-i}}{\overline{\sigma}^2_{-i} + \overline{\mu}^2_{-i}} \right)^{-1}, \tag{27}$$

the ij-th element of the network adjacency matrix, denoted by $\widetilde{\mathbf{W}}$, is given by

$$\widetilde{w}_{ij} = \frac{\overline{\mu}_{-i}\mu_{ji} + 2\rho_{ij}\sigma_{ij}\sigma_{ji} + \overline{\mu}_{-j}\mu_{ij}}{\overline{\sigma}^2_{-i} + \overline{\mu}^2_{-i}}. \tag{28}$$

and the expression of $\widetilde{a}_i$, the planner's choice of network-independent bank lending financed by deposits, is provided in the appendix. Throughout this paper, "$\widetilde{\cdot}$" differentiates the variable in the planner's solution from its counterpart in the market equilibrium. The planner's network attenuation factor differs from ϕ_i in (15) and depends more on bank i due to the additional term, $(\tau_2 - \theta_2)\overline{\sigma}^2_{-i}$, in the denominator that reflects the payment risk spillover of bank i's choice of y_i. Moreover, the ij-th element of the adjacency matrix in (28) differs from its decentralized counter-

part in (16) by incorporating the hedging and liquidity externalities of bank i's choice of y_i.

Let $\widetilde{\Phi}$ denote the diagonal matrix with the i-th diagonal element equal to $\widetilde{\phi}_i$ and $\mathbf{U}$ denote the matrix with the ij-th element equal to μ_{ij}. We rewrite the planner's solution (26) in vector form:

$$\mathbf{y}^* = \widetilde{\Phi}\widetilde{\mathbf{W}}\mathbf{y} - \widetilde{\Phi}\mathbf{U}\mathbf{U}^\top\mathbf{y} + \widetilde{\alpha} \tag{29}$$

where $\widetilde{\mathbf{a}} = [\widetilde{a}_1, ..., \widetilde{a}_N]$, and we have the closed-form solution

$$\mathbf{y}^* = \left(\mathbf{I} - \widetilde{\Phi}\widetilde{\mathbf{W}} + \widetilde{\Phi}\mathbf{U}\mathbf{U}^\top\right)^{-1}\widetilde{\alpha}\,. \tag{30}$$

Proposition 2 *Suppose* $\rho\left(\widetilde{\Phi}\widetilde{\mathbf{W}} + \widetilde{\Phi}\mathbf{U}\mathbf{U}^\top\right) < 1$*, where* $\rho(\cdot)$ *denotes the spectral radius. Then, the planner's optimal solution is uniquely defined and given by (30).*

Discussion: Payment network vs. other networks. The modern payment system settles depositors' transactions by requiring the payment senders' banks to transfer reserves and deposits to the recipients' banks (Piazzesi and Schneider, 2016). In our model, the interconnectedness between banks emerges from transactions among depositors. The literature on interbank network focuses instead on banks' transactions rather than depositors' transactions.[18] In particular, the interbank network of reserve borrowing and lending has attracted most attention.[19]

[18]The literature considers three types of network: (1) interbank financial contracts, mainly reserve loans (e.g., Allen and Gale, 2000; Furfine, 2000; Boss et al., 2004; Upper and Worms, 2004; Wells, 2004; Brusco and Castiglionesi, 2007; Degryse and Nguyen, 2007; Cocco et al., 2009; Bech and Atalay, 2010; Iyer and Peydró, 2011; Castiglionesi and Wagner, 2013; Kuo et al., 2013; Zawadowski, 2013; Farboodi, 2014; Gabrieli and Georg, 2014; Acemoglu et al., 2015; Elliott et al., 2015; Babus, 2016; Bräuning and Fecht, 2016; Erol and Ordoñez, 2017; Gofman, 2017; Blasques et al., 2018; Castiglionesi and Eboli, 2018; Craig and Ma, 2021; Corbae and Gofman, 2019; Anderson et al., 2020; Jasova et al., 2021), (2) linkages via common assets (e.g., Cifuentes et al., 2005; Leitner, 2005; Acharya and Yorulmazer, 2007; Ibragimov et al., 2011; Allen et al., 2012; Greenwood et al., 2015; Caccioli et al., 2015; Cabrales et al., 2017; Albuquerque et al., 2019; Heipertz et al., 2019; Kopytov, 2019), (3) connections from OTC bilateral trading (e.g., Duffie et al., 2009; Hugonnier et al., 2014; Afonso and Lagos, 2015; Bech and Monnet, 2016; Farboodi et al., 2017; Chang and Zhang, 2019; Eisfeldt et al., 2022; Li and Schürhoff, 2019; Üslü, 2019; Hendershott et al., 2020).

[19]The interbank network literature is reviewed by Allen and Babus (2009), Glasserman and Young (2016), and Jackson and Pernoud (2021). One reason behind the exclusive focus on interbank reserve borrowing rather than the more primitive network of depositor payment flows is a legacy institutional setup, deferred net settlement (DNS) that was phased out in the U.S. in 1980s (Bech and Hobijn, 2007). In DNS, banks facing payment outflows automatically obtain a loan from counterparties that experience inflows; in contrast, under the current protocol of real-time gross settlement, payments are no longer settled via interbank credit but by same-day transfer of reserves. In DNS, interbank borrowing happens simultaneously with depositors' payments, so, in a way, the network of interbank reserve borrowing is correlated with that of interbank depositor payment. Under RTGS, the two networks are no longer coupled.

The network of depositors' transactions and that of interbank credit differ but can be related. The interbank credit network can help mitigate the impact of payment flows, allowing the payment recipients' banks to lend to the senders' banks that experience liquidity loss (Bhattacharya and Gale, 1987). However, as previously discussed, the interbank reserve market has frictions, captured via the quadratic cost of liquidity loss. By analyzing the network of depositors' interbank payment flows, we uncover a new source of externality and systemic risk. Moreover, our network analysis is not subject to the common challenges in the literature, such as a lack of bilateral linkage data, endogenous linkages, and randomness in linkages. In our setting, depositor-initiated payments are observed from Fedwire, and this network is not endogenous to banks' choices (unlike, for example, the network of interbank credit) but results from depositors' payments. Finally, we directly model a random graph and quantify the joint probability distribution of depositors' payment flows across banks (i.e., g_{ij}). The randomness in payment flows is a key feature of our model and is important empirically in explaining banks' incentive to finance lending with deposits (Li and Li, 2021).

3 Empirical Methodology

3.1 Data

We obtain confidential transaction-level data from the Fedwire Funds Service ("Fedwire") that spans from 2010 to 2020. Fedwire is a system for real-time gross settlement (RTGS) used to electronically settle U.S. dollar payments among member institutions (including more than two thousand banks). The system processes trillions of dollars daily. The Federal Reserve maintains accounts for both payment sender banks and receiver banks and settles transactions by transferring reserves between banks without netting. In 2020, the average weekly transaction value exceeded the U.S. annual GDP. Fedwire accounts for roughly two-thirds of payment volume in the U.S. The rest of the transactions are mainly settled through the Clearing House Interbank Payments System (CHIPS) of more than forty member banks, which, unlike Fedwire, allows netting (and potentially members' exposure to counterparty risks) and thus does not fit our setting where payments are settled on gross terms and the concern for banks is reserve loss rather than counterparty risks.[20] In

[20]Kahn and Roberds (2009) review the payment literature. Related studies analyze intraday reserve constraints, coordination failure in payment timing (Poole, 1968; Hamilton, 1996; McAndrews and Potter, 2002; Bech and Garratt, 2003; Ashcraft and Duffie, 2007; Bech, 2008; Afonso, Kovner, and Schoar, 2011; Afonso and Shin, 2011; Ashcraft, McAndrews, and Skeie, 2011; Bech, Martin, and McAndrews, 2012; Ihrig, 2019; Afonso, Duffie, Rigon, and

Appendix A, we provide more details on the structure of U.S. payment system. Bech and Hobijn (2007) provide an overview on the adoption of RTGS around the world.

For each transaction, Fedwire records the time and date of the transaction, identities of sender bank and receiver bank, payment amount, and type (instructed by customers or by banks themselves). We focus on transactions instructed by customers (depositors), which are out of the banks' control as in our theoretical model. In particular, we exclude bank-scheduled transfers and banks' purchases and sales of federal funds. Customer-initiated transactions make up about 85% of transactions (in terms of the number of transactions). We obtain data on bank balance sheets and income statements from U.S. Call Report. We merge the Fedwire data with the Call Report data using Federal Reserve's internal identity system. Our merged sample covers 83% of banks in the Call Report (in terms of total assets). We provide the summary statistics in Table D.1 in the appendix.

3.2 Reduced-form motivating facts

Before describing the structural estimation strategy, we show that there are several empirical facts that are challenging to explain or interpret without considering banks' interconnectedness. First, we examine banks' response to changes in the effective FFR depending on their liquidity ratios. We run the following regression:

$$\ell_{it} = \beta \cdot \Delta FFR_{t-1} \times LR_{it} + \gamma X_{it} + \alpha_i + \varepsilon_{it} \tag{31}$$

where LR_{it} is the ratio of the banks' safe assets to total assets, α_i is bank FEs, and X_{it} includes the same control variables as in the model (excluding the payment network). The results are in Columns 1 and 2 of Table 1. Generally, lending growth declines when FFR changes increase. However, the decline is milder for the banks with more liquid assets. This fact implies that banks' lending decisions under constraints depend on banks' safe assets, which is consistent with the model predictions. We find similar results if we use LIBOR-Treasury spread changes in Columns 5-6.

Next, we construct a measure of money velocity by dividing nominal GDP by M2 to test

Shin, 2022; Yang, 2022), stress in short-term funding markets (Ashcraft and Bleakley, 2006; Ashcraft, McAndrews, and Skeie, 2011; Acharya and Merrouche, 2013; Chapman, Gofman, and Jafri, 2019; Correa, Du, and Liao, 2020; d'Avernas and Vandeweyer, 2021; Copeland, Duffie, and Yang, 2021), and costs of payments for depositors (Higgins (2024); Sarkisyan (2024); Wang (2023); Liang et al. (2024); Ding et al. (2025)). Our focus is on how payment liquidity risk propagates into banks' decisions on lending and balance-sheet composition at lower (quarterly) frequencies.

how increased money velocity impacts the relation between interest rates and lending. We run the following regression:

$$\ell_{it} = \beta \cdot \Delta FFR_{t-1} \times Velocity_t + \gamma X_{it} + \alpha_i + \varepsilon_{it} \tag{32}$$

where α_i is bank FEs and X_{it} includes the same control variables as in the model (excluding the payment network) and also the velocity. The results are in Columns 3-4 of Table 1 below. We find that the velocity itself constrains lending, because rapid circulation of money creates liquidity pressure on banks and forces them to liquidate assets. However, during monetary contractions, velocity has an offsetting positive effect on lending growth. This fact seems puzzling, but can be rationalized when considering the network. High interest rates force balance movements across banks. If money velocity is high, the movements are faster and more efficient, resulting in higher lending growth. The results are robust to using LIBOR-OIS spread change, as we show in Columns 7-8.

The goal of regressions (31) and (32) is to explain as much variation in lending growth as possible using the variables from the model and liquidity/velocity constraints. The regression naturally excludes the network dependence, which we will derive through the lens of the model. If network structure explains part of the cross-sectional correlation (i.e., $corr(\varepsilon_{it}, \varepsilon_{jt})$), then we should observe a significant correlation between the residuals. Table 2 indeed reports the results from the Pesaran CD test and the Breusch-Pagan LM test. Both tests reject the null hypothesis of the absence of cross-sectional correlation. The implication is that the observable balance sheet variables themselves are not sufficient to explain the dependence of lending choices of banks on one another, which we aim to do through the network model.

We take one step further and create a heatmap of cross-sectional correlations between residuals of equations (31) and (32). We limit the sample to the top 30 banks for tractability. Figure 1 shows the results. Panels A and B show the results for equation (31) with FFR changes and changes to LIBOR-Treasury spread. Panels C and D show the results for equation (32). A significant part of the heatmap is either green or yellow, implying a very strong correlation between residuals. This fact implies the need to use the SEM model with a variable that can explain why one bank's choice of lending depends on other banks' choices.

Overall, the reduced-form findings imply that balance sheet variables, liquidity, and velocity do not explain a significant part of the cross-sectional correlation between banks' lending choices.

Table 1: **Liquidity Buffers, Velocity, and Monetary Contraction.** This table presents the results of estimation of regressions (31) in Columns 1-2 and equations (32) in Columns 3-4. Columns 5-8 report similar results, but instead of EFFR, we use the spread between LIBOR and 3-month Treasuries. Bank fixed effects are included. Robust standard errors are in parentheses. *,** , and *** correspond to 10-, 5-, and 1% significance level, respectively.

	Lending Growth							
	(1)	(2)	(3)	(4)	(5)	(6)	(7)	(8)
Effective FFR Change	-0.012^{***}	-0.014^{***}	-0.014^{***}	-0.014^{***}				
	(0.002)	(0.002)	(0.002)	(0.002)				
EFFR Change $\times$ LR	0.034^{***}	0.029^{***}						
	(0.010)	(0.010)						
EFFR Change $\times$ Velocity			0.011^{***}	0.015^{***}				
			(0.001)	(0.001)				
LIBOR-Treasury Change					0.048^{***}	0.047^{***}	0.046^{***}	0.045^{***}
					(0.004)	(0.004)	(0.004)	(0.004)
LIBOR-Treasury Change $\times$ LR					0.126^{***}	0.115^{***}		
					(0.021)	(0.021)		
LIBOR-Treasury Change $\times$ Velocity							0.027^{***}	0.030^{***}
							(0.003)	(0.003)
LR	-0.003	-0.013	-0.003	-0.009	-0.006	-0.018	-0.005	-0.012
	(0.010)	(0.013)	(0.010)	(0.013)	(0.010)	(0.013)	(0.010)	(0.013)
Velocity			-0.022^{***}	-0.075^{***}			-0.019^{***}	-0.069^{***}
			(0.004)	(0.005)			(0.004)	(0.005)
Bank FE	No	Yes	No	Yes	No	Yes	No	Yes
Controls	Yes	Yes	Yes	Yes	Yes	Yes	Yes	Yes
Obs.	21,500	21,500	21,500	21,500	21,000	21,000	21,000	21,000
R^2	0.023	0.012	0.024	0.006	0.034	0.018	0.034	0.009

Figure 1: **Heatmap of Cross-Sectional Correlation in Residuals**. This figure plots a heatmap of cross-sectional correlation in residuals after estimating equations (31) and (32). For tractability, only the top 30 banks in terms of average total assets are used. Panels A and B show the results for equation (31) with FFR changes and changes to LIBOR-Treasury spread. Panels C and D show the results for equation (32). Yellow and green colors mean high correlation, while darker colors mean low correlation.

Panel A: Liquidity + EFFR

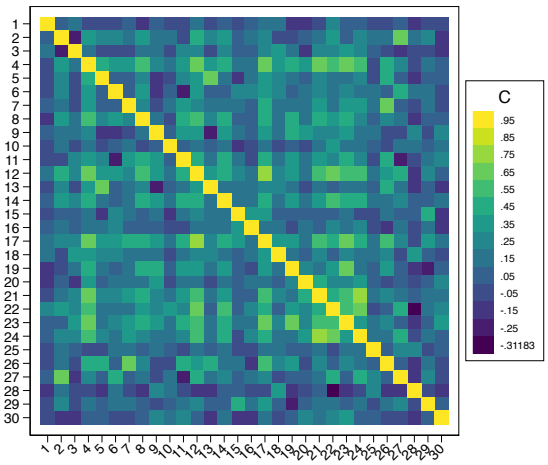

Panel B: Liquidity + LIBOR

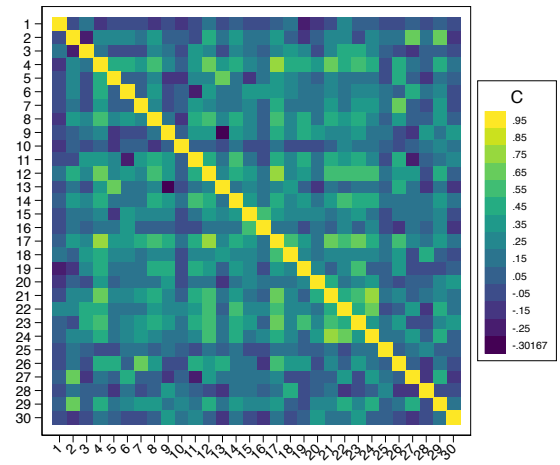

Panel C: Velocity + EFFR

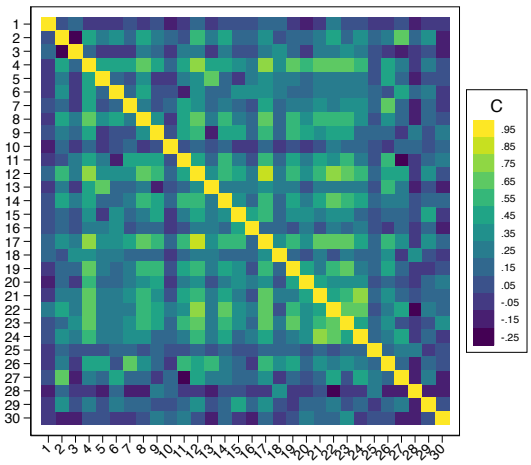

Panel D: Velocity + LIBOR

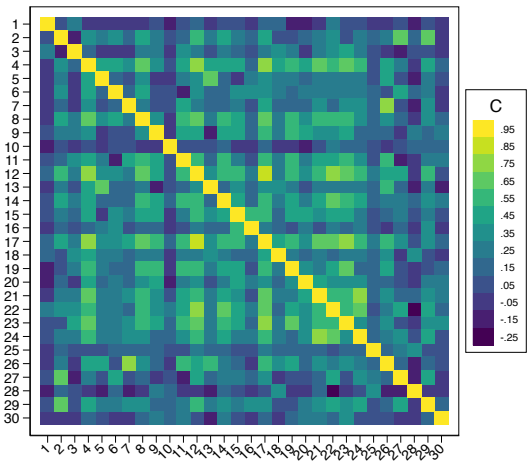

Table 2: **Cross-sectional Dependence Tests.** This table reports the statistics and corresponding p-values from the Pesaran CD test and Breusch-Pagan LM test. The corresponding regression results are reported in Table 1, and heatmaps are plotted in Figure 1.

	(1) Liquidity + EFFR	(2) Liquidity + LIBOR	(3) Velocity + FFR	(4) Velocity + LIBOR
Pesaran CD test				
Statistic	231.7	188.8	230	188.1
p-value	0.000	0.000	0.000	0.000
Breusch-Pagan LM				
Statistic ($\times 10^5$)	2.5	2.3	2.4	2.2
p-value	0.000	0.000	0.000	0.000

Banks also respond differently to policy rate changes, given their liquidity buffers and velocity. Next, we propose a methodology to estimate the network multiplier model and argue that the payment network can explain part of the cross-sectional correlation.

3.3 The empirical specification

We estimate the model with quarterly data. For quarter t, the amount of new loans extended by a bank, y_i, is calculated as the difference between loans in quarter t and loans in quarter $t-1$ (Call Report). As shown in (14), bank i's choice of y_i depends on other banks' y_j through w_{ij}, a function of statistics of g_{ij} and g_{ji} defined in (16). We calculate these statistics using daily observations of g_{ij} and g_{ji} in quarter $t-1$ so that w_{ij} is known (predetermined) when bank i chooses y_i for quarter t. Our results are robust when the statistics are calculated with lagged four quarters of data. To calculate daily observations of g_{ij}, we follow the definition in our model, dividing daily net payment flow from bank i to j in quarter $t-1$ (Fedwire) by bank i's deposits in quarter $t-1$ (Call Report). In Figure 2, we report the frequency distribution of g_{ij}. Note that our sample only contains Fedwire payments instructed by customers (depositors) as our model focuses on interbank reserve transfer due to depositors' payment activities rather than banks transacting with one another.

To maintain the standard assumption of stationarity of data generating processes (Hayashi, 2000), we use banks' quarterly loan growth rates instead of loan amounts. We divide (14) by the

loan amount at quarter $t-1$ to obtain the loan growth rate of bank i in quarter t, denoted by $n_{i,t}$

$$n_{i,t} \equiv \frac{y_{i,t}}{y_{i,t-1}} = \phi_i \sum_{j \neq i} w_{ij} \frac{y_{j,t}}{y_{i,t-1}} + \frac{a_{i,t}}{y_{i,t-1}} \,. \tag{33}$$

To simplify the notation, we use $a'_{i,t}$ to denote $a_{i,t}/y_{i,t-1}$. For the decomposition in (22), we have

$$a'_{i,t} = \bar{\alpha}'_i + \nu'_{i,t} \,, \tag{34}$$

where, $\bar{\alpha}'_i = \bar{\alpha}_i / y_{i,t-1}$, and the shock, $\nu'_{i,t}$, has a zero mean and a conditional variance $\delta_i'^2$ ($\delta'_i = \delta_i / y_{i,t-1}$). Next, we substitute bank j's loan growth rate, $n_{j,t} = \frac{y_{j,t}}{y_{j,t-1}}$ in (33) to obtain:

$$n_{i,t} = \phi_i \sum_{j \neq i} w'_{ij} n_{j,t} + \bar{\alpha}'_i + \nu'_{i,t} \,, \tag{35}$$

where the loan amount-adjusted adjacency matrix, denoted by $\mathbf{W}'$, has the ij-th element given by

$$w'_{ij} \equiv w_{ij} \frac{y_{j,t-1}}{y_{i,t-1}} \,. \tag{36}$$

A key target of our estimation is ϕ_i, $i \in \{1, 2, ..., N\}$. We consider a random coefficient model—that is, ϕ_i is drawn from a Normal distribution with mean μ_ϕ and variance σ^2_ϕ. An estimate of μ_ϕ that is statistically significant from zero suggests that the average bank experiences a significant peer effect, and σ^2_ϕ reveals the degree of bank heterogeneity. And, together with the network adjacency matrix, $\mathbf{W}'$, these parameters determine whether banks' lending decisions are strategic complements (i.e., $\phi_i w_{ij} > 0$) or substitutes (i.e., $\phi_i w_{ij} < 0$).

Instead of directly estimating the equilibrium condition (35) using observations of loan growth rates and w_{ij} from last quarter, we recognize that empirically, a bank's lending decision depends on bank characteristics and macroeconomic variables outside of our theoretical model. Therefore, our empirical model of loan growth rate will contain two components, $q_{i,t}$ that is outside of our model (driven by bank characteristics and macro variables), and $n_{i,t}$, which is the component that reflects the mechanism in our model. In data, we only observe $l_{i,t} = q_{i,t} + n_{i,t}$, not $q_{i,t}$ and $n_{i,t}$ separately. However, by observing bank characteristics (denoted by $x^m_{i,t}$) and macroeconomic variables (denoted by x^p_t) that drive $q_{i,t}$, we are able to estimate the distribution of ϕ_i, effectively using the regression residuals of $l_{i,t}$. In our estimation, the bank characteristics include the log-

Figure 2: **Distribution of** g_{ij}. This figure reports the frequency distribution of g_{ij}. The x-axis shows the logarithm (base 10) of g_{ij} (for example, -2 corresponds to -0.01) and the y-axis shows the fraction of observations in a bin.

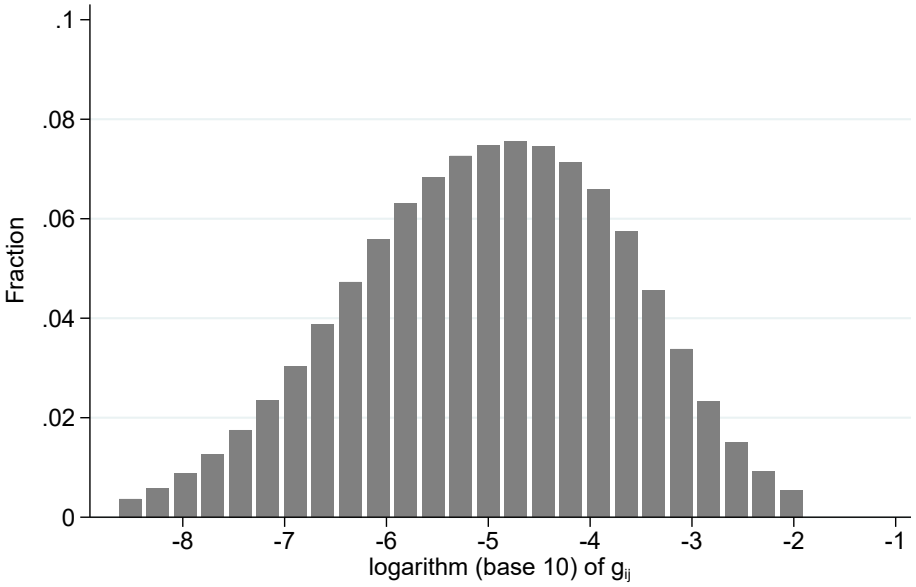

arithm of total assets, the ratio of liquid securities (reserves and available-for-trade securities) to total assets, the ratio of equity capital to total assets, the ratio of deposits to total assets, the ratio of loans to total assets, the return on assets, and the macroeconomic variables (from FRED) include the change in effective federal funds rate (EFFR), real GDP growth, inflation, stock market return, and housing price growth.[21] All control variables are lagged by one quarter for predeterminacy. We include the constant as well. Table D.1 in the appendix provides the summary statistics.

In sum, our empirical model of the observed loan growth rate is

$$l_{i,t} = \sum_{m=1}^{M} \beta_m^{bank} x_{i,t}^m + \sum_{p=1}^{P} \beta_p^{macro} x_t^p + n_{i,t}, \tag{37}$$

[21] The stock market return is the quarterly change of the Wilshire 5000 Total Market Index (a market-capitalization-weighted index of the market value of all American-stocks actively traded in the United States). The housing price growth is the quarterly change of the S&P/Case-Shiller U.S. National Home Price Index.

where, according to (35), we have

$$n_{i,t} = \phi_i \sum_{j \neq i} w'_{ij} n_{j,t} + \bar{\alpha}'_i + \nu'_{i,t} \quad \nu'_{i,t} \sim \mathcal{N}\left(0, \delta_i^{'2}\right). \tag{38}$$

Equation (37) and (38) together constitute a spatial error model (SEM) (e.g., Anselin, 1988; Elhorst, 2010). Such models allow the joint estimation of β coefficients in the observational equation (37), and $\bar{\alpha}'_i$, $\delta_i^{'2}$, μ_ϕ, and σ_ϕ in the error (or residual) equation (38). Therefore, even though the econometrician does not observe $n_{i,t}$ directly, the parameters of the network game can still be recovered. In Appendix C.1, we explain the estimation algorithm for both the simulated MLE under heterogeneous ϕ_i and the standard MLE for the simpler version of model with homogeneous ϕ.

We can rewrite the system of (37) and (38) in vector form:

$$\boldsymbol{\ell}_t = X_t \beta + \mathbf{n}_t, \tag{39}$$

$$\mathbf{n}_t = \Phi \mathbf{W}' \mathbf{n}_t + \bar{\alpha}' + \nu'_t, \tag{40}$$

where $\Phi \equiv \mathrm{diag}(\boldsymbol{\phi})$ and $\boldsymbol{\phi} = (\phi_1, \ldots, \phi_N)^\top$. Following Proposition 1, we require $\rho(\Phi \mathbf{W}') < 1$, where $\rho(\cdot)$ denotes the spectral radius. Under this restriction,

$$\mathbf{n}_t = \left(\mathbf{I} - \Phi \mathbf{W}'\right)^{-1} \left(\bar{\alpha}' + \nu'_t\right). \tag{41}$$

The control variables, X_t, absorb part of the variation in loan growth rates and only leave the residual variation for estimating the network effect, ϕ_i. This is a conservative approach. Any comovement in $\boldsymbol{\ell}_t$ across banks that is driven by common variation in bank characteristics or common loadings on macroeconomic factors (X_t) cannot be attributed to peer effects. Given the strong heterogeneity in bank sizes, w'_{ij} in (36) can be prohibitively large if i is much smaller than j, which then implies that for small banks, the component related to network effects, $n_{i,t}$, will mechanically account for a large share of loan growth relative to $q_{i,t}$. Since our model does not address the relative importance of $n_{i,t}$ and $q_{i,t}$, $\mathbf{W}'$ is normalized to be right-stochastic (row sums equal to one); thus the relative importance of $n_{i,t}$ and $q_{i,t}$ is not mechanically driven by size. The normalization also prevents the estimate of μ_ϕ from being disproportionately influenced by small banks.

We estimate the parameters using MLE. Conditional on a realization of $\boldsymbol{\phi} = (\phi_1, \ldots, \phi_N)^\top$,

the model implies the following Gaussian likelihood for loan growth:

$$-\frac{T}{2}\ln\big((2\pi)^N|\Delta'|\big)-\frac{1}{2}\sum_{t=1}^{T}\Big[\big(\mathbf{I}-\Phi\mathbf{W}'\big)(\boldsymbol{\ell}_t-X_t\beta)-\bar{\boldsymbol{\alpha}}'\Big]^{\top}\Delta'^{-1}\Big[\big(\mathbf{I}-\Phi\mathbf{W}'\big)(\boldsymbol{\ell}_t-X_t\beta)-\bar{\boldsymbol{\alpha}}'\Big],$$

where N denotes the number of banks, T denotes the number of quarters, and Δ' is a diagonal covariance matrix with the i-th diagonal element equal to $\delta_i'^2$. The diagonal structure of Δ' imposes the identifying restriction that the structural shocks $\boldsymbol{\nu}_t'$ are uncorrelated across banks. In the next subsection, we discuss its implication for identifying ϕ. Empirically, it is reasonable to assume that, after controlling for a sufficiently large set of bank characteristics and macroeconomic variables (X_t), comovement in the residual loan growth rates, $n_{i,t}$, has been significantly reduced, and after teasing out the network propagation mechanism, the structural shocks, ν_t', should be uncorrelated across banks. In other words, comovement in loan growth rate, $l_{i,t}$, across banks has two sources, from X_t and from the network propagation mechanism, i.e., $(\mathbf{I}-\Phi\mathbf{W}')^{-1}$ in (41), that transmits individual banks' uncorrelated shocks to their peers.

For the case of homogeneous ϕ (i.e., the diagonal matrix Φ is replaced by a single parameter, ϕ), we conduct standard MLE by maximizing the likelihood function above. For the case of heterogeneous ϕ_i that is drawn from a Normal distribution $\mathcal{N}(\mu_\phi, \sigma_\phi^2)$, the complete likelihood function is obtained by integrating the conditional likelihood above over the distribution of ϕ. We estimate the parameters $(\mu_\phi,\ \sigma_\phi)$ jointly with $(\bar{\boldsymbol{\alpha}}',\ \boldsymbol{\delta}',\ \beta)$ using simulated MLE, approximating the integral over $\boldsymbol{\phi}$ via the Monte Carlo method.

Note that when the shocks ν_t' are normally distributed, we have an MLE estimator. If the shocks are not normally distributed, the estimator is quasi-MLE. When the score of normal log-likelihood has the martingale difference property and the first two conditional moments are correctly specified, the quasi-MLE estimator is consistent and has a limiting normal distribution (Bollerslev and Wooldridge, 1992). For inference, we apply the classic delta method.[22]

3.4 Parameter identification

To clarify the intuition about how the key parameter, ϕ_i, is identified from the data, it is useful to consider a simplified version of the model in equations (37) and (38) under homogeneous ϕ.

Let $L_t \in \mathbb{R}^N$ denote the vector containing loan growth rates of individual banks at quarter t,

[22] We follow Bollerslev and Wooldridge (1992) to calculate the asymptotic standard errors robust to non-normality.

and, to simplify exposition, let us disregard $\bar{\alpha}_i'$ in equation (38) and assume that the network matrix has constant weights $\mathbf{W}'$. The model given by (39) and (40) can be rewritten in vector form:

$$\boldsymbol{\ell}_t = X_t\beta + \mathbf{n}_t, \quad \mathbf{n}_t \sim \mathcal{N}\left(\mathbf{0}_N, \Omega\right), \tag{42}$$

where $\mathbf{0}_N$ denotes an N-dimensional vector of zeros, $\Omega = \mathbf{M}\Delta'\mathbf{M}^\top$ with $M = \left(\mathbf{I} - \phi\mathbf{W}'\right)^{-1}$, Δ' is a diagonal matrix with elements given by $\left\{\delta_i'^2\right\}_{i=1}^N$. In deriving the covariance Ω, we used equation (38), i.e., that in equilibrium we can rewrite $\mathbf{n}_t$ (having, for now, removed $\bar{\alpha}_i$) as $\mathbf{n}_t = \left(\mathbf{I} - \phi\mathbf{W}'\right)^{-1}\nu_t'$, where ν_t' has a distribution with zero mean and a diagonal covariance matrix Δ'.

We can consistently estimate β via linear projection, and use the residuals to construct a consistent estimator of covariance matrix Ω.[23] The key question is whether we can recover the structural parameters ϕ and $\left\{\delta_i'^2\right\}_{i=1}^N$. Being symmetric, the estimated $\widehat{\Omega}$ gives $N(N+1)/2$ equations, while we have to recover $N+1$ parameters in $\mathbf{M}\Delta'\mathbf{M}^\top$. Therefore, as long as Ω is full-rank, the system is over-identified. The identification is akin to that of structural vector autoregressions (Sims and Zha, 1999) where shock propagation is recovered from residual covariance.

To further sharpen the intuition, let us consider a system of three banks and the simplest network, a chain: Bank 1 is connected with Bank 2, and 2 with 3, so

$$\mathbf{W}' = \begin{bmatrix} 0 & 1 & 0 \\ 0 & 0 & 1 \\ 0 & 0 & 0 \end{bmatrix}, \text{ and } \mathbf{M}\Delta'\mathbf{M}^\top = \begin{bmatrix} \delta_1'^2 + \phi^2\delta_2'^2 + \phi^4\delta_3'^2 & \phi\delta_2'^2 + \phi^3\delta_3'^2 & \phi^2\delta_3'^2 \\ \phi\delta_2'^2 + \phi^3\delta_3'^2 & \delta_2'^2 + \phi^2\delta_3'^2 & \phi\delta_3'^2 \\ \phi^2\delta_3'^2 & \phi\delta_3'^2 & \delta_3'^2 \end{bmatrix}.$$

The volatility of n_1 is $\delta_1'^2 + \phi^2\delta_2'^2 + \phi^4\delta_3'^2$. The first term is the volatility of Bank 1's shock, ν_1'. The second term is the volatility of Bank 2's shock transmitted to Bank 1, i.e., ϕn_2, and the third term reflects Bank 3's shock transmitted in two steps (via Bank 2) to Bank 1, i.e., $\phi^2 n_3$. By the same logic, the volatility of n_2 is $\delta_2'^2 + \phi^2\delta_3'^2$, capturing Bank 2's exposure to its own shock and Bank 3's shock, while Bank 3 only loads on its own shock, so the volatility of n_3 is $\delta_3'^2$. The covariance between n_1 and n_2 is $\phi\delta_2'^2 + \phi^3\delta_3'^2$, reflecting Bank 1's and 2's exposure to 2's and 3's shocks. The covariance between n_2 and n_3 is $\phi\delta_3'^2$ as it only arises from the one-step transmission of Bank 3's shock to 2, i.e., ϕn_3. Covariances emerge from network linkages, and their estimates identify the network effect, ϕ. Given $\delta_3'^2 = \{\widehat{\Omega}\}_{3,3}$, we can solve for ϕ using either the covariance between n_1 and n_3, i.e., $\{\widehat{\Omega}\}_{1,3} = \phi^2\delta_3'^2$, or the covariance between n_2 and n_3, i.e., $\{\widehat{\Omega}\}_{2,3} = \phi\delta_3'^2$, so the

[23] The model in (42) has the same structure and properties as the Seemingly Unrelated Regressions (Zellner, 1962).

system is clearly over-identified. Moreover, given the estimates of $\delta_3^{'2}$ and ϕ, either the volatility of n_2, i.e., $\{\widehat{\Omega}\}_{2,2} = \delta_2^{'2} + \phi^2\delta_3^{'2}$, or the covariance between n_1 and n_2, i.e., $\{\widehat{\Omega}\}_{1,2} = \phi\delta_2^{'2} + \phi^3\delta_3^{'2}$, gives a solution for $\delta_2^{'2}$. In the last step, given ϕ, $\delta_2^{'2}$, and $\delta_3^{'2}$, $\{\widehat{\Omega}\}_{1,1}$ pins down $\delta_1^{'2}$.

The structural shocks, ν_i', are uncorrelated across banks. Thus, after controlling for bank characteristics and macro variables, the residuals' (n_i's) correlations are from the network linkages. Therefore, the network effect, μ_ϕ, is identified by such correlations. Accordingly, we saturate the empirical model with a rich set of control variables (X_t) so that the residual correlations are driven by the network linkages instead of missing variables that induce comovement between banks.

3.5 Systemic risk

In this section, we develop systemic risk metrics. When presenting our results, we will consider the mean of ϕ_i estimated from the heterogeneous-ϕ model – μ_ϕ. Intuitively, we are going to consider an average systemic risk.

As shown in (40), an increase in $\bar{\alpha}_i'$ or a positive shock to bank i, $\nu_{i,t}' > 0$, is transmitted to other banks via $\mu_\phi \mathbf{W}'$ and, after rounds of propagation, all routes of transmission are summarized by

$$\mathbf{M}\left(\mu_\phi, \mathbf{W}'\right) \equiv \mathbf{I} + \mu_\phi \mathbf{W}' + \mu_\phi^2 \mathbf{W}'^2 + \mu_\phi^3 \mathbf{W}'^3 + \ ... \ = \sum_{k=0}^{\infty} \mu_\phi^k \mathbf{W}'^k = \left(\mathbf{I} - \mu_\phi \mathbf{W}'\right)^{-1}, \tag{43}$$

as shown in (41). Consider an increase of $\bar{\alpha}_i'$ by ϵ for all banks or a shock $\nu_{i,t}' = \epsilon$ to all banks. Under $\mathbf{W}'$ being right-stochastic (i.e., $\mathbf{W}'\mathbf{1} = \mathbf{1}$), we have the equilibrium impact given by

$$\mathbf{M}\left(\mu_\phi, \mathbf{W}'\right)\mathbf{1}\epsilon = \left(\mathbf{I} + \mu_\phi \mathbf{W}'\mathbf{1} + \mu_\phi^2 \mathbf{W}'^2\mathbf{1} + \mu_\phi^3 \mathbf{W}'^3\mathbf{1} + \ ...\right)\epsilon = \frac{1}{1-\mu_\phi}\mathbf{1}\epsilon\,. \tag{44}$$

Therefore, for the same variation in $\bar{\alpha}_i'$ across banks or the same shock, $\nu_{i,t}'$, to all banks, the network multiplier, $1/(1-\mu_\phi)$, is a sufficient statistic for the equilibrium impact. If $\mu_\phi > 0$, the network amplifies the impact, i.e., $\frac{1}{1-\mu_\phi} > 1$; under $\mu_\phi < 0$, the network dampens the impact.

Definition 1 (Network Multiplier) *The average network multiplier is defined as* $\frac{1}{1-\mu_\phi}$.

Given the estimates of μ_ϕ, σ_ϕ,$\bar{\alpha}_i'$, and $\delta_i'^2$, we use our structural model to identify systemically important banks. A bank is systemically important if it has a disproportionately large impact on the

aggregate credit supply. Let N_t denote the network-dependent component of aggregate lending:

$$N_t = \sum_{i=1}^{N} y_{i,t-1} n_{i,t} = \mathbf{y}_{t-1}^{\top} \mathbf{n}_t \,. \tag{45}$$

Substituting the solution of loan growth rates, $\mathbf{n}_t$, given by (41), we obtain

$$N_t = \mathbf{y}_{t-1}^{\top} \left(\mathbf{I} - \mu_\phi \mathbf{W}'\right)^{-1} \left(\bar{\alpha}' + \nu_t'\right) = \mathbf{y}_{t-1}^{\top} \mathbf{M}\left(\mu_\phi, \mathbf{W}'\right) \left(\bar{\alpha}' + \nu_t'\right). \tag{46}$$

Before the shocks, ν_t', are realized for quarter t, we calculate the conditional mean of N_t,

$$\mathbb{E}_{t-1}[N_t] = \mathbf{y}_{t-1}^{\top} \mathbf{M}\left(\mu_\phi, \mathbf{W}'\right) \bar{\alpha}' \,, \tag{47}$$

and the conditional variance of N_t,

$$\mathrm{Var}_{t-t}\left(N_t\right) = \mathbf{y}_{t-1}^{\top} \mathbf{M}\left(\mu_\phi, \mathbf{W}'\right) \Delta' \mathbf{M}\left(\mu_\phi, \mathbf{W}'\right)^{\top} \mathbf{y}_{t-1} \,, \tag{48}$$

where Δ' is the covariance matrix of ν_t', a diagonal matrix whose i-th diagonal element is $\delta_i'^2$.

Definition 2 (Network Impulse Response Function and Volatility Key Bank) *The impulse response of aggregate credit supply to a one standard-deviation shock to a bank i is given by*

$$NIRF_{i,t-1}\left(\mu_\phi, \delta_i', \mathbf{W}'\right) \equiv \frac{\partial N_t}{\partial \nu_{i,t}'} \delta_i' = \mathbf{y}_{t-1}^{\top} \left\{\mathbf{M}\left(\mu_\phi, \mathbf{W}'\right)\right\}_{.i} \delta_i' \tag{49}$$

where the operator $\{\}_{.i}$ returns the i-th column of its argument. Volatility key bank is defined as

$$i_{t-1}^{*} = \underset{i \in \{1, \ldots, N\}}{\arg\max} \; NIRF_{i,t-1}\left(\mu_\phi, \delta_i', \mathbf{W}'\right). \tag{50}$$

A bank's NIRF records the impact of its shock on the aggregate credit supply. It depends on the average network attenuation factor, μ_ϕ, the network topology given by $\mathbf{W}'$, and the size of the bank's shock, δ_i'. Our estimation method allows us to identify both μ_ϕ and δ_i'. We construct confidence intervals for NIRFs using the estimate of σ_ϕ. We also construct NIRFs by using Monte Carlo simulations of ϕ_i from the Normal distribution with mean μ_ϕ and variance σ_ϕ. Next, we show that NIRFs measure banks' contributions to the conditional volatility of aggregate credit supply.

Proposition 3 (Credit-Supply Volatility Decomposition) *Let "vec" denote the vectorization operator. NIRFs decompose the conditional volatility of aggregate credit supply:*

$$\mathrm{Var}_{t-t}\left(N_t\right) = vec\left(\left\{NIRF_{i,t-1}\left(\mu_\phi, \delta_i', \mathbf{W}'\right)\right\}_{i=1}^{N}\right)^\top vec\left(\left\{NIRF_{i,t-1}\left(\mu_\phi, \delta_i', \mathbf{W}'\right)\right\}_{i=1}^{N}\right) . \quad (51)$$

3.6 Comparing the planner's solution and market equilibrium

We compare the conditional expectation and conditional volatility of aggregate credit supply from the market equilibrium with those from the planner's solution under homogeneous ϕ.

First, we show how to utilize the parameter estimates to compute the planner's solution. Following Section 3.3, we define

$$\widetilde{w}_{ij}' = \widetilde{w}_{ij}\frac{y_{j,t-1}}{y_{i,t-1}}, \quad (52)$$

where $\widetilde{w}_{ij}$ is defined in (28), and

$$\mu_{ij}' = \mu_{ij}\frac{y_{j,t-1}}{y_{i,t-1}}. \quad (53)$$

Throughout this paper, we use "$\widetilde{\ }$" to denote variables in the planner's solution. Dividing the planner's solution (26) by $y_{i,t-1}$ and substituting $y_{j,t}$ with $y_{j,t-1}\widetilde{n}_{j,t}$, we obtain

$$\widetilde{n}_{i,t} = \widetilde{\phi}_i \sum_{j\neq i} \widetilde{w}_{ij}'\widetilde{n}_{j,t} - \widetilde{\phi}_i \sum_{j\neq i} \mu_{ij}\left(\sum_{k\neq j}\mu_{kj}'\widetilde{n}_{k,t}\right) + \widetilde{a}_{i,t}' \quad (54)$$

where $\widetilde{\phi}_i$ is defined in (27) and $\widetilde{a}_{i,t}' = \widetilde{a}_{i,t}/y_{i,t-1}$. Let $\widetilde{\mathbf{W}}'$ and $\mathbf{U}'$ denote the matrices whose the ij-th elements are equal to $\widetilde{w}_{ij}'$ and μ_{ij}', respectively. Let $\widetilde{\mathbf{a}}_t'$ denote the vector for $\widetilde{a}_{i,t}'$. And, let $\widetilde{\Phi}$ denote the diagonal matrix with the i-th diagonal element equal to $\widetilde{\phi}_i$. In vector form, we have:

$$\widetilde{\mathbf{n}}_t = \widetilde{\Phi}\left(\widetilde{\mathbf{W}}' - \mathbf{U}\mathbf{U}'^\top\right)\widetilde{\mathbf{n}}_t + \widetilde{\mathbf{a}}_t'. \quad (55)$$

The planner's choice of individual banks' lending can be solved as follows:

$$\widetilde{\mathbf{n}}_t = \widetilde{\mathbf{M}}\left(\widetilde{\Phi}, \widetilde{\mathbf{W}}', \mathbf{U}, \mathbf{U}'\right)\widetilde{\mathbf{a}}_t'. \quad (56)$$

where we define

$$\widetilde{\mathbf{M}}\left(\widetilde{\Phi}, \widetilde{\mathbf{W}}', \mathbf{U}, \mathbf{U}'\right) \equiv \left(\mathbf{I} - \widetilde{\Phi}\widetilde{\mathbf{W}}' + \widetilde{\Phi}\mathbf{U}\mathbf{U}'^\top\right)^{-1}. \quad (57)$$

Following the definition (28), we compute $\widetilde{w}_{ij}$ using the statistics of g_{ij} and g_{ji} discussed in Section 3.3 and compute $\widetilde{w}'_{ij}$ in (52) and μ'_{ij} in (53). Comparing the planner's solution (55) and the market equilibrium (40), we can see that $\widetilde{\mathbf{W}}' - \mathbf{U}\mathbf{U}'^{\top}$ plays a similar role in the planner's solution, capturing the peer effects, as $\mathbf{W}'$ in the market equilibrium. Therefore, we normalize $\widetilde{\mathbf{W}}' - \mathbf{U}\mathbf{U}'^{\top}$ to be right-stochastic as we do for $\mathbf{W}'$ in Section 3.3. We calculate $\widetilde{\phi}_i$, defined in (27), using the estimate of ϕ and the statistics of g_{ij} and g_{ji}. To compute the mean and standard deviation of $\widetilde{a}'_{i,t}$, we solve the connection between $\widetilde{a}'_{i,t}$ and $a'_{i,t}$, given by (34) from the market equilibrium:

$$\widetilde{a}'_{i,t} = \frac{b_{i,t}}{y_{i,t-1}} + \frac{\widetilde{\phi}_i}{\phi} a'_{i,t}\,. \tag{58}$$

The details are provided in equation (C.27) the appendix, and $b_{i,t}$ is defined in (C.28). We define $b'_{i,t} = b_{i,t}/y_{i,t-1}$ and rewrite the planner's solution (56) in vector form:

$$\widetilde{\mathbf{n}}_t = \widetilde{\mathbf{M}}\left(\widetilde{\Phi}, \widetilde{\mathbf{W}}', \mathbf{U}, \mathbf{U}'\right) \mathbf{b}'_{t-1} + \widetilde{\mathbf{M}}\left(\widetilde{\Phi}, \widetilde{\mathbf{W}}', \mathbf{U}, \mathbf{U}'\right) \frac{1}{\phi} \widetilde{\Phi}\, \mathbf{a}'_t\,. \tag{59}$$

The aggregate credit supply by banks chosen by the planner is

$$\widetilde{N}_t = \sum_{i=1}^{N} y_{i,t-1} \widetilde{n}_{i,t} = \mathbf{y}_{t-1}^{\top} \widetilde{\mathbf{n}}_t\,. \tag{60}$$

With the estimates of ϕ, $\bar{\alpha}'_i$ (the mean of $a'_{i,t}$) and δ'_i (the volatility of $a'_{i,t}$), our goal is to compute the conditional mean and volatility of planner's choice of bank lending. Because the first term in $\widetilde{\mathbf{n}}_t$, $\widetilde{\mathbf{M}}(\widetilde{\Phi}, \widetilde{\mathbf{W}}', \mathbf{U}, \mathbf{U}')\mathbf{b}'_{t-1}$, is not random, we solve the conditional volatility of $\widetilde{N}_t$:

$$\mathrm{Var}_{t-1}\left[\widetilde{N}_t\right] = \frac{1}{\phi^2} \mathbf{y}_{t-1}^{\top} \widetilde{\mathbf{M}}\left(\widetilde{\Phi}, \widetilde{\mathbf{W}}', \mathbf{U}, \mathbf{U}'\right) \widetilde{\Phi}\, \Delta' \widetilde{\Phi}^{\top} \widetilde{\mathbf{M}}\left(\widetilde{\Phi}, \widetilde{\mathbf{W}}', \mathbf{U}, \mathbf{U}'\right)^{\top} \mathbf{y}_{t-1}, \tag{61}$$

where, as previously defined, Δ' is a diagonal matrix with the i-th diagonal element equal to $\delta_i'^2$. The calculation of the conditional mean of $\widetilde{N}_t$,

$$\mathbb{E}_{t-1}\left[\widetilde{N}_t\right] = \mathbf{y}_{t-1}^{\top} \widetilde{\mathbf{M}}\left(\widetilde{\Phi}, \widetilde{\mathbf{W}}', \mathbf{U}, \mathbf{U}'\right) \mathbf{b}'_{t-1} + \mathbf{y}_{t-1}^{\top} \widetilde{\mathbf{M}}\left(\widetilde{\Phi}, \widetilde{\mathbf{W}}', \mathbf{U}, \mathbf{U}'\right) \frac{1}{\phi} \widetilde{\Phi}\, \bar{\alpha}'\,, \tag{62}$$

requires $\mathbf{b}'_{t-1}$ (and $b_{i,t}$ given by (C.28) in the appendix) that depends on τ_1, τ_2, θ_1, and θ_2 that cannot be identified in our estimation (as we only estimate the composite parameter, $\phi = \frac{\tau_2 - \theta_2}{\kappa + \tau_2 - \theta_2}$

defined in (15)). Therefore, when comparing the conditional mean of N_t of the market equilibrium and that of $\widetilde{N}_t$, we focus on the second component of $\mathbb{E}_{t-1}[\widetilde{N}_t]$ that can be computed with our parameter estimates. This second component, $\mathbf{y}_{t-1}^{\top}\widetilde{\mathbf{M}}(\widetilde{\Phi}, \widetilde{\mathbf{W}}', \mathbf{U}, \mathbf{U}')\frac{1}{\phi}\widetilde{\Phi}\,\bar{\alpha}'$, is more comparable to the market equilibrium, $\mathbb{E}_{t-1}[N_t] = \mathbf{y}_{t-1}^{\top}\mathbf{M}\left(\phi, \mathbf{W}'\right)\bar{\alpha}'$ in (47). The differences are in the network propagation ($\widetilde{\mathbf{M}}(\widetilde{\Phi}, \widetilde{\mathbf{W}}', \mathbf{U}, \mathbf{U}')$ vs. $\mathbf{M}\left(\phi, \mathbf{W}'\right)$) and the deviations of $\widetilde{\phi}_i$ from ϕ (captured by $\frac{1}{\phi}\widetilde{\Phi}$).

4 Estimation Results

4.1 The network multiplier

Table 3 reports the estimates of μ_ϕ and σ_ϕ (the mean and standard deviation of ϕ_i) for the heterogeneous-ϕ_i model and the estimate of ϕ for the homogeneous-ϕ model. We also report the implied network multiplier given by (44). Our estimation is done on different samples of banks ranked by the size of their deposits. The main specification includes the top 500 banks, and we also report results for the top 300 and 700 banks.[24]

As discussed in Section 3.3, under $\phi = \mu_\phi > 0$ (or $1/(1-\mu_\phi) > 1$), the network amplifies a common variation in all banks' $\bar{\alpha}_i'$ (expected level of network-independent lending) or a common shock to banks' network-independent lending, say, $\bar{\nu}_{i,t}' = \epsilon$, by $1/(1-\mu_\phi) - 1$. An estimate of μ_ϕ equal to 0.1898 in the sample of top 500 banks implies an average multiplier equal to 1.23 and an average amplification effect of 23%. As we demonstrate in Panel B, the amplification effect is slightly smaller if we remove banks' deposit and loan market power in the case of homogeneous ϕ, but there is still a significant amplification. As discussed in Section 2, the sign of $\phi_i w_{ij}'$ determines whether banks' decisions are strategic complements or substitutes. In our sample, only 0.39% of non-zero w_{ij}' are negative.[25] Therefore, $\mu_\phi > 0$ indicates strategic complementarity, which is the source of the network amplification effect.

We have hundreds of banks in each sample, so there are hundreds of $\bar{\alpha}_i'$ and δ_i'. Since the samples differ in the number of banks, we present the estimates of $\bar{\alpha}_i'$ and δ_i' through their distribution for each sample. Figure D.1 in Appendix D reports the results. Across samples, the distributions of these parameters are fairly consistent, which suggests that once we have include the largest hundreds of banks, the distribution of network-independent level of expected loan growth rate and

[24] The network adjacency matrix, $\mathbf{W}'$, is independently constructed for banks in each subsample.

[25] Among all the potential pairs, there are 6.47% that have non-zero w_{ij}', so the payment-flow network is sparse.

Table 3: **Network multiplier**. The table reports the estimates of μ_ϕ, σ_ϕ, ϕ for the case without bank heterogeneity, and the implied (average) network multiplier given by (44). The quasi-SML standard errors are reported in parentheses under the estimated coefficients. The average network multiplier, $1/(1-\widehat{\mu}_\phi)$, is reported in the second line, and the R^2 in the third line is the fraction of variation explained by the control variables (i.e., the bank characteristics and macroeconomic variables). Panel A shows the results for the model with endogenous deposit and loan rates, while Panel B shows the results with homogeneous ϕ, in which case the t-stats are calculated with quasi-MLE.

Number of Banks:	300	500	700
Panel A: Baseline model – heterogeneous ϕ_i			
$\widehat{\mu}_\phi$	0.0873 (0.00)	0.1898 (0.00)	0.1765 (0.04)
$\widehat{\sigma}_\phi$	0.0283 (0.01)	0.1058 (0.00)	0.1961 (0.05)
$1/\left(1-\widehat{\mu}_\phi\right)$	1.0956	1.2342	1.2143
R^2	0.1119	0.1215	0.1324
Panel B: Exogenous rates – homogeneous ϕ			
$\widehat{\phi}$	0.1075 (0.04)	0.1086 (0.04)	0.0953 (0.04)
$1/\left(1-\widehat{\phi}\right)$	1.1204	1.1219	1.1054
R^2	0.1120	0.1217	0.1325

volatility (i.e., $\bar{\alpha}_i'$ and δ_i') can be reliably estimated. In the appendix, we also report the estimates of control variable coefficients in Table D.2 for the homogenous-ϕ model. We also plot the distribution of ϕ_i for different sizes in Figure D.2 in Appendix D. In the following, our analysis will be based on the sample of top 500 banks.

In Figure 3, we report a placebo exercise designed to address the standard omitted-variable concern in spatial autoregressive models, namely that cross-sectional dependence may reflect common exposure to unobserved factors rather than genuine network interactions. Instead of using the observed payment network, we construct a geographic network based on bilateral physical distances between banks. Because geographic proximity captures a broad set of shared local fundamentals—such as regional economic conditions, demand shocks, and regulatory environments—it provides a stringent alternative source of cross-sectional correlation unrelated to payment flows.

Figure 3: **Distribution of ϕ_i: actual vs placebo**. This figure reports the distribution of ϕ_i for the sample of 500 banks. The blue bars plot the distribution using the actual payment network. The orange bars plot the distribution using the placebo geographic network. The difference in the Bayesian Information Criterion is 4521.78, in favor of an actual network.

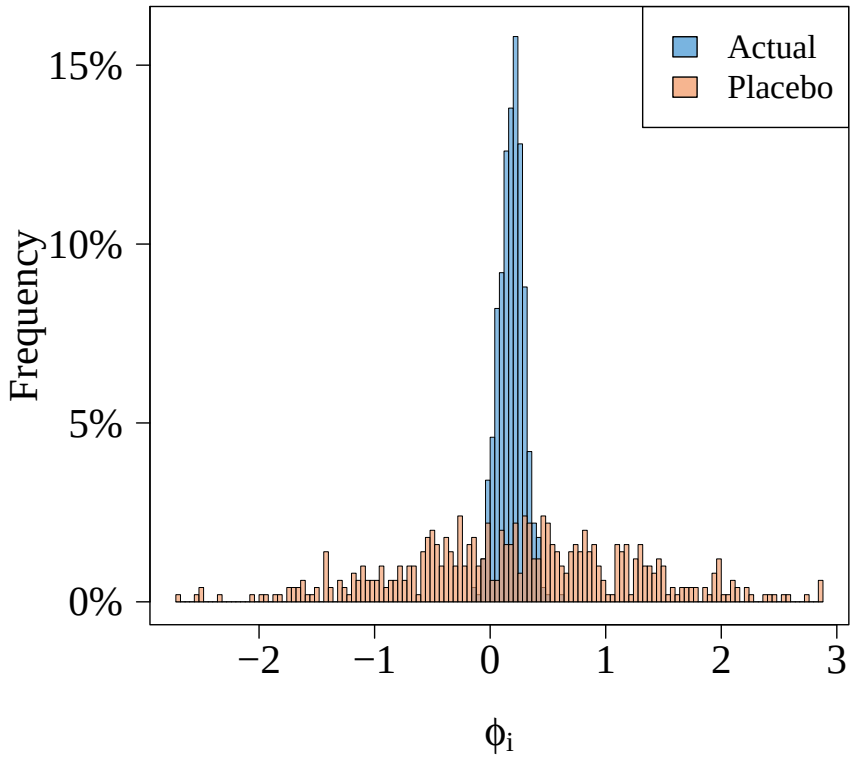

The estimation results under the geographic network differ sharply from those obtained using the actual payment network. The implied cross-sectional distribution of ϕ_i is essentially flat, with a very large estimate of σ_ϕ and no statistically meaningful dispersion. Both μ_ϕ and σ_ϕ are statistically indistinguishable from zero, with t-statistics of 0.1 and 0.05, respectively. Hence, once network interactions are defined by geographic proximity rather than payment linkages, the heterogeneous propagation mechanism is not identified in the data.

We formally compare the two specifications using the Bayesian Information Criterion (BIC). Because both models are estimated on the same sample and have identical dimensionality, differences in BIC are driven entirely by differences in maximized likelihood. The payment network specification is overwhelmingly preferred, with a BIC difference of 4521.78 in its favor. This magnitude constitutes decisive evidence against the geographic placebo, indicating that the cross-

sectional dependence captured by the model is intrinsically tied to the topology of the payment network rather than to spatial proximity or other latent regional confounders.

4.2 The importance of network topology

The estimate of $\mu_\phi > 0$ in Table 3 indicates that the network is an amplification mechanism for the average bank. In Section 3.5, we have shown that when $\bar{\alpha}'_i$ changes by the same amount for all banks, or when all banks are hit by shocks of the same size ($\nu'_{i,t}$), the network multiplier is a sufficient statistic for the network amplification effect. Our estimation reveals that $\bar{\alpha}'_i$ differs across banks, and the size of shock, measured by δ'_i, the standard deviation or volatility of $\nu'_{i,t}$, also differs across banks. In the following, we further demonstrate the network amplification mechanism by incorporating the heterogeneity in $\bar{\alpha}'_i$ and δ'_i. Under such heterogeneity, the network multiplier is no longer a sufficient statistic for the amplification mechanism, and the topology of network linkages, encoded in the network adjacency matrix, $\mathbf{W}'$, plays an important role.

First, we check how well liquidity, interest rate, and profitability variables explain lending growth with and without the payment network. Columns 1 and 2 of Table 4 regress lending growth on liquidity ratio, ROA, deposit rates, loan rates, and stock return. Columns 3 and 4 use the lending growth net of the topology effects, i.e., $\bar{\alpha}' + \nu'_t$ from equation (39). With the network, R^2 is higher – 17.8% as opposed to 13.7%. After accounting for the network, the liquidity ratio also does not predict lending growth as strongly as without accounting for the network.

As discussed in Section 2.1, the main mechanism in our model can be summarized in two steps. When extending loans funded by deposits, banks face potential liquidity loss due to depositors' payment outflows and have to rely on their liquid assets. Therefore, the network-independent level of lending, a_i, depends on the liquidity base, m_i, in Proposition 1. The liquidity constraint is then relaxed by liquidity churn within the system: when depositors at different banks transact with one another, one bank's payment outflow is another's inflow. Such liquidity churn is captured by the network amplification operator in Proposition 1, which, as a reminder, is reproduced here

$$\mathbf{M}(\Phi, \mathbf{W}) \equiv (\mathbf{I} - \Phi\mathbf{W})^{-1} = \sum_{k=0}^{\infty} (\Phi\mathbf{W})^k \tag{63}$$

As discussed in Section 2.2, we directly estimate the distributional properties of $a'_{i,t} = a_{i,t}/y_{i,t-1}$ (mean, $\bar{\alpha}'_i$, and standard deviation, δ'_i) rather than unpacking its internal structure, for example,

Table 4: **The importance of the network topology**. The table reports the coefficients from regressing lending growth on liquidity ratio, ROA, deposit rates, loan rates, and stock return. Deposit (loan) rates are defined as interest expense (income) divided by total deposits (loans). Columns 1 and 2 use lending growth from the Call Reports. Columns 3 and 4 use lending growth net of the network, defined as $\bar{\alpha}' + \nu_t'$ from equation (39). Bank and time fixed effects are included. Standard errors are robust and displayed in parentheses. *,** , and *** correspond to 10-, 5-, and 1% significance level, respectively.

	Lending Growth			
	(1)	(2)	(3)	(4)
LR	0.025^{***}	0.038^{***}	0.014	0.030^{***}
	(0.008)	(0.009)	(0.009)	(0.009)
ROA	1.127^{***}	1.197^{***}	-0.357	-0.498^{**}
	(0.215)	(0.208)	(0.222)	(0.217)
Deposit rate	-0.010^{***}	-0.010^{***}	-0.010^{***}	-0.013^{***}
	(0.001)	(0.002)	(0.001)	(0.002)
Loan rate	-0.003^{***}	-0.002^{***}	-0.003^{***}	-0.002^{***}
	(0.001)	(0.001)	(0.001)	(0.001)
Stock Return	-0.001^{***}		-0.000^{***}	
	(0.000)		(0.000)	
Network	No	No	Yes	Yes
Bank FE	Yes	Yes	Yes	Yes
Time FE	No	Yes	No	Yes
Obs.	22,000	22,000	22,000	22,000
Adj. R^2	0.089	0.137	0.149	0.178

how $a_{i,t}$ depends on bank i's liquid assets in quarter t. Therefore, our empirical exercise focuses on characterizing this network amplification operator, i.e., the second step of the model mechanism.

As shown in (41), the network amplification mechanism increases the equilibrium level of bank lending relative to the level without network effects (i.e., $(\mathbf{I} - \Phi\mathbf{W})^{-1}\bar{\alpha}'$ vs. $\bar{\alpha}'$) but it also amplifies the sensitivity of aggregate bank lending to shocks through strategic complementarity in banks' decisions (i.e., $(\mathbf{I} - \Phi\mathbf{W})^{-1}\nu_t'$ vs. ν_t'). Next, we characterize how the network amplification mechanism affects both the expected level of bank lending and volatility.

For implications of network amplification on loan amount, we multiply the model-implied

Figure 4: **Network propagation and aggregate credit supply**. This figure reports the mean (Panel A) and volatility (Panel B) of aggregate credit supply conditional on the outstanding loan amounts of the previous period (i.e., $\{y_{i,t-1}\}_{i=1}^{N}$) equal to the sample average. In both panels, the statistics are decomposed into each round of network propagation. We report results from our data network and the uniform network with equally connected banks.

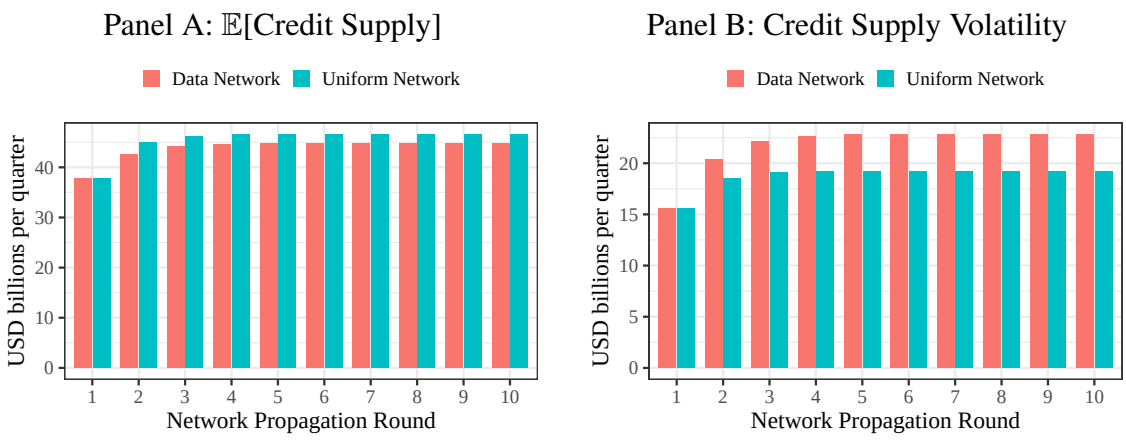

loan growth rate, $n_{i,t}$, by the average loan amounts in our sample. We compute the expected level and volatility of $y_{i,t}$, i.e., $\mathbb{E}_{t-1}[y_{i,t}] = y_{i,t-1}\mathbb{E}_{t-1}[n_{i,t}]$ and $\sqrt{\mathbf{Var}_{t-1}[y_{i,t}]} = y_{i,t-1}\sqrt{\mathbf{Var}_{t-1}[n_{i,t}]}$, conditional on $y_{i,t-1}$ being equal to the sample average. The steps have been laid out in (45) to (48) in Section 3.5. When computing the equilibrium, we use the estimates of μ_ϕ, σ_ϕ, $\bar{\alpha}'_i$, and δ'_i and, for the adjacency matrix, we take the average of $\mathbf{W}'$ across the 44 quarters in our sample.

In Figure 4, we decompose the mean (Panel A) and volatility (Panel B) of aggregate bank lending into rounds of network propagation as shown in (63). In both panels, the first column shows the value without network effects, and each subsequent column corresponds to the cumulative effect after each round of network propagation. For both mean and volatility, the second and third columns correspond respectively to direct network linkages and first-degree of indirect linkages. Both direct and first-degree indirect linkages have significant influence on the equilibrium level of aggregate lending. Linkages that are more than two steps away are less important. This feature can be attributed to both $\mathbf{W}'$ and ϕ_i. The smaller ϕ_i is, the weaker the effects of distant linkages are. As shown in (63), ϕ_i is effectively the discount factor for network linkages.

In Figure 4, we demonstrate the importance of network topology. In the counterfactual network ("uniform network"), banks are equally connected or edges are evenly distributed among bank pairs ($w'_{ij} = 1/(N-1)$). The network amplification mechanism depends on Φ and $\mathbf{W}'$. By comparing the data network and this counterfactual network, we focus on the role of $\mathbf{W}'$ as

Figure 5: **Network topology.** This figure compares the data network given by the average adjacency matrix W' and the uniform network. We only keep 10% of linkages and 20% of nodes for tractability. The size of node i is proportional to δ_i' (the volatility of structural shock to loan growth).

Panel A: Data Network Panel B: Uniform Network

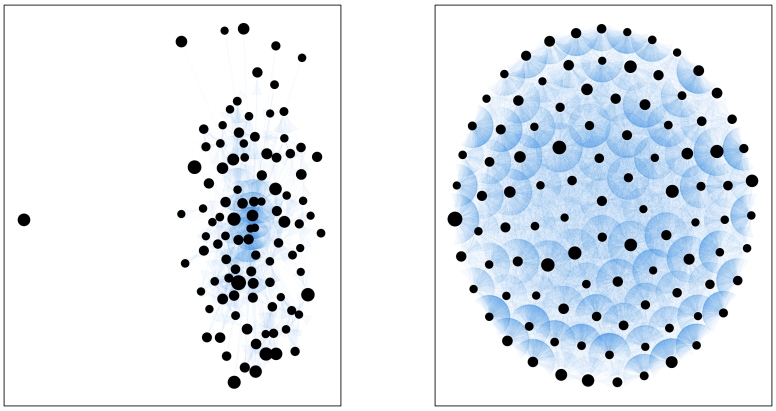

the amplification effects of both networks incorporate $\phi_i > 0$. In Panel A, relative to the uniform network, the data network generates a slightly lower expected level of aggregate credit supply, and in each round of network propagation, the cumulative effects of data network are dominated by those of the uniform network. In Panel B, relative to the uniform network, the data network generates a much higher volatility. In both panels, the first columns under the two networks have the same value because they represent the values without network effects. The divergence starts in the first round of network propagation, which is captured by the second column.

In Figure 5, we compare the data network, given by the average adjacency matrix W', and uniform network. The size of node i is proportional to δ_i' (volatility of bank-level shock). The most connected nodes are placed at the center while the least connected are at the periphery (Fruchterman and Reingold, 1991).[26] The distribution of edges of the data network is much more uneven than that of the uniform network, suggesting stronger heterogeneity in banks' network positions.

The topology of network is important for the aggregation of idiosyncratic shocks (Acemoglu et al., 2012). We show in Figure 6 that the data network generates a higher volatility than the uniform network. We simulate 10,000 times a vector of 500 i.i.d. standard normal shocks, ν'. For each simulation, we calculate the simple average (which has a standard deviation of $\sqrt{\frac{1}{500}} = 0.045$) and

[26] In Fruchterman and Reingold (1991), linked nodes are close and nodes should be distributed widely for visibility.

Figure 6: **Network and fat tails.** We simulate 10,000 times a vector of 500 i.i.d. standard normal shocks and, for each simulation, we calculate the average of the shocks and the averages of shocks (denoted by ν) amplified by two networks, i.e., the averages of vector $(\mathbf{I} - \Phi\mathbf{G})^{-1}\nu$ where the two networks are $\mathbf{G} = \mathbf{W}'$ (the data network) and the uniform network. The figure reports the frequency distribution of the three averages over 10,000 simulations.

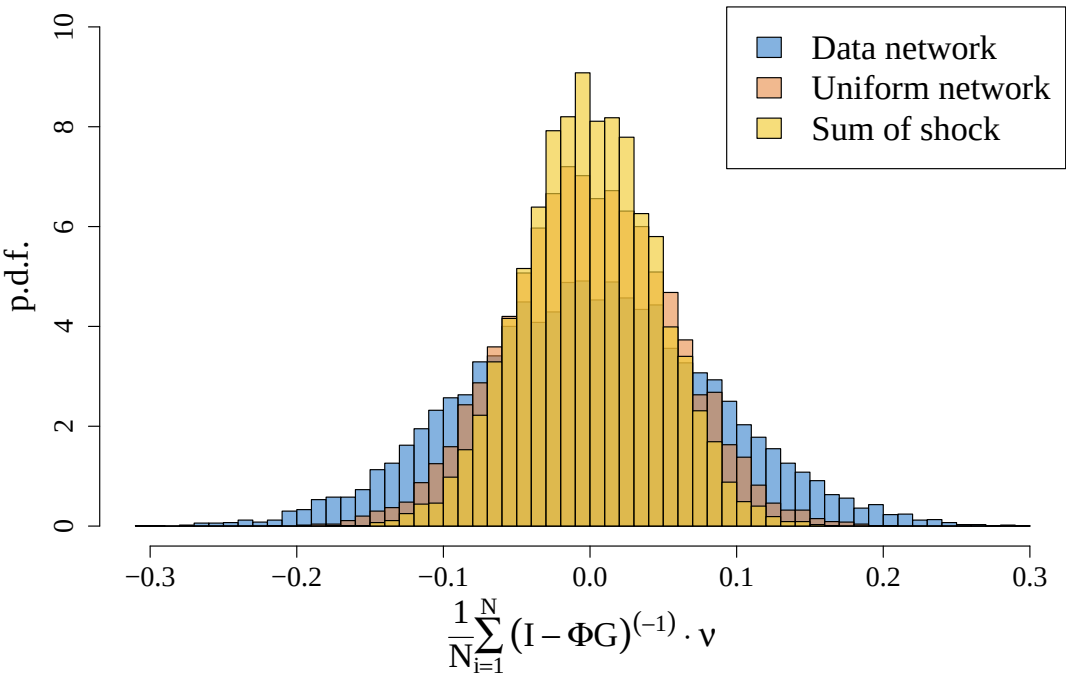

the average of shocks amplified by two networks, i.e., the averages of vector $(\mathbf{I} - \Phi\mathbf{G})^{-1}\nu'$ where the two networks are $\mathbf{G} = \mathbf{W}'$ (the data network) and the uniform network. The simple average represents one hypothetical scenario without any network propagation of shocks, and intuitively, the aggregation exhibits the smallest volatility (dispersion of outcome of the 10,000 experiments). The case with shocks propagated by a uniform network features network amplification, and the aggregation generates a higher volatility than that from the simple average. Finally, the data network generates the highest volatility, suggesting that, relative to the uniform network, the data network has a topology of linkages that is more prone to amplify the fluctuation of aggregate bank lending.

4.3 Identifying systemically important banks

In the homogeneous-ϕ model, we define volatility key bank in (49) as the bank with the highest network impulse response function (NIRF). In (51), we show that the volatility of aggregate credit supply can be decomposed into individual banks' NIRFs. Therefore, ranking banks by their NIRFs is equivalent to ranking banks by their contributions to credit-supply fluctuation. Next, we demonstrate how banks' positions in the network, given by the adjacency matrix $\mathbf{W}'$, and the sizes of their structural shocks, $\{\delta_i'^2\}_{i=1}^N$, determine their NIRFs. Banks differ significantly in both aspects that are reflected in their NIRFs.

In Figure 7, we plot the loan amount implied by the size of bank-specific shock to growth rate (i.e., $y_{t-1}\delta_i'$), and network impulse response function (NIRF) for the top 500 banks. For both quantities, we set the average loan amounts from the previous period, y_{t-1}, to the sample average. When $y_{t-1}\delta_i'$ and NIRF are close for a bank, the payment network does not generate powerful externality for this bank; in other words, what the bank contributes is close to the size of its own shock. In contrast, when NIRF and $y_{t-1}\delta_i'$ differ for a bank, the bank's position in payment network significantly affects its contribution to the volatility of aggregate credit supply. In Figure 7, we see the wedge between NIRF and $y_{t-1}\delta_i'$ is particularly large for a handful of banks. This finding suggests that the payment network amplifies the shocks to a relatively small number of banks and therefore generates heterogeneity in banks' contribution to the volatility of aggregate credit supply that is beyond the heterogeneity from banks' difference in the size of their shocks δ_i'.

Next, in Figure 8, we examine how shocks propagate within and across the tightly-connected cluster of banks identified in the Fedwire payment network. We partition banks into a cluster C and a periphery P using the Louvain community-detection algorithm applied to the positive part of the adjacency matrix $\mathbf{W}'$, whose (i,j)-th element w_{ij}', defined in (36), aggregates the mean and variance of bilateral payment flows between banks i and j. The algorithm maximizes modularity—the excess of within-group edge weight over its expectation under a null model of random connections—so the resulting cluster comprises banks whose mutual payment flows are disproportionately large relative to their overall connectivity. By construction, the block $\mathbf{W}'_{CC}$ is dense while the cross-block matrices $\mathbf{W}'_{CP}$ and $\mathbf{W}'_{PC}$ are sparse, yielding the near-block-diagonal structure of $\mathbf{W}'$ that underlies the propagation patterns documented below.

Panel A decomposes the cumulative volatility of aggregate credit supply, following Proposition 3, into within- and outside-cluster contributions round by round. The within-cluster term dominates at every horizon: it accounts for the bulk of total volatility already by the second round,

Figure 7: **Bank shock size and NIRF.** In this figure, we plot the size of bank-specific shock, δ_i', and network impulse response function (NIRF) for the top five hundred banks (ranked by the size of NIRF) in our sample. Both δ_i' and NIRF are scaled using average lending in the previous period. Panel A computes NIRFs using the estimate of μ_ϕ. The confidence intervals are 95% intervals computed using the estimate of σ_ϕ. Panel B uses 500 Monte Carlo simulations to generate a distribution of NIRF along with standard errors. The correlation between NIRFs using two methods exceeds 99%.

Panel A: NIRF based on mean and variance

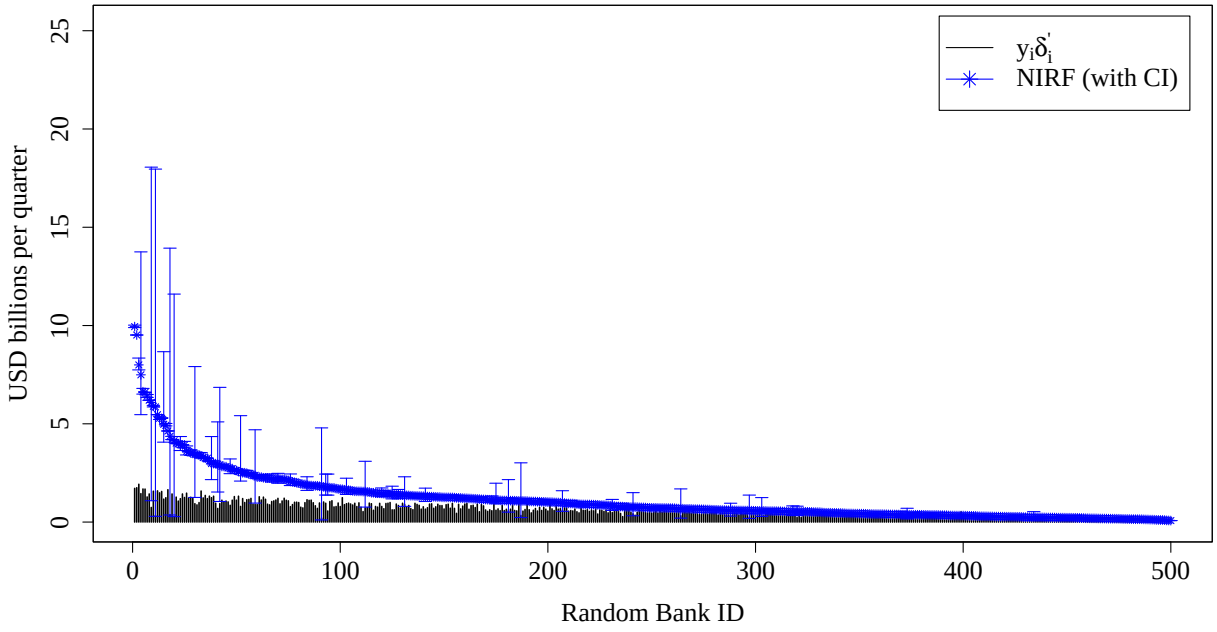

Panel B: NIRF based on Monte Carlo simulations

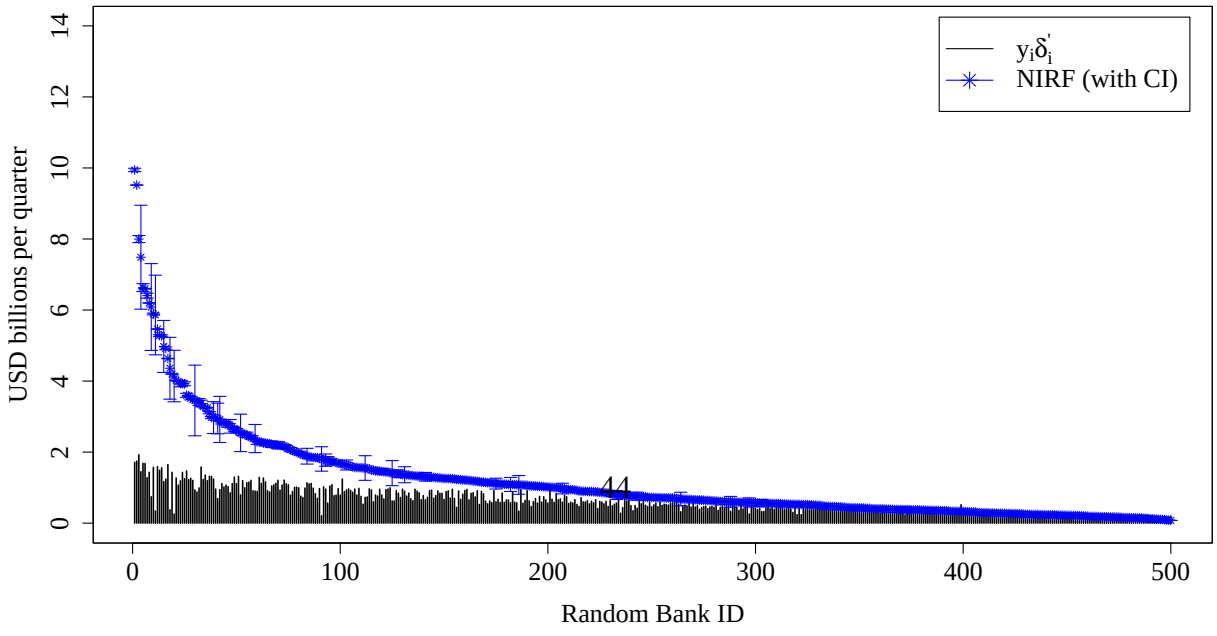

Figure 8: **Cluster Shock Propagation: Internal Echo and Leakage.** We group banks into a cluster and a periphery using a community-detection algorithm applied to the payment-flow network $\mathbf{W}'$. Panel A decomposes cumulative credit-supply volatility into within-cluster and outside-cluster contributions across rounds of network propagation. Panel B traces the average impulse response of cluster banks to a unit shock hitting the cluster, and breaks it into three components: the portion that stays and circulates within the cluster (echo), the portion that escapes to the periphery (leakage), and the portion that returns from the periphery back into the cluster (re-entry).

Panel A: Within- vs. Outside-Cluster Volatility

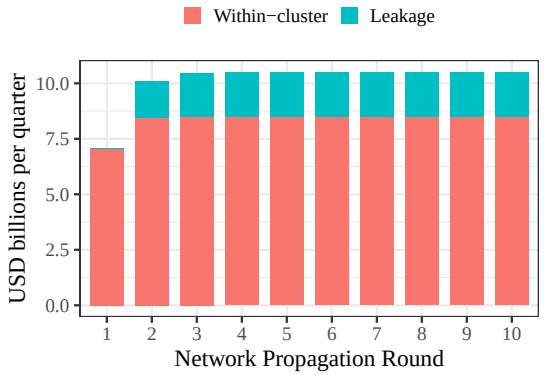

Panel B: Echo, Leak, and Re-Entry IRF

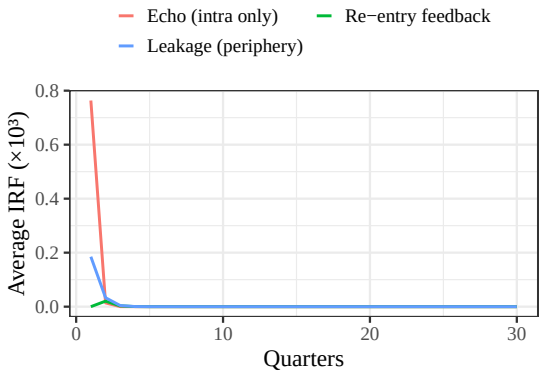

while the outside-cluster contribution remains negligible throughout. This concentration mirrors the finding in Section 4.2 that the real network generates substantially higher credit-supply volatility than the uniform benchmark of Figure 4; here we show that this excess volatility originates almost entirely within the dense cluster, whose members recycle liquidity and amplify shocks among themselves through the strategic complementarity mechanism of Proposition 1.

Panel B decomposes the cluster's impulse response into three analytically distinct phases, each tied to a specific block of the propagation matrix $\mathbf{M}(\Phi, \mathbf{W}')$ defined in (20). Let $A_{CC} = \Phi_{CC}\mathbf{W}'_{CC}$ denote the intra-cluster block of the effective propagation matrix. The *echo* phase is captured by $A^h_{CC}\varepsilon_0$: the shock circulates purely within the cluster at a rate governed by $\rho(A_{CC})$, the spectral radius of A_{CC}. The *leakage* is the periphery's average response to the same shock, driven by the cross-block $\mathbf{W}'_{PC}$. The *re-entry* feedback is the residual between the full cluster response and the echo term; it corresponds to the round-trip $C \to P \to C$ through the periphery. Formally, integrating out the periphery via the Schur complement yields an effective cluster interaction matrix $\widetilde{\mathbf{W}}_{CC} = \mathbf{W}'_{CC} + \mathbf{W}'_{CP}(\mathbf{I} - \mathbf{W}'_{PP})^{-1}\mathbf{W}'_{PC}$, where the second term captures how a shock that leaks from C to P propagates through the periphery—at a speed determined by $(\mathbf{I} - \mathbf{W}'_{PP})^{-1}$—and re-enters C via $\mathbf{W}'_{CP}$; the re-entry component in Panel B is the difference between the impulse response under $\widetilde{\mathbf{W}}_{CC}$ and that under $\mathbf{W}'_{CC}$ alone.

Figure 9: **Network propagation: The planner's solution vs. market equilibrium**. This figure reports the mean (Panel A) and volatility (Panel B) of aggregate credit supply conditional on the outstanding loan amounts of the previous period (i.e., $\{y_{i,t-1}\}_{i=1}^{N}$). The loan amounts of the previous period are set to the full-sample average. In both Panel A and B, the statistics are decomposed into each round of network propagation.

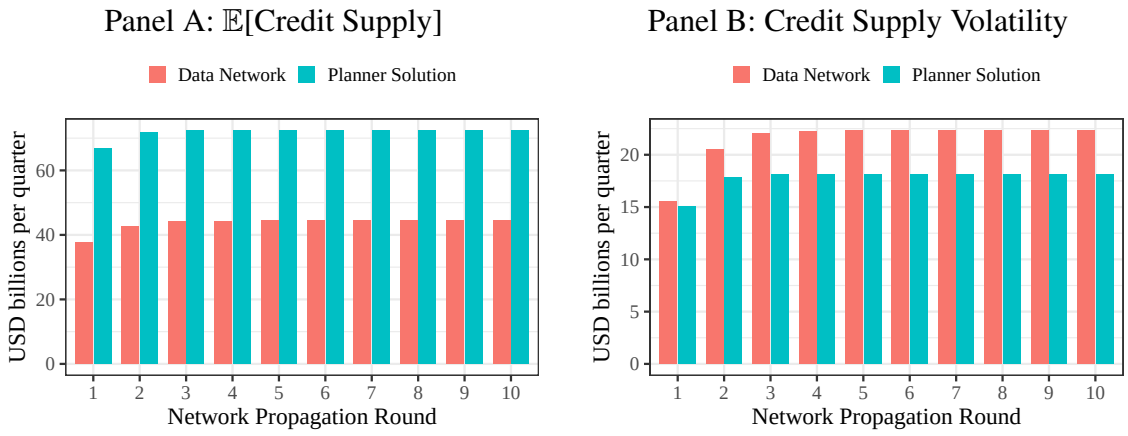

Taken together, the two panels confirm the concentration result of Section 3.5 – a relatively small subset of banks drives the volatility, while also showing that the cluster is not fully closed: a non-negligible share of the shock energy it generates eventually reaches the broader banking system.

4.4 Quantifying the network externalities

Network propagation. We apply the framework in Section 3.6 to compare the market equilibrium and the planner's solution. The planner maximizes the total profits of all banks, internalizing the network externality generated by depositors' payment flows. As a result, the planner does not internalize the net interest margin effect coming from endogenous interest rates. In Panel A of Figure 9, we decompose the expected aggregate credit supply (conditional on lagged loan amounts, i.e., $\{y_{i,t-1}\}_{i=1}^{N}$, equal to the sample average) into rounds of network propagation. The first column in both cases is generated by the loan growth rate absent of network effects (i.e., $\bar{\alpha}_i'$ for the market equilibrium and $\widetilde{\phi}_i\alpha_i'/\phi$ in the planner's solution). The second column adds to the first column impact of direct network linkages, and the third column adds to the second column impact of first-degree indirect linkages. Once the network effects are activated (starting from the second column), the planner's solution features a higher expected level of credit supply. The wedge is stable across rounds of network propagation, suggesting that the main difference between the

Figure 10: **Rolling estimation.** Each rolling window has 20 quarters. We report the estimate of the mean of the network multiplier constructed using the estimate of σ_ϕ in Panel A. Panel B plots the conditional volatility in the rolling window.

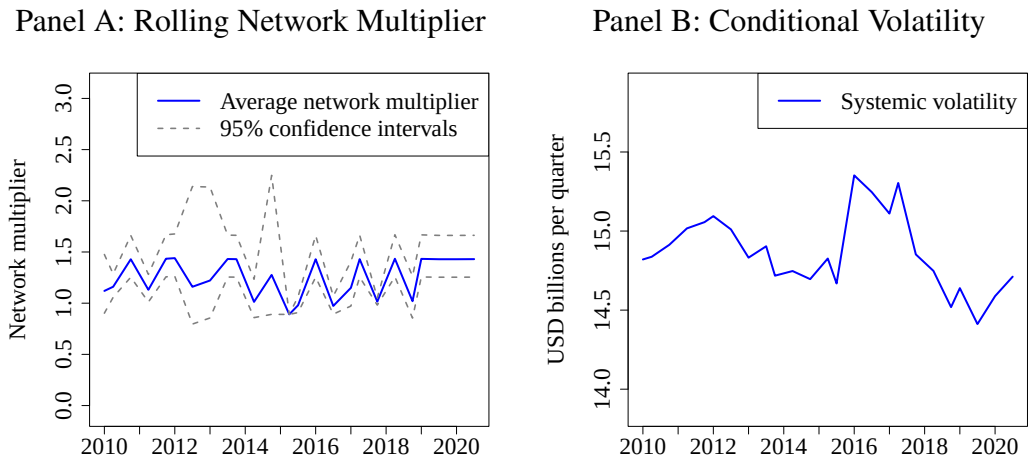

planner's solution and market equilibrium is due to direct network linkages. In Panel B of Figure 9, we decompose the volatility of aggregate credit supply (conditional on $\{y_{i,t-1}\}_{i=1}^N$) into rounds of network propagation. By internalizing the spillover effects of individual banks' lending decisions, the planner becomes less responsive to shocks than the market equilibrium, generating a volatility that is around 10% lower.

Overall, the results in Figure 9 show that, by internalizing the liquidity spillover effects of payment network, the planner generates a higher expected level and lower volatility of aggregate bank lending than the market equilibrium; in other words, payment network externality induces a lower expected level of credit supply and higher volatility without a planner's intervention.

Rolling-sample estimation. In Figure 10, we present the rolling-window estimation results. We plot the estimates of the mean of ϕ_i and construct confidence intervals using the estimates of σ_ϕ. Each window contains 20 quarters. The horizon axis marks the last quarter of a rolling sample. The multiplier is stable over time, but its variance demonstrates significant variation over time. For example, after the GFC and at the onset of the COVID-19 pandemic, banks experienced larger shocks and greater heterogeneity in shock exposure, so, intuitively, our estimate of μ_ϕ contains more noise (a wider confidence interval).

5 Conclusion

When financing loans with deposits, a bank must hold enough liquid assets to cover potential deposit outflow, as loans are illiquid and cannot be readily sold for cash. The money multiplier—the ratio of loans funded by deposits to a bank's liquid assets—cannot be overstretched. Except for the extreme events of bank run, deposit outflows occur because depositors make payments to one another, causing liquidity to churn among banks. The payment senders' banks lose deposits and reserves (the settlement assets in payment system), while the recipients' banks gain deposits and reserves. Therefore, banks' liquidity conditions are intrinsically interconnected, and the equilibrium money multiplier depends on the random graph of depositors' interbank payment flows.

The payment function of deposits gives rise to strategic complementarity in banks' lending decisions, amplifying shocks to individual banks and contributing to the fluctuation in aggregate credit supply. Our network analysis reveals a subset of systemically important banks that drive the aggregate fluctuation due to their special positions in the payment-flow network. We also quantify the network externality by comparing the planner's solution and market equilibrium. Policy interventions targeted at correcting the network externality can improve aggregate credit conditions and alleviate the misallocation of lending opportunities across banks.

Our paper offers a new perspective on money multiplier and velocity. The traditional concept of money multiplier is often explained in an artificial setting that is disconnected from the practice of modern banking (McLeay et al., 2014). We formalize the money multiplier through the natural link between the monetary base and the creation of credit and deposits: When financing lending with deposits, banks must have enough reserves to cover subsequent payment outflows. Moreover, we provide a network perspective on money velocity. The network structure of how deposits circulate across banks determines banks' liquidity risk and to what extent liquidity recycling within the banking system relaxes this liquidity constraint on banks' credit and money creation. Overall, we highlight the dual role of deposits as sources of funds for banks and means of payment for the rest of the economy, building a bridge between payment system and macro finance.

In the foreseeable future, payment system will undergo fundamental technological changes. In the area of digital payment, entrants with new technologies provide payment netting services, effectively rewiring payment flows and changing the network topology of interbank liquidity churn. Central banks around the world have been actively researching on new payment systems and their own digital payment platforms that will challenge the central role of deposits in payment systems

and change how payment systems redistribute liquidity across banks. So far, the discussion on payment systems has largely focused on operational efficiency and technological vulnerabilities. Our paper draws attention to bank credit supply and provides a novel framework for quantifying the impact of changes in payment-flow networks on aggregate credit conditions.

References

Acemoglu, D., V. M. Carvalho, A. Ozdaglar, and A. Tahbaz-Salehi (2012). The network origins of aggregate fluctuations. *Econometrica 80*(5), 1977–2016.

Acemoglu, D., A. Ozdaglar, and A. Tahbaz-Salehi (2015). Systemic risk and stability in financial networks. *American Economic Review 105*, 564–608.

Acharya, V. and O. Merrouche (2013). Precautionary hoarding of liquidity and interbank markets: Evidence from the subprime crisis. *Review of Finance 17*(1), 107–160.

Acharya, V. V., R. S. Chauhan, R. G. Rajan, and S. Steffen (2022). Liquidity dependence: Why shrinking central bank balance sheets is an uphill task. Working paper, Frankfurt School of Finance & Management, New York University, and University of Chicago.

Acharya, V. V., L. H. Pedersen, T. Philippon, and M. Richardson (2016, 10). Measuring Systemic Risk. *The Review of Financial Studies 30*(1), 2–47.

Acharya, V. V. and T. Yorulmazer (2007). Too many to fail—an analysis of time-inconsistency in bank closure policies. *Journal of Financial Intermediation 16*(1), 1–31.

Adrian, T. and M. K. Brunnermeier (2016, July). Covar. *American Economic Review 106*(7), 1705–41.

Afonso, G., D. Duffie, L. Rigon, and H. S. Shin (2022). Interbank payment timing is still closely coupled. Working paper, Bank for International Settlements, Federal Reserve Bank of New York, and Stanford University.

Afonso, G., A. Kovner, and A. Schoar (2011). Stressed, not frozen: The federal funds market in the financial crisis. *The Journal of Finance 66*(4), 1109–1139.

Afonso, G. and R. Lagos (2015). Trade dynamics in the market for federal funds. *Econometrica 83*(1), 263–313.

Afonso, G. and H. S. Shin (2011). Precautionary demand and liquidity in payment systems. *Journal of Money, Credit and Banking 43*(s2), 589–619.

Albuquerque, R., L. Cabral, and J. Guedes (2019, 03). Incentive Pay and Systemic Risk. *The Review of Financial Studies 32*(11), 4304–4342.

Allen, F. and A. Babus (2009). Chapter 21 - networks in finance. The Network Challenge: Strategy, Profit, and Risk in an Interlinked World. Pearson Education.

Allen, F., A. Babus, and E. Carletti (2012). Asset commonality, debt maturity and systemic risk. *Journal of Financial Economics 104*(3), 519–534. Market Institutions, Financial Market Risks and Financial Crisis.

Allen, F. and D. Gale (2000). Financial contagion. *Journal of Political Economy 108*(1), 1–33.

Alvarez, F., A. Atkeson, and C. Edmond (2009). Sluggish responses of prices and inflation to monetary shocks in an inventory model of money demand. *The Quarterly Journal of Economics 124*(3), 911–967.

Alvarez, F. and F. Lippi (2009). Financial innovation and the transactions demand for cash. *Econometrica 77*(2), 363–402.

Anderson, H., S. Erol, and G. Ordoñez (2020, August). Interbank networks in the shadows of the federal reserve act. Working Paper 27721, National Bureau of Economic Research.

Anselin, L. (1988). *Spatial econometrics: methods and models*. Studies in operational regional science. Kluwer Academic Publishers.

Artavanis, N., D. Paravisini, C. Robles-Garcia, A. Seru, and M. Tsoutsoura (2022). One Size Doesn't Fit All: Heterogeneous Depositor Compensation During Periods of Uncertainty. Working Papers 30369, National Bureau of Economic Research.

Ashcraft, A. and C. H. Bleakley (2006). On the market discipline of informationally-opaque firms: Evidence from bank borrowers in the federal funds market. Staff Reports 257, Federal Reserve Bank of New York.

Ashcraft, A., J. McAndrews, and D. Skeie (2011). Precautionary reserves and the interbank market. *Journal of Money, Credit and Banking 43*(s2), 311–348.

Ashcraft, A. B. and D. Duffie (2007, May). Systemic illiquidity in the federal funds market. *American Economic Review 97*(2), 221–225.

Babus, A. (2016). The formation of financial networks. *The RAND Journal of Economics 47*(2), 239–272.

Bai, J., A. Krishnamurthy, and C.-H. Weymuller (2018). Measuring liquidity mismatch in the banking sector. *The Journal of Finance 73*(1), 51–93.

Ballester, C., A. Calvó-Armengol, and Y. Zenou (2006). Who's who in networks. Wanted: The key player. *Econometrica 74*, 1403–1417.

Baron, M. (2020). Countercyclical Bank Equity Issuance. *The Review of Financial Studies 33*(9), 4186–4230.

Baumol, W. J. (1952). The transactions demand for cash: An inventory theoretic approach. *The Quarterly Journal of Economics 66*(4), 545–556.

Bech, M. (2008). Intraday liquidity management: A tale of games banks play. *Economic Policy Review 14*.

Bech, M. and E. Atalay (2010). The topology of the federal funds market. *Physica A: Statistical Mechanics and its Applications 389*(22), 5223–5246.

Bech, M. and B. Hobijn (2007). Technology diffusion within central banking: The case of real-time gross settlement. *International Journal of Central Banking 3*(3), 147–181.

Bech, M., A. Martin, and J. McAndrews (2012). Settlement liquidity and monetary policy implementation–lessons from the financial crisis. *Economic Policy Review 18*(1).

Bech, M. and C. Monnet (2016). A search-based model of the interbank money market and monetary policy implementation. *Journal of Economic Theory 164*, 32–67. Symposium Issue on Money and Liquidity.

Bech, M. L. and R. Garratt (2003). The intraday liquidity management game. *Journal of Economic Theory 109*(2), 198 – 219. Festschrift for Karl Shell.

Begenau, J. (2020). Capital requirements, risk choice, and liquidity provision in a business-cycle model. *Journal of Financial Economics 136*(2), 355–378.

Benoit, S., J.-E. Colliard, C. Hurlin, and C. Pérignon (2016, 06). Where the Risks Lie: A Survey on Systemic Risk. *Review of Finance 21*(1), 109–152.

Bhattacharya, S. and D. Gale (1987). Preference shocks, liquidity, and central bank policy. In W. Barnett and K. Singleton (Eds.), *New approaches to monetary economics*. Cambridge, UK: Cambridge University Press.

Bianchi, J. and S. Bigio (2022). Banks, liquidity management, and monetary policy. *Econometrica 90*(1), 391–454.

Bigio, S. and Y. Sannikov (2019). A model of intermediation, money, interest, and prices. Working paper, Stanford and UCLA.

Billio, M., M. Getmansky, A. W. Lo, and L. Pelizzon (2012). Econometric measures of connectedness and systemic risk in the finance and insurance sectors. *Journal of Financial Economics 104*(3), 535–559.

Blasques, F., F. Bräuning, and I. van Lelyveld (2018). A dynamic network model of the unsecured interbank lending market. *Journal of Economic Dynamics and Control 90*, 310–342.

Blume, L. E., W. A. Brock, S. N. Durlauf, and R. Jayaraman (2015). Linear social interactions models. *Journal of Political Economy 123*(2), 444–496.

Bollerslev, T. and J. M. Wooldridge (1992). Quasi-maximum likelihood estimation and inference in dynamic models with time-varying covariances. *Econometric Reviews 11*(2), 143–172.

Bolton, P., H. Chen, and N. Wang (2011). A unified theory of Tobin's q, corporate investment, financing, and risk management. *The Journal of Finance 66*(5), 1545–1578.

Bolton, P., Y. Li, N. Wang, and J. Yang (2020). Dynamic banking and the value of deposits. Working Paper 28298, National Bureau of Economic Research.

Boss, M., H. Elsinger, M. Summer, and S. Thurner (2004). Network topology of the interbank market. *Quantitative Finance 4*(6), 677–684.

Bramoullé, Y., H. Djebbari, and B. Fortin (2009). Identification of peer effects through social networks. *Journal of Econometrics 150*(1), 41–55.

Bräuning, F. and F. Fecht (2016, 08). Relationship Lending in the Interbank Market and the Price of Liquidity*. *Review of Finance 21*(1), 33–75.

Brown, M., B. Guin, and S. Morkoetter (2020). Deposit withdrawals from distressed banks: Client relationships matter. *Journal of Financial Stability 46*, 100707.

Brunnermeier, M. K. and Y. Sannikov (2016). The I theory of money. Working paper, Princeton University.

Brusco, S. and F. Castiglionesi (2007). Liquidity coinsurance, moral hazard, and financial contagion. *Journal of Finance 62*(5), 2275–2302.

Cabrales, A., P. Gottardi, and F. Vega-Redondo (2017, 07). Risk Sharing and Contagion in Networks. *The Review of Financial Studies 30*(9), 3086–3127.

Caccioli, F., J. D. Farmer, N. Foti, and D. Rockmore (2015). Overlapping portfolios, contagion, and financial stability. *Journal of Economic Dynamics and Control 51*, 50–63.

Calomiris, C. W. and J. R. Mason (1997). Contagion and bank failures during the great depression: The june 1932 chicago banking panic. *The American Economic Review 87*(5), 863–883.

Calvó-Armengol, A., E. Patacchini, and Y. Zenou (2009). Peer effects and social networks in education. *The Review of Economic Studies 76*(4), 1239–1267.

Castiglionesi, F. and M. Eboli (2018, 05). Liquidity Flows in Interbank Networks*. *Review of Finance 22*(4), 1291–1334.

Castiglionesi, F. and W. Wagner (2013). On the efficiency of bilateral interbank insurance. *Journal of Financial Intermediation 22*(2), 177–200.

Cavalcanti, R. d. O. and N. Wallace (1999). A model of private bank-note issue. *Review of Economic Dynamics 2*(1), 104 – 136.

Chang, B. and S. Zhang (2019). Endogenous market making and network formation. Working paper, Wisconsin University and LSE.

Chapman, J., M. Gofman, and S. Jafri (2019). High-frequency analysis of financial stability. Working paper, Bank of Canada and University of Rochester.

Cifuentes, R., G. Ferrucci, and H. S. Shin (2005). Liquidity risk and contagion. *Journal of the European Economic Association 3*(2/3), 556–566.

Cocco, J. F., F. J. Gomes, and N. C. Martins (2009). Lending relationships in the interbank market. *Journal of Financial Intermediation 18*(1), 24–48.

Cohen-Cole, E., A. Kirilenko, and E. Patacchini (2014). Trading networks and liquidity provision. *Journal of Financial Economics 113*(2), 235–251.

Cohen-Cole, E., E. Patacchini, and Y. Zenou (2015). Static and dynamic networks in interbank markets. *Network Science 3*(1), 98–123.

Copeland, A., D. Duffie, and Y. Yang (2021). Reserves were not so ample after all. Staff Reports 974, Federal Reserve Bank of New York.

Corbae, D. and M. Gofman (2019). Interbank trading, collusion, and financial regulation. Working paper, University of Rochester and University of Wisconsin - Madison.

Correa, R., W. Du, and G. Y. Liao (2020). U.S. banks and global liquidity. Working Paper 27491, National Bureau of Economic Research.

Craig, B. and Y. Ma (2021). Intermediation in the interbank lending market. *Journal of Financial Economics*.

d'Avernas, A. and Q. Vandeweyer (2021). Intraday liquidity and money market dislocations. Working paper, Stockholm School of Economics and University of Chicago Booth School of Business.

de Paula, A. (2017). Econometrics of network models. In *Advances in Economics and Econometrics: Theory and Applications, Eleventh World Congress*, pp. 268–323. Cambridge University Press.

Décamps, J.-P., T. Mariotti, J.-C. Rochet, and S. Villeneuve (2011). Free cash flow, issuance costs, and stock prices. *The Journal of Finance 66*(5), 1501–1544.

Degryse, H. and G. Nguyen (2007). Interbank exposures: An empirical examination of contagion risk in the belgian banking system. *International Journal of Central Banking 3*(2), 123–171.

Denbee, E., C. Julliard, Y. Li, and K. Yuan (2021). Network risk and key players: A structural analysis of interbank liquidity. *Journal of Financial Economics 141*(3), 831–859.

Diamond, D. W. and P. H. Dybvig (1983). Bank runs, deposit insurance, and liquidity. *Journal of Political Economy 91*(3), 401–419.

Diebold, F. X. and K. Yılmaz (2014). On the network topology of variance decompositions: Measuring the connectedness of financial firms. *Journal of Econometrics 182*(1), 119–134.

Ding, D., R. B. Gonzalez, Y. Ma, and Y. Zeng (2025). The Effect of Instant Payments on the Banking System: Liquidity Transformation and Risk-taking. *Banco Central do Brasil Working Paper Series*.

Donaldson, J. R., G. Piacentino, and A. Thakor (2018). Warehouse banking. *Journal of Financial Economics 129*(2), 250 – 267.

Drechsler, I., A. Savov, and P. Schnabl (2017, 05). The Deposits Channel of Monetary Policy. *The Quarterly Journal of Economics 132*(4), 1819–1876.

Drechsler, I., A. Savov, and P. Schnabl (2018). Liquidity, risk premia, and the financial transmission of monetary policy. *Annual Review of Financial Economics 10*(1), 309–328.

Drechsler, I., A. Savov, and P. Schnabl (2021). Banking on deposits: Maturity transformation without interest rate risk. *The Journal of Finance 76*(3), 1091–1143.

Duarte, F. and T. M. Eisenbach (2021). Fire-sale spillovers and systemic risk. *The Journal of Finance 76*(3), 1251–1294.

Duffie, D., S. Malamud, and G. Manso (2009). Information percolation with equilibrium search dynamics. *Econometrica 77*(5), 1513–1574.

Eisfeldt, A. L., B. Herskovic, and S. Liu (2023). Interdealer price dispersion. Working paper, UCLA.

Eisfeldt, A. L., B. Herskovic, S. Rajan, and E. Siriwardane (2022, 09). OTC Intermediaries. *The Review of Financial Studies 36*(2), 615–677.

Elhorst, J. P. (2010). Spatial panel data models. In M. M. Fischer and A. Getis (Eds.), *Handbook of Applied Spatial Analysis*, pp. 377–407. Springer Berlin Heidelberg.

Elliott, M., B. Golub, and M. O. Jackson (2015). Financial networks and contagion. *American Economic Review 104*(10), 3115–3153.

Erol, S. and G. Ordoñez (2017). Network reactions to banking regulations. *Journal of Monetary Economics 89*(C), 51–67.

Farboodi, M. (2014). Intermediation and voluntary exposure to counterparty risk. Working paper, University of Chicago.

Farboodi, M., G. Jarosch, and R. Shimer (2017, March). The emergence of market structure. Working Paper 23234, National Bureau of Economic Research.

Fruchterman, T. M. J. and E. M. Reingold (1991). Graph drawing by force-directed placement. *Software: Practice and Experience 21*(11), 1129–1164.

Furfine, C. H. (2000). Interbank payments and the daily federal funds rate. *Journal of Monetary Economics 46*(2), 535 – 553.

Gabrieli, S. and C.-P. Georg (2014). A network view on interbank market freezes. Discussion Papers 44/2014, Deutsche Bundesbank.

Galeotti, A., S. Goyal, M. O. Jackson, F. Vega-Redondo, and L. Yariv (2010, 01). Network Games. *The Review of Economic Studies 77*(1), 218–244.

Gersbach, H. (1998, January). Liquidity Creation, Efficiency, and Free Banking. *Journal of Financial Intermediation 7*(1), 91–118.

Glaeser, E. L. and J. Scheinkman (2000, December). Non-market interactions. Working Paper 8053, National Bureau of Economic Research.

Glasserman, P. and H. P. Young (2016, September). Contagion in financial networks. *Journal of Economic Literature 54*(3), 779–831.

Gofman, M. (2017). Efficiency and stability of a financial architecture with too-interconnected-to-fail institutions. *Journal of Financial Economics 124*(1), 113–146.

Gorton, G. (1988). Banking panics and business cycles. *Oxford Economic Papers 40*(4), 751–781.

Graham, B. S. (2008). Identifying social interactions through conditional variance restrictions. *Econometrica 76*(3), 643–660.

Greenwood, R., A. Landier, and D. Thesmar (2015). Vulnerable banks. *Journal of Financial Economics 115*, 471–485.

Gu, C., F. Mattesini, C. Monnet, and R. Wright (2013). Banking: A new monetarist approach. *The Review of Economic Studies 80*(2 (283)), 636–662.

Gurley, J. G. and E. S. Shaw (1960). *Money in a Theory of Finance*. Washington, D.C.: Brookings Institution.

Hamilton, J. D. (1996). The daily market for federal funds. *Journal of Political Economy 104*(1), 26–56.

Hart, O. and L. Zingales (2014). Banks are where the liquidity is. Working paper, Harvard University.

Hayashi, F. (2000). *Econometrics*. Princeton University Press: Princeton.

Heipertz, J., A. Ouazad, and R. Rancière (2019, July). The transmission of shocks in endogenous financial networks: A structural approach. Working Paper 26049, National Bureau of Economic Research.

Hendershott, T., D. Li, D. Livdan, and N. Schürhoff (2020). Relationship trading in over-the-counter markets. *The Journal of Finance 75*(2), 683–734.

Herskovic, B. (2018). Networks in production: Asset pricing implications. *The Journal of Finance 73*(4), 1785–1818.

Herskovic, B., B. Kelly, H. Lustig, and S. Van Nieuwerburgh (2020). Firm volatility in granular networks. *Journal of Political Economy 128*(11), 4097–4162.

Higgins, S. (2024). Financial Technology Adoption: Network Externalities of Cashless Payments in Mexico. *American Economic Review 114*(11), 3469–3512.

Hugonnier, J., B. Lester, and P.-O. Weill (2014). Heterogeneity in decentralized asset markets. Working paper, National Bureau of Economic Research.

Ibragimov, R., D. Jaffee, and J. Walden (2011). Diversification disasters. *Journal of Financial Economics 99*(2), 333–348.

Ihrig, J. (2019). Banks' demand for reserves in the face of liquidity regulations. On the economy blog, march 5, 2019, Federal Reserve Bank of St. Louis.

Iyer, R. and J.-L. Peydró (2011). Interbank contagion at work: Evidence from a natural experiment. *Review of Financial Studies 24*(4), 1337–1377.

Iyer, R. and M. Puri (2012, June). Understanding bank runs: The importance of depositor-bank relationships and networks. *American Economic Review 102*(4), 1414–45.

Jackson, M. O. and A. Pernoud (2021). Systemic risk in financial networks: A survey. *Annual Review of Economics 13*(1), 171–202.

Jackson, M. O. and Y. Zenou (2015). Chapter 3 - games on networks. Volume 4 of *Handbook of Game Theory with Economic Applications*, pp. 95–163. Elsevier.

Jasova, M., L. Laeven, C. Mendicino, J.-L. Peydró, and D. Supera (2021). Systemic risk and monetary policy: The haircut gap channel of the lender of last resort. CEPR Discussion Papers 16240, C.E.P.R. Discussion Papers.

Jiang, Z. and R. Richmond (2021). Origins of international factor structures. Working paper, NYU Stern and Northwestern Kellogg.

Jiménez, G., S. Ongena, J.-L. Peydró, and J. Saurina (2012, May). Credit supply and monetary policy: Identifying the bank balance-sheet channel with loan applications. *American Economic Review 102*(5), 2301–26.

Jiménez, G., S. Ongena, J.-L. Peydró, and J. Saurina (2014). Hazardous times for monetary policy: What do twenty-three million bank loans say about the effects of monetary policy on credit risk-taking? *Econometrica 82*(2), 463–505.

Kahn, C. M. and W. Roberds (2007). Transferability, finality, and debt settlement. *Journal of Monetary Economics 54*(4), 955–978.

Kahn, C. M. and W. Roberds (2009). Why pay? An introduction to payments economics. *Journal of Financial Intermediation 18*(1), 1–23.

Katz, L. (1953, March). A new status index derived from sociometric analysis. *Psychometrika 18*(1), 39–43.

Keynes, J. M. (1936). *The General Theory of Employment, Interest and Money*. Palgrave Macmillan: London.

Kiyotaki, N. and J. Moore (2000). Inside money and liquidity. Working paper, London School of Economics.

Kiyotaki, N. and J. Moore (2002). Evil is the root of all money. *American Economic Review 92*(2), 62–66.

Kopytov, A. (2019). Financial networks over the business cycle. 2019 Meeting Papers 159, Society for Economic Dynamics.

Krishnamurthy, A. and A. Vissing-Jørgensen (2012). The aggregate demand for treasury debt. *Journal of Political Economy 120*(2), 233–267.

Krishnamurthy, A. and A. Vissing-Jørgensen (2015). The impact of Treasury supply on financial sector lending and stability. *Journal of Financial Economics 118*(3), 571–600.

Kuo, D., D. R. Skeie, J. I. Vickery, and T. Youle (2013). Identifying term interbank loans from fedwire payments data. Staff Reports 603, Federal Reserve Bank of New York.

Lee, L., X. Liu, and X. Lin (2010). Specification and estimation of social interaction models with network structures. *The Econometrics Journal 13*(2), 145–176.

Lee, L.-f. and J. Yu (2010, April). A spatial dynamic panel data model with both time and individual fixed effects. *Econometric Theory 26*(02), 564–597.

Leitner, Y. (2005). Financial networks: Contagion, commitment, and private sector bailouts. *The Journal of Finance 60*, 2925–2953.

Li, D. and N. Schürhoff (2019). Dealer networks. *The Journal of Finance 74*(1), 91–144.

Li, Y. and Y. Li (2021). Payment risk and bank lending. Dice center working paper, The Ohio State University Fisher College of Business.

Liang, P., M. Sampaio, and S. Sarkisyan (2024). Digital Payments and Monetary Policy Transmission. *SSRN Electronic Journal*.

Lins, K. V., H. Servaes, and P. Tufano (2010). What drives corporate liquidity? An international survey of cash holdings and lines of credit. *Journal of Financial Economics 98*(1), 160 – 176.

Lopez-Salido, D. and A. Vissing-Jørgensen (2023). Reserve demand, interest rate control, and quantitative tightening. Working paper, Board of Governors of the Federal Reserve System.

Lu, L. and S. Luo (2019). The global effects of U.S. monetary policy on equity and bond markets: A spatial panel data model approach. Working paper, Federal Reserve Bank of Boston.

Lucas, R. E. J. and J. P. Nicolini (2015). On the stability of money demand. *Journal of Monetary Economics 73*, 48 – 65.

Martin, C., M. Puri, and A. Ufier (2018, May). Deposit inflows and outflows in failing banks: The role of deposit insurance. Working Paper 24589, National Bureau of Economic Research.

McAndrews, J. J. and S. M. Potter (2002). Liquidity effects of the events of September 11, 2001. *Federal Reserve Bank of New York Economic Policy Review 8*(2).

McLeay, M., A. Radia, and R. Thomas (2014). Money creation in the modern economy. Quarterly Bulletin 2014Q1, Bank of England.

Nagel, S. (2016, 07). The Liquidity Premium of Near-Money Assets*. *The Quarterly Journal of Economics 131*(4), 1927–1971.

Ozdagli, A. and M. Weber (2017, May). Monetary policy through production networks: Evidence from the stock market. Working Paper 23424, National Bureau of Economic Research.

Parlour, C. A., U. Rajan, and J. Walden (2020). Payment system externalities and the role of central bank digital currency. *Journal of Finance forthcoming*.

Piazzesi, M., C. Rogers, and M. Schneider (2019). Money and banking in a new keynesian model. Working paper, Stanford University.

Piazzesi, M. and M. Schneider (2016). Payments, credit and asset prices. Working paper, Stanford University.

Poole, W. (1968). Commercial bank reserve management in a stochastic model: Implications for monetary policy. *The Journal of Finance 23*(5), 769–791.

Quadrini, V. (2017). Bank liabilities channel. *Journal of Monetary Economics 89*, 25 – 44. Carnegie-Rochester-NYU Conference Series on the Macroeconomics of Liquidity in Capital Markets and the Corporate Sector.

Redding, S. J. and E. Rossi-Hansberg (2017). Quantitative spatial economics. *Annual Review of Economics 9*(Volume 9, 2017), 21–58.

Riddick, L. A. and T. M. Whited (2009). The corporate propensity to save. *The Journal of Finance 64*(4), 1729–1766.

Sarkisyan, S. (2024). Instant Payment Systems and Competition for Deposits. *SSRN Electronic Journal*.

Schumpeter, J. A. (1954). *History of Economic Analysis*. Oxford, U.K.: Oxford University Press.

Sidrauski, M. (1967). Rational choice and patterns of growth in a monetary economy. *The American Economic Review 57*(2), 534–544.

Sims, C. A. and T. Zha (1999). Error bands for impulse responses. *Econometrica 67*(5), 1113–1155.

Tobin, J. (1956). The interest-elasticity of transactions demand for cash. *The Review of Economics and Statistics 38*(3), 241–247.

Tobin, J. (1963). Commercial banks as creators of "money". Cowles Foundation Discussion Papers 159, Cowles Foundation for Research in Economics, Yale University.

Upper, C. and A. Worms (2004). Estimating bilateral exposures in the german interbank market: Is there a danger of contagion? *European Economic Review 48*(4), 827 – 849.

Üslü, S. (2019). Pricing and liquidity in decentralized asset markets. *Econometrica 87*(6), 2079–2140.

Wang, L. (2023). Regulating Competing Payment Networks. *Working Paper*.

Wang, T. (2019). Banks' wealth, banks' creation of money, and central banking. *International Journal of Central Banking 15*(3), 89–135.

Wells, S. (2004, September). Financial interlinkages in the United Kingdom's interbank market and the risk of contagion. Bank of England working papers 230, Bank of England.

Wicksell, K. (1907). The influence of the rate of interest on prices. *The Economic Journal 17*(66), 213–220.

Yang, Y. (2022). What quantity of reserves is sufficient? Working paper, Stanford University.

Zawadowski, A. (2013, 03). Entangled Financial Systems. *The Review of Financial Studies 26*(5), 1291–1323.

Zellner, A. (1962). An efficient method of estimating seemingly unrelated regressions and tests for aggregation bias. *Journal of the American Statistical Association 57*(298), 348–368.

A Appendix: Background Information on Payment Systems

The Fedwire Funds Service is the primary payment system in U.S. for large-value domestic and international USD payments. It is a real-time gross settlement system that enables participants to initiate funds transfer that are immediate, final, and irrevocable once processed. The service is operated by the Federal Reserve Banks. Financial institutions that hold an account with a Federal Reserve Bank are eligible to participate in the service and electronically transfer funds between each other. Such institutions include Federal Reserve member banks, nonmember depository institutions, and certain other institutions, such as U.S. branches and agencies of foreign banks.

Participants originate funds transfers by instructing a Federal Reserve Bank to debit funds from their own accounts and credit funds to the account of another participant. To make transfers, the following information is submitted to the Federal Reserve: the receiving bank's routing number, account number, name, and dollar amount being transferred. Each transaction is processed individually and settled upon receipt. Wire transfers sent via Fedwire are completed the same business day, with many being completed instantly. Participants may originate funds transfers online, by initiating a secure electronic message, or offline, via telephone procedures.

Participants of Fedwire Funds Service can use the platform to send or receive payments for their own accounts or on behalf of corporate or individual clients (i.e., the depositors). In the paper, we focus on Fedwire fund transfers made on behalf of banks' corporate or individual clients, which make up about 85% of total transactions in terms of transaction number.

The Fedwire Funds Service business day begins at 9:00 p.m. Eastern Standard Time (EST) on the preceding calendar day and ends at 7:00 p.m. EST, Monday through Friday, excluding designated holidays. For example, the Fedwire Funds Service opens for Monday at 9:00 p.m. on the preceding Sunday. The deadline for initiating transfers on behalf of a third party (i.e., a bank's depositor) is 6:00 p.m. EST on each business day and 7:00 p.m. EST for banks' own transactions. Under certain circumstances, Fedwire Funds Service operating hours may be extended.

To facilitate the smooth operation of the Fedwire Funds Service, the Federal Reserve Banks offer intraday credit, in the form of daylight overdrafts, to financially healthy Fedwire participants with regular access to the discount window. Many Fedwire Funds Service participants use daylight credit to facilitate payments throughout the operating day. Nevertheless, the Federal Reserve Policy on Payment System Risk prescribes daylight credit limits, which can constrain some Fedwire Funds Service participants' payment operations. Each participant is aware of these constraints and

is responsible for managing its account throughout the day.

The usage of Fedwire Funds Service grows over our sample period from 2010 to 2020, with the total number of transfers and transaction dollar value increasing by 47% and 38%, respectively. In 2020, approximately 5,000 participants initiate funds transfers over the Fedwire Funds Service, which processed an average daily volume of 727,313 payments, with an average daily value of approximately $3.3 trillion.[27] The distribution of these payments is highly skewed, with a median value of $24,500 and an average value of approximately $4.6 million. In particular, only about 7% of Fedwire fund transfers are for more than $1 million.

The other important interbank payment system in U.S. is the Clearing House Interbank Payments System (CHIPS), which is a private clearing house for large-value transactions between banks. In 2020, CHIPS processed an average daily volume of 462,798 payments, with an average daily value of approximately $1.7 trillion, about half of the daily value processed by Fedwire.[28] There are three key differences between CHIPS and Fedwire Funds Service. First, CHIPS is privately owned by The Clearing House Payments Company LLC, while Fedwire is operated by the Federal Reserve. Second, CHIPS has less than 50 member participants as of 2020, compared with thousands of banking institutions sending and receiving funds via Fedwire. Third, CHIPS is not a real-time gross settlement (RTGS) system like Fedwire, but a netting engine that uses bilateral and multi-lateral netting to consolidates pending payments into single transactions. The netting mechanism significantly reduces the impact of payment flows on banks' decision making (and therefore our sample focuses on the RTGS, Fedwire) but exposes banks to potential counterparty risks.

[27]Data source: www.frbservices.org. Federal Reserve also operates two smaller payment systems, National Settlement Service (NSS) with an average daily settlement value of $93 billions in 2020 (source: www.frbservices.org), and ACH with an average daily settlement value of $122.8 billion in 2020 (source: www.federalreserve.gov).

[28]Data source: https://www.theclearinghouse.org

B Appendix: Bank Depositor Liquidity Management

In this section, we microfound the component, $\theta_1 x_i + \frac{\theta_2}{2} x_i^2$, of bank i's objective function by modeling the liquidity management problem of bank i's depositors.

In aggregate, bank i's depositors lose liquidity x_i, which is equal to the payment outflow to other banks' depositors. To cover the liquidity shortfall, bank i's depositors may borrow from bank i, for example, in the form of lines of credit.[29] Consider a unit mass of depositors and the evenly distributed loss of liquidity (i.e., each depositor's loss of liquidity is equal to x_i). A representative depositor chooses c, the amount of liquidity obtained from bank i (for example, the size of lines of credit). Bank i charges a proportional price P_c. The depositor's problem is given by

$$\max_c \xi_1 \left[c - x_i - \frac{1}{2\xi_2}(c - x_i)^2 \right] - cP_c \,, \tag{B.1}$$

where the parameter ξ_1 (> 0) captures the overall demand for liquidity and the parameter ξ_2 (> 0) captures the decreasing return to liquidity. A key economic force is that a higher x_i increases the marginal benefit of c. In other words, when bank i's depositors lose liquidity through payment outflows to other banks' depositors, they rely more on bank i for liquidity provision.

From the depositor's first order condition for c,

$$\xi_1 - \frac{\xi_1}{\xi_2}(c - x_i) = P_c \,, \tag{B.2}$$

we solve the optimal c:

$$c = \xi_2 \left(1 - \frac{P_c}{\xi_1} \right) + x_i \,. \tag{B.3}$$

The depositor's liquidity demand is stronger following a greater payment outflow, x_i and when the marginal value of liquidity declines slower (i.e., under a greater value of ξ_2). A higher value of ξ_1 or a lower price P_c also increase c. Under the homogeneity of bank i's depositors, equation (B.3) is also the aggregate liquidity demand for the unit mass of bank i's depositors.

Bank i sets the price P_c to maximize its profits from liquidity provision:

$$\max_{P_c} \left[\xi_2 \left(1 - \frac{P_c}{\xi_1} \right) + x_i \right] P_c \,. \tag{B.4}$$

[29] Empirically, cash and lines of credit are substitutes (Lins, Servaes, and Tufano, 2010).

Here we assume relationship banking so bank i's depositors cannot obtain liquidity elsewhere. This translates into bank i's market power and monopolistic profits. From the first-order condition for P_c,

$$-\frac{\xi_2}{\xi_1}P_c + \xi_2\left(1 - \frac{P_c}{\xi_1}\right) + x_i = 0\,, \tag{B.5}$$

we solve the optimal P_c:

$$P_c = \frac{\xi_1}{2}\left(1 + \frac{x_i}{\xi_2}\right)\,. \tag{B.6}$$

Substituting the optimal P_c into bank i's profits, we obtain the maximized profits:

$$\frac{\xi_1\xi_2}{4}\left(1 + \frac{x_i}{\xi_2}\right)^2 = \frac{\xi_1\xi_2}{4} + \frac{\xi_1}{2}x_i + \frac{\xi_1}{4\xi_2}x_i^2\,, \tag{B.7}$$

which corresponds to the component, $\theta_1 x_i + \frac{\theta_2}{2}x_i^2$, of bank i's objective function in the main text with

$$\theta_1 = \frac{\xi_1}{2}\,, \text{ and, } \theta_2 = \frac{\xi_1}{2\xi_2}\,. \tag{B.8}$$

The constant $\frac{\xi_1\xi_2}{4}$ is omitted in bank i's objective function in the main text.

C Appendix: Derivation Details

C.1 Maximum likelihood formulation

For the homogeneous ϕ case, we rewrite the variables and coefficients of the model in equations (37) and (38) in matrix form following Lee and Yu (2010):

$$\begin{aligned}
B &\equiv [\beta_1^{bank}, .., \beta_m^{bank}, ..., \beta_M^{bank}, \beta_1^{macro}, ..., \beta_p^{macro}, ..., \beta_P^{macro}]^\top, \\
L &\equiv [l_{1,1}, ..., l_{N,1}, ..., l_{i,t}, ..., l_{1,T}, ..., l_{N,T}]^\top, \\
\mathbf{n} &\equiv [n_{1,1}, ..., n_{N,1}, ..., n_{i,t}, ..., n_{1,T}, ..., n_{N,T}]^\top \\
\nu' &\equiv [\nu'_{1,1}, ..., \nu'_{N,1}, ..., \nu'_{i,t}, ..., \nu'_{1,T}, ..., \nu'_{N,T}]^\top \\
\underline{\alpha} &\equiv \mathbf{1}_T \otimes \bar{\alpha}' = \mathbf{1}_T \otimes [\bar{\alpha}'_1, ..., \bar{\alpha}'_N]^\top,
\end{aligned}$$

and

$$\mathbf{W}' \equiv diag\left(\mathbf{W}_t\right)_{t=1}^T = \begin{bmatrix} \mathbf{W}'_1 & \mathbf{0} & ... & \mathbf{0} \\ \mathbf{0} & \mathbf{W}'_2 & ... & ... \\ ... & ... & ... & \mathbf{0} \\ \mathbf{0} & ... & \mathbf{0} & \mathbf{W}'_T \end{bmatrix}, \quad \mathbf{X} \equiv \left[\mathbf{X}^{bank}, \mathbf{X}^{macro}\right],$$

where we define

$$\mathbf{X}^{macro} = \begin{bmatrix} x_1^1 & ... & x_1^p & ... & x_1^P \\ ... & ... & ... & ... & ... \\ x_t^1 & ... & x_t^p & ... & x_t^P \\ ... & ... & ... & ... & ... \\ x_T^1 & ... & x_T^p & ... & x_T^P \end{bmatrix} \otimes \mathbf{1}_N, \quad \mathbf{X}^{bank} = \begin{bmatrix} x_{1,1}^1 & ... & x_{1,1}^m & ... & x_{1,1}^M \\ ... & ... & ... & ... & ... \\ x_{N,1}^1 & ... & x_{N,1}^m & ... & x_{N,1}^M \\ ... & ... & ... & ... & ... \\ x_{N,T}^1 & ... & x_{N,T}^m & ... & x_{N,T}^M \end{bmatrix},$$

we can then rewrite the empirical model as

$$L = \mathbf{X}B + \mathbf{n}, \quad \mathbf{n} = \phi\mathbf{W}'\mathbf{n} + \underline{\alpha} + \nu', \quad \nu'_{i,t} \sim \mathcal{N}\left(0, \delta_i'^2\right). \tag{C.1}$$

This, in turn, implies that

$$\nu'\left(B, \underline{\alpha}, \phi\right) = \left(I_{N\times T} - \phi\mathbf{W}'\right)\left(L - \mathbf{X}B\right) - \underline{\alpha}. \tag{C.2}$$

Using the Gaussian distribution to model the exogenous error terms ν' yields the log likelihood

$$\ln \mathcal{L}\left(B, \phi, \underline{\alpha}, \left\{\delta_i'^2\right\}_{i=1}^N\right) \equiv -\frac{TN}{2}\ln\left(2\pi\right) - \frac{T}{2}\sum_{i=1}^N \ln \delta_i'^2 - \sum_{i=1}^N \frac{1}{2\delta_i'^2}\sum_{t=1}^T \nu'_{i,t}\left(B, \underline{\alpha}, \phi\right)^2, \tag{C.3}$$

We maximize the likelihood to estimate the parameters, $B, \phi, \underline{\alpha}, \left\{\delta_i^{'2}\right\}_{i=1}^N$. In the numeric solution of likelihood maximization, we first estimate B using ordinary least squares (OLS), and use the first-order condition for $\delta_i^{'2}$, i.e.,

$$\widehat{\delta_i^{'2}} = \frac{1}{T}\sum_{t=1}^{T} \nu'_{i,t}\left(B, \underline{\alpha}, \phi\right)^2,$$

to substitute out $\delta_i^{'2}$ in the log likelihood function, forming a concentrated likelihood that only depends on ϕ. By maximizing the concentrated likelihood, we obtain $\hat{\phi}$. Next, using the aforementioned first-order conditions for $\delta_i^{'2}$, we obtain estimates of $\delta_i^{'2}$. We then re-estimate B as in feasible generalized least squares (FGLS), using $\hat{\phi}$ and $\delta_i^{'2}$ to form the heteroskedastic covariance matrix in the observational equation of L. Next, $\hat{B}$ is used to form a new concentrated likelihood, which is used to update the estimate of ϕ. We iterate this process until convergence. In the above formulation, the identification of ϕ is ensured by the conditions in Bramoullé, Djebbari, and Fortin (2009). In Section 3.4, we explain the intuition.

C.2 Solving the bank's optimization

First, it is straightforward to derive the moments in the bank's objective function:

$$\begin{aligned}
\mathbb{E}\left[(x_i - m_i)^2\right] &= \mathrm{Var}(x_i) + \mathbb{E}\left[x_i - m_i\right]^2 \qquad \text{(C.4)}\\
&= \mathrm{Var}\left(\sum_{j\neq i} g_{ij}y_i - \sum_{j\neq i} g_{ji}y_j\right) + \mathbb{E}\left[\sum_{j\neq i} g_{ij}y_i - \sum_{j\neq i} g_{ji}y_j - m_i\right]^2\\
&= \sum_{j\neq i}\left(y_i^2\sigma_{ij}^2 + y_j^2\sigma_{ji}^2 - 2y_iy_j\sigma_{ij}\sigma_{ji}\rho_{ij}\right) + \left(\sum_{j\neq i}\mu_{ij}y_i - \sum_{j\neq i}\mu_{ji}y_j - m_i\right)^2,\\
\mathbb{E}\left[x_i^2\right] &= \mathrm{Var}(x_i) + \mathbb{E}\left[x_i\right]^2 = \mathrm{Var}(x_i) + \mathbb{E}\left[\sum_{j\neq i} g_{ij}y_i - \sum_{j\neq i} g_{ji}y_j\right]^2\\
&= \sum_{j\neq i}\left(y_i^2\sigma_{ij}^2 + y_j^2\sigma_{ji}^2 - 2y_iy_j\sigma_{ij}\sigma_{ji}\rho_{ij}\right) + \left(\sum_{j\neq i}\mu_{ij}y_i - \sum_{j\neq i}\mu_{ji}y_j\right)^2, \qquad \text{(C.5)}\\
\mathbb{E}\left[z_i^2\right] &= \mathrm{Var}(z_i) + \mathbb{E}\left[z_i\right]^2 = \mathrm{Var}(z_i) + \mathbb{E}\left[\sum_{j\neq i} g_{ij}y_i\right]^2 = y_i^2(\overline{\sigma}_{-i}^2 + \overline{\mu}_{-i}^2), \qquad \text{(C.6)}
\end{aligned}$$

To simplify the notations, we define

$$\overline{\mu}_{-i} \equiv \sum_{j \neq i} \mu_{ij} \tag{C.7}$$

$$\overline{\sigma}^2_{-i} = \sum_{j \neq i} \sigma^2_{ij}. \tag{C.8}$$

To solve the first-order condition for y_i, note that

$$\frac{\partial \mathbb{E}\left[x_i - m_i\right]}{\partial y_i} = \sum_{j \neq i} \mu_{ij} = \overline{\mu}_{-i}\,, \tag{C.9}$$

$$\frac{\partial \mathbb{E}\left[x_i\right]}{\partial y_i} = \sum_{j \neq i} \mu_{ij} = \overline{\mu}_{-i}\,, \tag{C.10}$$

$$\frac{\partial \mathbb{E}\left[(x_i - m_i)^2\right]}{\partial y_i} = 2 \sum_{j \neq i} \left(y_i \sigma^2_{ij} - \rho_{ij} \sigma_{ij} \sigma_{ji} y_j \right) + 2 \left(y_i \overline{\mu}_{-i} - \sum_{j \neq i} \mu_{ji} y_j - m_i \right) \overline{\mu}_{-i} \tag{C.11}$$

$$\frac{\partial \mathbb{E}\left[x_i^2\right]}{\partial y_i} = 2 \sum_{j \neq i} \left(y_i \sigma^2_{ij} - \rho_{ij} \sigma_{ij} \sigma_{ji} y_j \right) + 2 \left(y_i \overline{\mu}_{-i} - \sum_{j \neq i} \mu_{ji} y_j \right) \overline{\mu}_{-i} \tag{C.12}$$

$$\frac{\partial \mathbb{E}\left[z_i^2\right]}{\partial y_i} = 2 y_i (\overline{\sigma}^2_{-i} + \overline{\mu}^2_{-i}) \tag{C.13}$$

Under parameter restriction, $\tau_2 + \kappa > \theta_2$, that ensures the concavity of objective function in y_i, we solve y_i from the first-order condition:

$$\begin{aligned} 0 =& \varepsilon_i + R - r_i - \tau_1 \overline{\mu}_{-i} + \theta_1 \overline{\mu}_{-i} - y_i \kappa (\overline{\sigma}^2_{-i} + \overline{\mu}^2_{-i}) \\ & - \tau_2 \left[\sum_{j \neq i} \left(y_i \sigma^2_{ij} - \rho_{ij} \sigma_{ij} \sigma_{ji} y_j \right) + \left(y_i \overline{\mu}_{-i} - \sum_{j \neq i} \mu_{ji} y_j - m_i \right) \overline{\mu}_{-i} \right] \\ & + \theta_2 \left[\sum_{j \neq i} \left(y_i \sigma^2_{ij} - \rho_{ij} \sigma_{ij} \sigma_{ji} y_j \right) + \left(y_i \overline{\mu}_{-i} - \sum_{j \neq i} \mu_{ji} y_j \right) \overline{\mu}_{-i} \right] \end{aligned}$$

which can be further simplified to

$$\begin{aligned} 0 =& \varepsilon_i + R - r_i - (\tau_1 - \theta_1) \overline{\mu}_{-i} + \tau_2 \overline{\mu}_{-i} m - y_i \left(\kappa + \tau_2 - \theta_2 \right) \left(\overline{\sigma}^2_{-i} + \overline{\mu}^2_{-i} \right) \\ & + (\tau_2 - \theta_2) \sum_{j \neq i} \left(\rho_{ij} \sigma_{ij} \sigma_{ji} + \overline{\mu}_{-i} \mu_{ji} \right) y_j. \end{aligned} \tag{C.14}$$

From this condition, we solve the optimal y_i in the main text, and we obtain

$$a_i \equiv \frac{R_i - r_i + \varepsilon_i - (\tau_1 - \theta_1)\overline{\mu}_{-i} + \tau_2 \overline{\mu}_{-i} m_i}{(\kappa + \tau_2 - \theta_2)(\overline{\sigma}^2_{-i} + \overline{\mu}^2_{-i})} \,. \tag{C.15}$$

and the following derivatives of a_i,

$$\frac{d^2 a_i}{d\varepsilon_i} = \frac{1}{(\kappa + \tau_2 - \theta_2)(\overline{\sigma}^2_{-i} + \overline{\mu}^2_{-i})} > 0 \tag{C.16}$$

$$\frac{da_i}{dm_i} = \frac{\tau_2 \overline{\mu}_{-i}}{(\kappa + \tau_2 - \theta_2)(\overline{\sigma}^2_{-i} + \overline{\mu}^2_{-i})} > 0. \tag{C.17}$$

$$\frac{da_i}{d\tau_1} = -\frac{\overline{\mu}_{-i}}{(\kappa + \tau_2 - \theta_2)(\overline{\sigma}^2_{-i} + \overline{\mu}^2_{-i})} < 0 \,. \tag{C.18}$$

$$\frac{d^2 a_i}{dm_i d\overline{\mu}_{-i}} = \frac{\tau_2}{(\kappa + \tau_2 - \theta_2)(\overline{\sigma}^2_{-i} + \overline{\mu}^2_{-i})} > 0. \tag{C.19}$$

$$\frac{d^2 a_i}{d\tau_1 d\overline{\mu}_{-i}} = -\frac{1}{(\kappa + \tau_2 - \theta_2)(\overline{\sigma}^2_{-i} + \overline{\mu}^2_{-i})} < 0 \,. \tag{C.20}$$

$$\frac{da_i}{d\overline{\sigma}^2_{-i}} = -\frac{R_i - r_i + \varepsilon_i - (\tau_1 - \theta_1)\overline{\mu}_{-i} + \tau_2 \overline{\mu}_{-i} m_i}{(\kappa + \tau_2 - \theta_2)(\overline{\sigma}^2_{-i} + \overline{\mu}^2_{-i})^2} = -\frac{a_i}{(\overline{\sigma}^2_{-i} + \overline{\mu}^2_{-i})} < 0 \tag{C.21}$$

C.3 Solving the planner's optimization

To solve the planner's solution, we calculate the following derivatives:

$$\begin{aligned}
\frac{\partial \mathbb{E}\left[(x_j - m_j)^2\right]}{\partial y_i} &= \frac{\partial \left\{ \sum_{k \neq j} \left(y_j^2 \sigma_{jk}^2 + y_k^2 \sigma_{kj}^2 - 2 y_j y_k \sigma_{jk} \sigma_{kj} \rho_{jk} \right) + \left(\sum_{k \neq j} \mu_{jk} y_j - \sum_{k \neq j} \mu_{kj} y_k - m_j \right)^2 \right\}}{\partial y_i} \\
&= 2 \left(y_i \sigma_{ij}^2 - \rho_{ij} \sigma_{ij} \sigma_{ji} y_j \right) - 2 \left(y_j \overline{\mu}_{-j} - \sum_{k \neq j} \mu_{kj} y_k - m_j \right) \mu_{ij}
\end{aligned} \tag{C.22}$$

$$\frac{\partial \mathbb{E}\left[x_j^2\right]}{\partial y_i} = \frac{\partial \left\{ \sum_{k\neq j} \left(y_j^2 \sigma_{jk}^2 + y_k^2 \sigma_{kj}^2 - 2 y_j y_k \sigma_{jk} \sigma_{kj} \rho_{jk} \right) + \left(\sum_{k\neq j} \mu_{jk} y_j - \sum_{k\neq j} \mu_{kj} y_k \right)^2 \right\}}{\partial y_i}$$

$$= 2\left(y_i \sigma_{ij}^2 - \rho_{ij}\sigma_{ij}\sigma_{ji} y_j \right) - 2\left(y_j \overline{\mu}_{-j} - \sum_{k\neq j} \mu_{kj} y_k \right) \mu_{ij} \tag{C.23}$$

$$\frac{\partial \mathbb{E}\left[z_j^2\right]}{\partial y_i} = 0 \tag{C.24}$$

The first-order condition for y_i:

$$\begin{aligned} 0 =& \varepsilon_i + R - r_i - \tau_1 \overline{\mu}_{-i} + \theta_1 \overline{\mu}_{-i} - y_i \kappa (\overline{\sigma}_{-i}^2 + \overline{\mu}_{-i}^2) \\ & - \tau_2 \left[\sum_{j\neq i} \left(y_i \sigma_{ij}^2 - \rho_{ij}\sigma_{ij}\sigma_{ji} y_j \right) + \left(y_i \overline{\mu}_{-i} - \sum_{j\neq i} \mu_{ji} y_j - m_i \right) \overline{\mu}_{-i} \right] \\ & + \theta_2 \left[\sum_{j\neq i} \left(y_i \sigma_{ij}^2 - \rho_{ij}\sigma_{ij}\sigma_{ji} y_j \right) + \left(y_i \overline{\mu}_{-i} - \sum_{j\neq i} \mu_{ji} y_j \right) \overline{\mu}_{-i} \right] + \sum_{j\neq i} (\tau_1 - \theta_1) \mu_{ij} \\ & - (\tau_2 - \theta_2) \left(y_i \sigma_{ij}^2 - \rho_{ij}\sigma_{ij}\sigma_{ji} y_j \right) + (\tau_2 - \theta_2) \left(y_j \overline{\mu}_{-j} - \sum_{k\neq j} \mu_{kj} y_k \right) \mu_{ij} - \tau_2 m_j \mu_{ij} \\ =& \varepsilon_i + R - r_i + \tau_2 \overline{\mu}_{-i} m - y_i \left(\kappa + 2\tau_2 - 2\theta_2 \right) \overline{\sigma}_{-i}^2 - y_i \left(\kappa + \tau_2 - \theta_2 \right) \overline{\mu}_{-i}^2 - \sum_{j\neq i} \tau_2 m_j \mu_{ij} \\ & + (\tau_2 - \theta_2) \sum_{j\neq i} \left(2\rho_{ij}\sigma_{ij}\sigma_{ji} + \overline{\mu}_{-i}\mu_{ji} + \overline{\mu}_{-j}\mu_{ij} \right) y_j - (\tau_2 - \theta_2) \sum_{j\neq i} \mu_{ij} \left(\sum_{k\neq j} \mu_{kj} y_k \right) \end{aligned} \tag{C.25}$$

From this condition, we solve the planner's optimal y_i in the main text. And, the planner's choice of network-independent bank lending financed by deposits is given by

$$\widetilde{a}_i \equiv \frac{\varepsilon_i + R_i - r_i + \tau_2 \overline{\mu}_{-i} m_i - \sum_{j\neq i} \tau_2 m_j \mu_{ij}}{\left(\kappa + \tau_2 - \theta_2 \right) \left(\overline{\sigma}_{-i}^2 + \overline{\mu}_{-i}^2 \right) + \left(\tau_2 - \theta_2 \right) \overline{\sigma}_{-i}^2} \,. \tag{C.26}$$

Different from the decentralized counterpart in (C.15), the numerator of $\widetilde{a}_i$ no longer has the expected outflow (which, from the planner's perspective, is offset by other banks' inflow) but it has an additional term $\sum_{j\neq i} \tau_2 m_j \mu_{ij}$ because the liquidity externality of bank i's lending is less valuable when bank j ($j \neq i$) already hold more liquid assets.

Next, we solve the connection between $\widetilde{a}_i$ in the planner's solution and a_i in (C.15) of the

market equilibrium:

$$\widetilde{a}_i = b_{i,t} + \frac{\widetilde{\phi}_i}{\phi} a_{i,t}\,, \tag{C.27}$$

where,

$$b_i \equiv \frac{\widetilde{\phi}_i}{(\overline{\sigma}^2_{-i} + \overline{\mu}^2_{-i})} \left[\left(\frac{\tau_1 - \theta_1}{\tau_2 - \theta_2} \right) \overline{\mu}_{-i} - \left(\frac{\tau_2}{\tau_2 - \theta_2} \right) \sum_{j \neq i} \mu_{ij} m_j \right]. \tag{C.28}$$

C.4 Heterogeneous ϕ_i

In the heterogeneous case, we can no longer use standard MLE because the likelihood involves integrating out a vector of latent bank-specific network coefficients, $\phi \equiv (\phi_1, \ldots, \phi_N)^\top$. We therefore estimate the model by simulated maximum likelihood (SML). We maintain the Gaussian parametric restriction

$$\phi_i \sim \mathcal{N}(\mu_\phi, \sigma^2_\phi), \qquad i = 1, \ldots, N, \tag{C.29}$$

where (μ_ϕ, σ_ϕ) are parameters to be estimated.[30]

Let $\theta \equiv (B, \underline{\alpha}, \mu_\phi, \sigma_\phi, \delta_i'^2)$ denote the parameter vector. Conditional on a realization of ϕ, the model remains Gaussian and can be written as

$$L = \mathbf{X}B + \mathbf{n}, \qquad \mathbf{n} = \Phi \mathbf{W}' \mathbf{n} + \underline{\alpha} + \nu', \qquad \nu'_{i,t} \sim \mathcal{N}(0, \delta_i'^2). \tag{C.30}$$

Equivalently,

$$\nu'\left(B, \underline{\alpha}, \phi\right) \equiv \left(I_{N \times T} - \Phi \mathbf{W}'\right)\left(L - \mathbf{X}B\right) - \underline{\alpha}. \tag{C.31}$$

Therefore, conditional on ϕ, the log likelihood is

$$\ln \mathcal{L}\left(\theta \mid \phi\right) \equiv -\frac{TN}{2} \ln(2\pi) - \frac{T}{2} \sum_{i=1}^{N} \ln \delta_i'^2 - \sum_{i=1}^{N} \frac{1}{2\delta_i'^2} \sum_{t=1}^{T} \nu'_{i,t}\left(B, \underline{\alpha}, \phi\right)^2. \tag{C.32}$$

The unconditional likelihood integrates out ϕ under (C.29):

$$\mathcal{L}(\theta) = \int \mathcal{L}\left(\theta \mid \phi\right), f(\phi \mid \mu_\phi, \sigma_\phi), d\phi, \tag{C.33}$$

where $f(\phi \mid \mu_\phi, \sigma_\phi) = \prod_{i=1}^{N} \varphi\left(\frac{\phi_i - \mu_\phi}{\sigma_\phi}\right) \frac{1}{\sigma_\phi}$ and $\varphi(\cdot)$ is the standard normal density. Since the integral in (C.33) is high-dimensional, we approximate it by Monte Carlo simulation. Specifically,

[30] In implementation, we impose the stability condition $\rho(\Phi W_t') < 1$ for all t, where $\Phi \equiv \mathrm{diag}(\phi_1, \ldots, \phi_N)$, and discard draws that violate it.

for each draw $s = 1, \ldots, S$, we generate

$$\phi_i^{(s)} = \mu_\phi + \sigma_\phi z_i^{(s)}, \qquad z_i^{(s)} \overset{i.i.d.}{\sim} \mathcal{N}(0,1), \tag{C.34}$$

form $\Phi^{(s)} = \operatorname{diag}(\phi_1^{(s)}, \ldots, \phi_N^{(s)})$, and compute the corresponding residual vector

$$\nu'^{(s)} \equiv \left(IN \times T - \Phi^{(s)} \mathbf{W}'\right)(L - \mathbf{X}B) - \underline{\alpha}. \tag{C.35}$$

The simulated likelihood is then

$$\widehat{\mathcal{L}}_S(\theta) \equiv \frac{1}{S} \sum s = 1^S \mathcal{L}\left(\theta \mid \phi^{(s)}\right), \qquad \widehat{\ell}_S(\theta) \equiv \ln \widehat{\mathcal{L}}_S(\theta), \tag{C.36}$$

where $\mathcal{L}(\theta \mid \phi^{(s)}) = \exp \ln \mathcal{L}(\theta \mid \phi^{(s)})$ is obtained from (C.32) by replacing ν' with $\nu'^{(s)}$.

We estimate θ by maximizing the simulated log likelihood $\widehat{\ell S}(\theta)$. For a given draw $\phi^{(s)}$, the optimal $\delta_i'^2$ satisfies

$$\widehat{\delta}_i'^2\left(\phi^{(s)}\right) = \frac{1}{T} \sum t = 1^T \left(\nu_{i,t}'^{(s)}\right)^2, \tag{C.37}$$

which we substitute back into (C.32) to form a draw-specific concentrated likelihood. Using (C.37), we define the simulated concentrated log likelihood

$$\widehat{\ell}_S^c(B, \underline{\alpha}, \mu_\phi, \sigma_\phi) \equiv \ln \left[\frac{1}{S} \sum_{s=1}^{S} \exp \left\{ -\frac{T}{2} \sum_{i=1}^{N} \ln \widehat{\delta}_i'^2\left(\phi^{(s)}\right) \right\} \right] + C, \tag{C.38}$$

where C collects terms constant in $(B, \underline{\alpha}, \mu_\phi, \sigma_\phi)$. We maximize (C.38) numerically over $(B, \underline{\alpha}, \mu_\phi, \sigma_\phi)$, and then recover $\delta_i'^2$ by averaging (C.37) across draws at the optimum.[31]

[31] We use common random numbers across iterations to smooth the simulated objective.

D Appendix: Additional Tables and Figures

Table D.1: **Summary Statistics**. This table reports the number of observations, mean, standard deviation, and percentiles of variables in our sample. Our sample contains 500 banks and 44 quarters from 2010 to 2020. We calculate μ_{ij} (σ_{ij}) as the within-quarter average (standard deviation) of daily payment outflows from bank i to bank j divided by bank i's deposits at the beginning of the quarter. Therefore, $\sum_{j\neq i}\mu_{ij}$ is the average daily payment outflow as a fraction of deposits for bank i within a quarter and $\sum_{j\neq i}\sigma_{ij}^2$ measures the payment-flow risk for bank i.

Variable	**N**	**Mean**	**S.D.**	**P25**	**P50**	**P75**
Quarterly loan growth rate	22000	0.0230	0.0550	-0.0016	0.0143	0.0341
Bank Characteristics:						
log(Asset) (unit: log(USD '000))	22000	15.13	1.41	14.15	14.69	15.72
Liquid Assets/Total Assets	22000	0.18	0.12	0.10	0.16	0.24
Capital/Total Assets	22000	0.11	0.03	0.09	0.10	0.12
Deposits/Total Assets	22000	0.68	0.12	0.63	0.70	0.75
Return on asset	22000	0.0026	0.0025	0.0018	0.0025	0.0033
Loans/Total Assets	22000	0.67	0.15	0.60	0.70	0.77
Macroeconomic Variables:						
Effective Fed Funds Rate change (%)	22000	-0.0007	0.2361	-0.0101	0.0119	0.0521
GDP growth (%)	22000	0.51	3.09	-2.59	1.43	2.29
Inflation (%)	22000	0.43	0.66	0.11	0.46	0.82
Stock market return (%)	22000	3.68	8.06	0.51	4.52	7.97
Housing price growth (%)	22000	1.13	1.87	0.14	1.15	2.29
Cross-Section Payment Statistics:						
Average net daily payment flow/Deposits (%)	500	0.01	0.91	-0.14	0.01	0.17
s.d. of net daily payment flow/Deposits (%)	500	0.97	0.83	0.48	0.74	1.14
Average gross daily outflow/Deposits (%)	500	1.82	4.31	0.35	0.74	1.47
s.d. of gross daily outflow/Deposits (%)	500	1.11	1.34	0.41	0.70	1.18

Table D.2: **Control Variable Coefficients**. This table reports the estimates of control variable coefficients across samples of different sizes that contain banks ranked by the size of their deposits (with exogenous rates). The t-stats are in the parentheses. The abbreviation, EFFR, is for effective fund funds rate. *,** , and *** correspond to 10-, 5-, and 1% significance level, respectively.

Number of Banks:	500	300	400	600	700
Constant	0.0897 (0.90)	0.1449 (1.33)	0.0973 (0.96)	0.0765 (0.76)	0.0609 (0.60)
Bank Characteristics:					
log(Asset)	-0.0039 (-0.80)	-0.0067 (-1.37)	-0.0046 (-0.92)	-0.0042 (-0.81)	-0.0032 (-0.62)
Liquid Assets/Assets	0.0144^{*} (1.77)	-0.0011 (-0.12)	0.0098 (1.03)	0.0200^{***} (2.58)	0.0252^{***} (3.52)
Capital/Assets	0.0931^{***} (3.28)	0.1086^{***} (4.63)	0.0971^{***} (3.58)	0.0607 (1.51)	0.0531 (1.32)
Deposits/Assets	-0.0108^{**} (-2.27)	-0.0080 (-1.47)	-0.0079 (-1.51)	-0.0111^{***} (-2.65)	-0.0097^{**} (-2.34)
Return on asset	1.2726^{***} (4.19)	1.3469^{***} (3.54)	1.3646^{***} (4.00)	1.2911^{***} (4.55)	1.3236^{***} (4.67)
Loans/Assets	-0.0296^{***} (-2.96)	-0.0380^{***} (-4.14)	-0.0331^{***} (-3.47)	-0.0241^{**} (-2.32)	-0.0172 (-1.64)
Macro. Variables:					
EFFR change (%)	-0.0111 (-1.30)	-0.0102 (-1.41)	-0.0108 (-1.27)	-0.0125 (-1.37)	-0.0123 (-1.31)
GDP growth (%)	-0.0007 (-1.00)	-0.0005 (-0.85)	-0.0007 (-0.97)	-0.0009 (-1.16)	-0.0009 (-1.15)
Inflation (%)	0.0032 (1.11)	0.0032 (1.13)	0.0029 (1.03)	0.0036 (1.23)	0.0036 (1.23)
Stock return (%)	-0.0009^{**} (-2.28)	-0.0008^{**} (-2.50)	-0.0009^{**} (-2.26)	-0.0009^{**} (-2.22)	-0.0009^{**} (-2.17)
Housing price growth (%)	0.0022^{**} (2.52)	0.0018^{**} (2.19)	0.0020^{**} (2.25)	0.0024^{**} (2.56)	0.0025^{***} (2.64)

Figure D.1: **The estimates of $\bar{\alpha}_i'$ and δ_i'.** This figure reports the frequency distribution of the estimates of $\bar{\alpha}_i'$ (Panel A) and δ_i' (Panel B) across different samples of banks ranked by the size of their deposits.

Panel A: Estimates of $\bar{\alpha}_i$

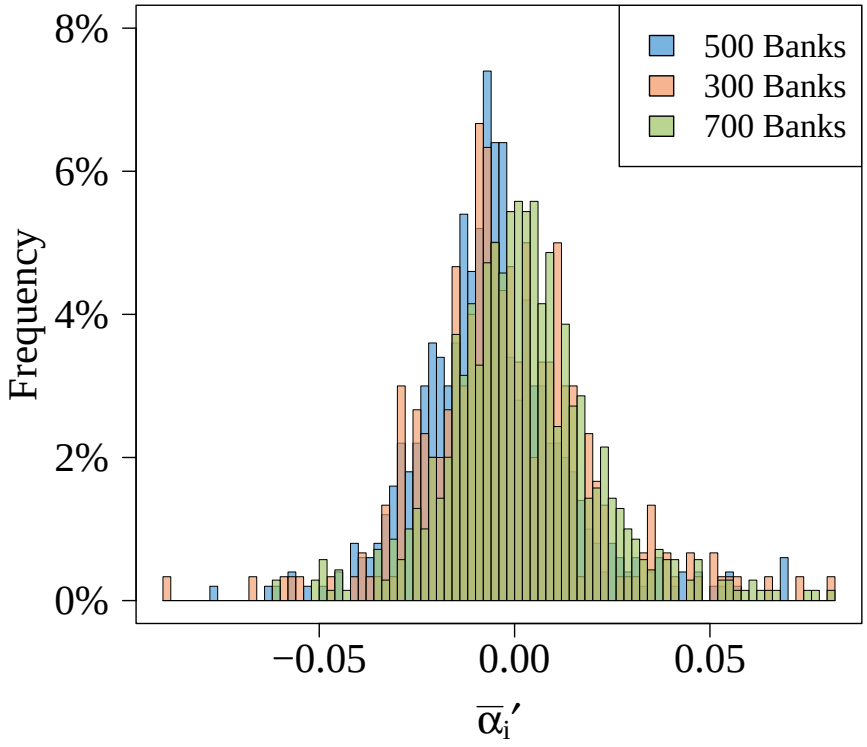

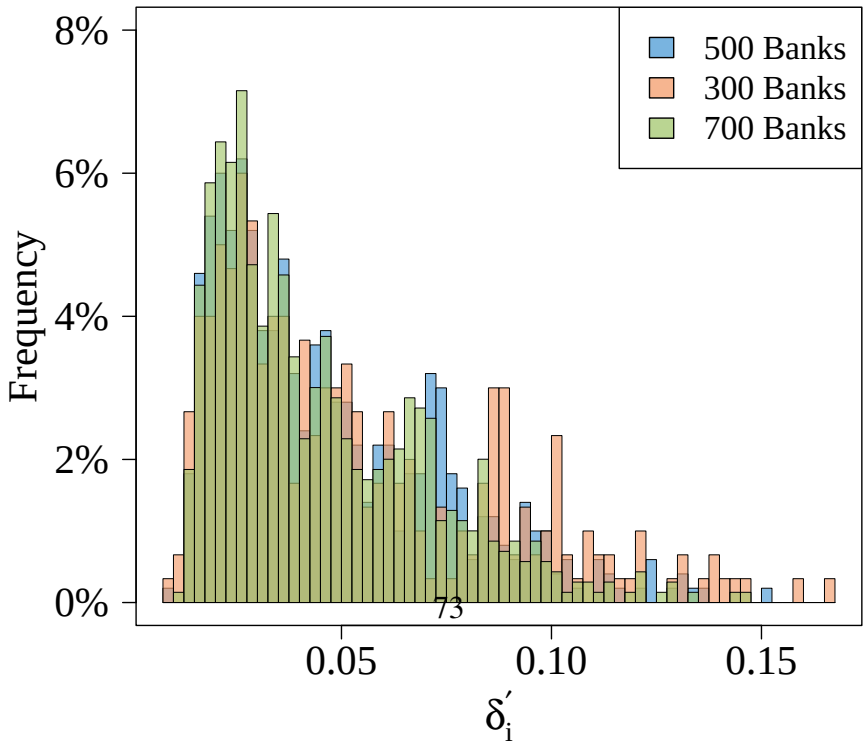

Figure D.2: **Distribution of** ϕ_i. This figure reports the distribution of ϕ_i for the banks of different sizes.

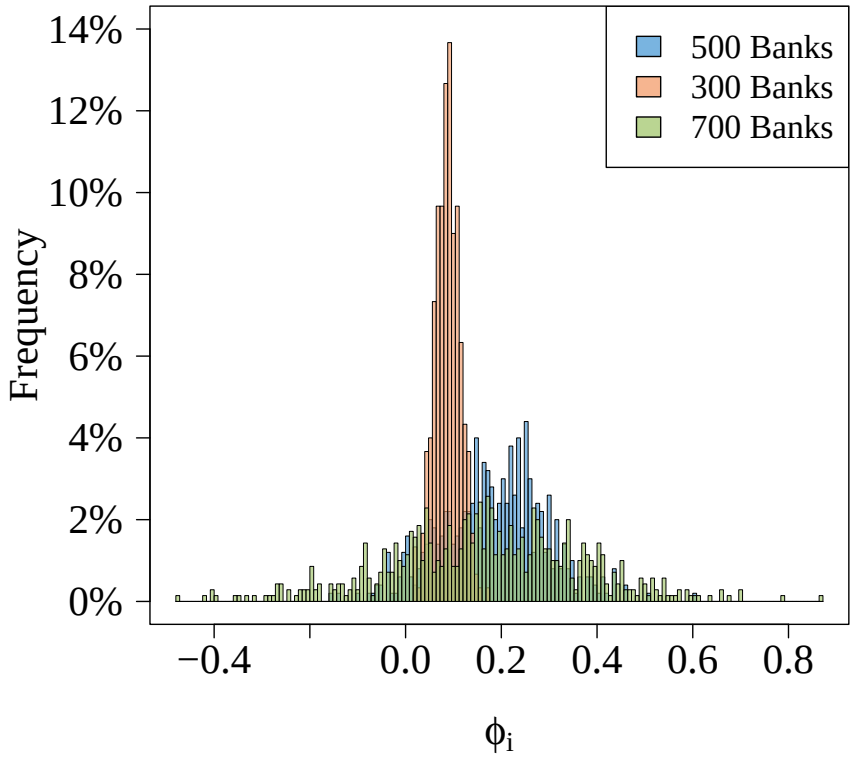

Figure D.3: **Control variable coefficients across samples**. This figure reports the ratio of an estimate from an alternative sample to the estimate from our main sample of the top 500 banks by deposit size. A ratio around one indicates that the two estimates are close. We plot the 95% confidence interval of each estimate from our main sample scaled by the estimate so the mid-point is equal to one.

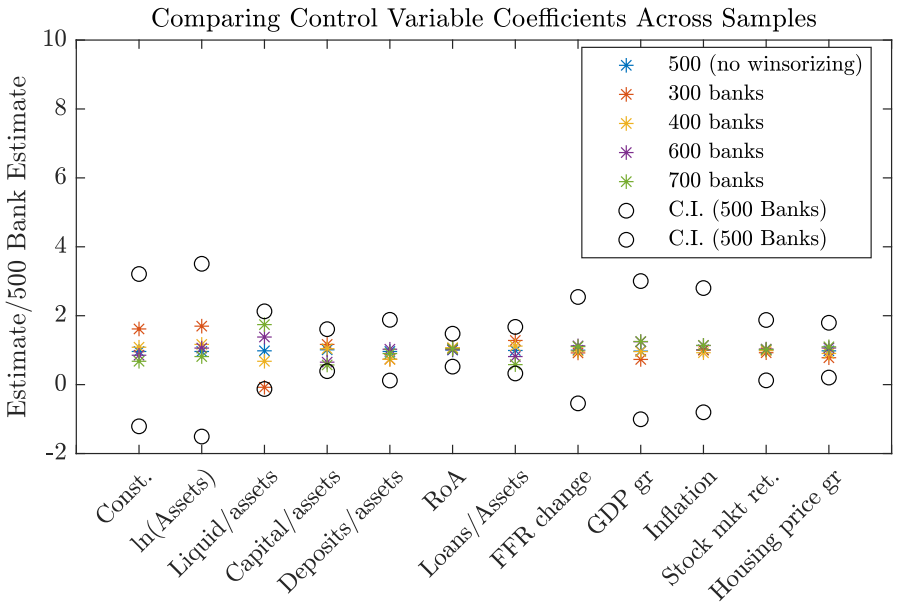

E Network Eigenvalues

Figure E.1: **Eigenvalues of network adjacency matrix.** In this figure, we plot the absolute values of the five largest eigenvalues of $\mathbf{W}'$. $\mathbf{W}'$ for quarter t is calculated from payment data from quarter $t-1$ (see Section 3.3).

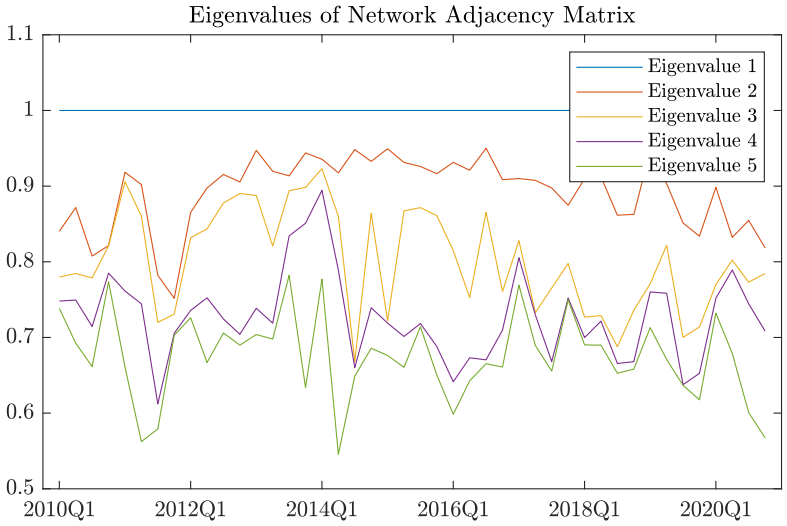

The eigenvalues of the network adjacency matrix are important in determining the strength of network propagation. With heterogeneous attenuation, define the diagonal matrix

$$\mathbf{\Phi} \equiv \text{diag}(\phi_1, \ldots, \phi_N), \tag{D.1}$$

and consider the effective propagation matrix $\mathbf{\Phi W}'$. Let $\widetilde{\mathbf{\Lambda}}$ denote the diagonal matrix whose diagonal elements are the eigenvalues of $\mathbf{\Phi W}'$, ranked by absolute value. In our sample, $\mathbf{\Phi W}'$ has linearly independent eigenvectors, so we apply the eigen decomposition

$$\mathbf{\Phi W}' = \widetilde{\mathbf{V}}, \widetilde{\mathbf{\Lambda}}, \widetilde{\mathbf{V}}^{-1}, \tag{D.2}$$

where $\widetilde{\mathbf{V}}$ is the $N \times N$ matrix whose i-th column is the ith largest eigenvector.

Substituting this decomposition into the definition of the network multiplier,

$$\mathbf{M}(\mathbf{\Phi}, \mathbf{W}') = (\mathbf{I} - \mathbf{\Phi W}')^{-1}, \tag{D.3}$$

we obtain

$$\mathbf{M!}\left(\mathbf{\Phi}, \mathbf{W}'\right) = \mathbf{I} + \widetilde{\mathbf{V}}, \widetilde{\mathbf{\Lambda}}, \widetilde{\mathbf{V}}^{-1} + \widetilde{\mathbf{V}}, \widetilde{\mathbf{\Lambda}}^2, \widetilde{\mathbf{V}}^{-1} +, \ldots, = \widetilde{\mathbf{V}} \left(\sum_{k=0}^{\infty} \widetilde{\mathbf{\Lambda}}^k \right) \widetilde{\mathbf{V}}^{-1}. \tag{D.4}$$

The matrix $\sum_{k=0}^{\infty} \widetilde{\mathbf{\Lambda}}^k$ is diagonal, and its i-th diagonal element is

$$\left\{ \sum_{k=0}^{\infty} \widetilde{\mathbf{\Lambda}}^k \right\}_{ii} = \left\{ \left(\mathbf{I} - \widetilde{\mathbf{\Lambda}} \right)^{-1} \right\}_{ii} = \frac{1}{1 - \widetilde{\mathbf{\Lambda}}_{ii}}, \tag{D.5}$$

where $\widetilde{\mathbf{\Lambda}}_{ii}$ is the i-th largest eigenvalue of $\mathbf{\Phi W}'$.

The strength of the network as a shock amplification mechanism therefore, depends on the eigenvalues of the effective propagation matrix $\mathbf{\Phi W}'$, which jointly capture the network topology (through $\mathbf{W}'$) and the heterogeneity in attenuation (through $\mathbf{\Phi}$). The stability of the eigenvalues over time suggests that the time variation of network effects is mainly driven by the cross-sectional distribution of $\phi_{i}{}_{i=1}^{N}$.

To see the mechanism more clearly, multiply both sides of the reduced-form shock equation by $\widetilde{\mathbf{V}}^{-1}$ and obtain

$$\widetilde{\mathbf{V}}^{-1} \boldsymbol{\epsilon}_t = \widetilde{\mathbf{V}}^{-1} \mathbf{M!}\left(\mathbf{\Phi}, \mathbf{W}'\right) \boldsymbol{\nu}_t' = \left(\sum_{k=0}^{\infty} \widetilde{\mathbf{\Lambda}}^k \right) \widetilde{\mathbf{V}}^{-1} \boldsymbol{\nu}_t'. \tag{D.6}$$

Up to a monotonic linear transformation given by $\widetilde{\mathbf{V}}^{-1}$, the ultimate impact of shocks on all banks depends on how strongly the network propagates shocks through the eigenvalues $\widetilde{\mathbf{\Lambda}}_{ii}$. We may decompose the propagation into two steps. First, the system-wide strength of amplification is governed by the eigenvalues of $\mathbf{\Phi W}'$. Second, after amplification, the distribution of shocks across banks depends on the eigenvectors collected in $\widetilde{\mathbf{V}}$.